Synthesis and Characterization of Electron-Responsive Materials

by

Yi LIU

A dissertation submitted to
Kochi University of Technology
In partial fulfillment of the requirements
for the degree of

DOCTOR OF PHILOSOPHY
KOCHI UNIVERSITY OF TECHNOLOGY
Kochi, Japan
September, 2013

ABSTRACT

Yi LIU. Synthesis and Characterization of Electron-Responsive Materials

(Under the supervision of Prof. Ryuichi Sugimoto**)**

As a new-type of photovoltaic devices, dye-sensitized solar cells (DSSCs) have been the subject of intensive research activities over the last quarter century. In DSSC devices, dyes play a key role in the conversion of solar energy into electricity. Compared with other dyes investigated so far, ruthenium poly(pyridine) complexes have been well-studied and found to be most effective. The robust immobilization of dye molecules onto a nanocrystalline semiconductor surface is critical to ensure effective electron injection and device durability. Generally, hydrophilic groups, such as -COOH, -PO_3OH, -SH, and -OH, are indispensable in the rational design of dyes for DSSCs. Up to now, dyes without these functional groups cannot be candidates for dye research. This drawback has limited the development of DSSCs. Therefore, the author made his endeavor to develop a novel separated electrolysis method to graft a new ruthenium poly(vinyl-substituted pyridine) complex onto a TiO_2 electrode surface and explored the capability of the incident photon-to-electricity conversion of the resulting TiO_2 electrode in DSSCs. The author confirmed that the deposition of the

ruthenium complex onto a TiO_2 electrode was strongly influenced by working potential, immobilization time and various solvents used as the electrolysis solvent, washing solvent, and immobilization solvent. Unfortunately, the DSSC fabricated with the resulting TiO_2 electrode just presented inferior incident photo-to-electricity conversion efficiency (at 440 nm, 1.2%). To improve the capacity of incident photo-to-electricity conversion of the resulting DSSC, sodium 4-vinylbenzenesulfonate was introduced into the immobilization system to form a composite film. The incident power conversion capacity of the composite film was sharply enhanced to 31.7% at 438 nm.

On the other hand, a photocathode which collects external circuit electrons and assists the regeneration of I^- from I^{3-} is also an essential component of DSSCs. Commonly, Pt film, which is optimal in electro-conductivity, catalytic activity of I^{3-} reduction, is coated onto a fluorine-doped tin oxide glass (FTO) to construct a photocathode. However, Pt is too expensive to apply in a large scale in DSSCs. Recently, poly(3-alkylthiophene)s, which are excellent in electro-conductivity, catalytic activity of I^{3-} reduction, and cost-effectiveness, have been employed to replace Pt to assemble a photocathode of DSSCs. For the large scale application of poly(3-alkylthiophene)s in DSSCs, it is essential that the polymerization of 3-

alkylthiophenes proceeds with a simple route and in high yield. To date, the $FeCl_3$ oxidative method is the most popular in the synthesis of poly(3-alkylthiophene)s. To the best of the author's knowledge, details on their synthesis is, however, still unavailable. Then, the author devoted his effort to investigate the polymerization of 3-alkylthiophene. By monitoring the progress of the polymerization of 3-hexylthiophene with $FeCl_3$ in $CHCl_3$, the author successfully constructed the reaction profile and estimated the activation energy of this polymerization reaction. The effect of solvent on the polymerization of 3-hexylthiophene with $FeCl_3$ was also studied. Other than chlorinated methanes, aromatic solvents, especially benzene and toluene, are applicable for the polymerization reaction. Different from the chlorination of the resulting polymer obtained the $FeCl_3$ oxidative method in $CHCl_3$, the incorporation of the solvent molecule(s) into the polymer was observed when the aromatic solvents were used. The author also found that the polymerization reaction proceeded by using TEMPO/$FeCl_3$ combination as the oxidant and discuss its reaction mechanism. Moreover, The polymerization activity of brominated 3-hexylthiophene with iron(III) halide was firstly established, even though the activity was rather low.

Table of contents

Chapter 1 Introduction

1.1 General introduction to electron-responsive materials

Electron-responsive materials, which give response to electrical stimuli, are classified into three categories: (1) conducting polymers, (2) coordination complexes, and (3) other electro-responsive materials, such as metals, metal oxides, and alloys. Electron-responsive materials are attracting a lot of attention, in view of their importance in fundamental research and practical applications. As excellent electron-responsive materials, coordination complexes (especially transition metal complexes)[1] and conducting polymers (especially poly(3-alkylthiophene))[2] have been investigated and applied in energy storage and conversion field (especially, in photon-to-electricity conversion field) in the past twenty years.

1.2 General introduction to dye-sensitized solar cells (DSSCs)

1.2.1 General introduction to solar energy utilization

With the rise of newly industrialized countries, the solution of energy crisis is an approaching challenge for the human society now. To date, fossil fuels, namely, coal, oil, and natural gas, which were formed millions of years ago from the fossilized remains of plants and animals are the main energy sources. However, the remaining reserves of these three non-renewable fossil fuels are too limited to support the sustainable development of human society. On the other hand, the tremendous consumption of fossil fuels has resulted in serious environmental and social catastrophes, such as global warming, extinction of species, and soil erosion. Thus, it is very urgent to explore alternative

energy sources. Several different clean and renewable energy sources like wind powder, bio-energy, and geothermal and solar energies, have been utilized to relieve the energy crisis.

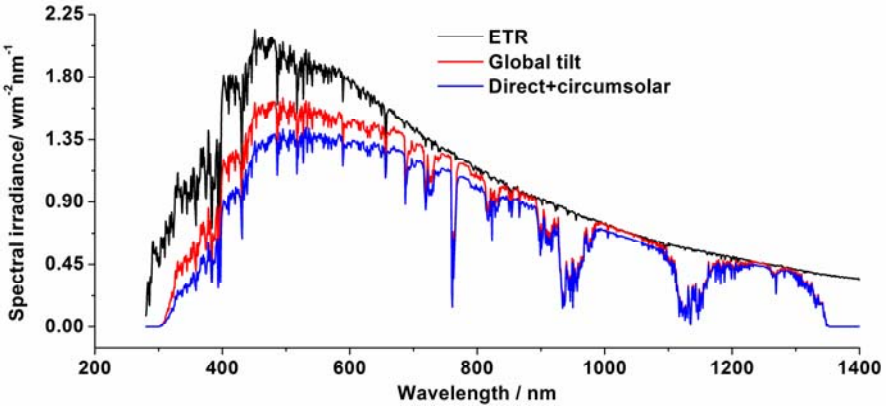

Scheme 1.2.1.1. Solar irradiance and photon flux at the AM 1.5G illumination[3]

Scheme 1.2.1.1 presents the solar irradiance and photon flux at the AM 1.5G illumination. The spectrum of sunlight reaches to the ground of the earth is influenced by water, CO_2, N_2, and dust particles etc. in the atmosphere. Comparing with other renewable energies, solar energy possesses obvious advantages: (1) Solar energy (pure radiant energy) is incredibly inexhaustible. Some theoretical calculations pointed out that the amount of energy reaching the earth from the sun for less than 28 minutes can meet the energy requirement of human in one year. (2) Solar energy is environmentally friendly. Processes for solar energy utilization do not lead to greenhouse gas emission. (3) Solar energy is available in anywhere, comparing with other sources. Generally, there are three methods to convert solar energy into other energies; (1) photon-to-thermal conversion by a solar heater, (2) photon-to-electricity conversion by a solar panel, and (3) conversion of solar energy into chemical energy by green plants (photosynthesis). The conversion of

light energy to thermal energy by a solar heater is very popular, convenient, and pollution-free. In view of the importance of electricity in real word, photon-to-electricity conversion by a solar panel is more attractive than photon-to-thermal conversion by a solar heater. A solar panel, which functions as a photon-absorber and a converter is the key component in a solar cell. Since Bell Labs announced the invention of a modern silicon-based solar cell in 1954, silicon-based solar cells have been becoming vital in space vehicle and industry. Although up to now a silicon-based solar cell still affords the highest photon-to-electricity efficiency (about 24% at 2012), the serious environmental pollution in the purification of silicon crystals has inhibited its further development.

1.2.2 Development of dye-sensitized solar cells

1.2.2.1 Work principle of dye-sensitized solar cells

As a promising alternative to traditional silicon-based solar cells, dye-sensitized solar cells (DSSCs) have been attracting much attention in the world in the last twenty years.[4] The history of DSSCs began in 1972 with the finding that photo-current was generated when a chlorophyll-sensitized zinc oxide electrode was exposed to light irradiation.[5] In the following years, a limited success was attained in the improvement of device efficiency. Poor photon-to-electricity conversion efficiency was attributed to the low photo-absorption ability of the sparse dye molecules on the flat semiconductor. Although an improved photo-absorption was achieved by stacking dye molecules each other, charge separation just occurred at the interface between a semiconductor and a dye molecule contacting with the semiconductor directly. To solve the dilemma, porous ZnO particles with a dramatically increased surface area were prepared and adopted to fabricate a photoanode for DSSCs in 1976.[6] The resulting DSSC devices outputted about

2.5% overall photon-to-electricity conversion efficiency. A big breakthrough in overall photon-to-electricity conversion efficiency of DSSCs came in 1991. Gräzel and O'regan improved the performance of DSSCs from 2.5% to 7.9% by the introduction of a nanoporous TiO_2 electrode and a ruthenium complex dye.[7] The performance improvement of DSSCs was largely attributed to the high surface area of the nanoporous TiO_2 electrode and the ideal spectral characteristics of the applied ruthenium complex dye. This achievement has triggered a boom of DSSCs research in the past 30 years. Now, the performance of DSSCs has rose up to 15%, exceeding the power conversion efficiency of traditional, amorphous silicon-based solar cells (13.4%).[8] The industrialization of DSSCs will have a bright future, owing to its low cost, feasibility in fabrication, pollution-free and colorfulness. Some real DSSC devices are exhibited in Scheme 1.2.2.1.1.

Scheme 1.2.2.1.1. Real DSSC devices (Annual Meeting of the Society of Polymer Science, Yokohama, May 29-31, 2012)

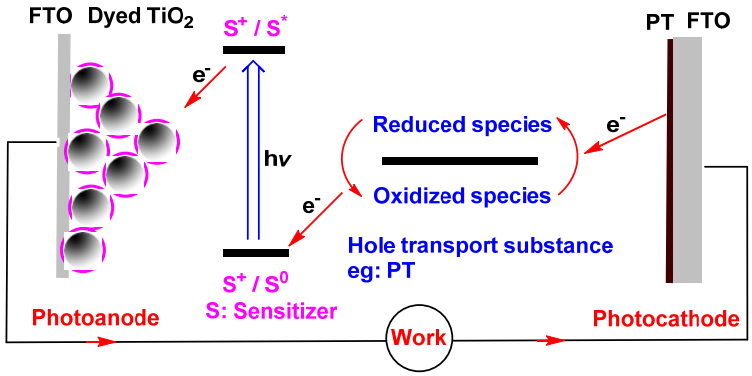

Scheme 1.2.2.1.2. Work principle of DSSCs

Scheme 1.2.2.1.2 depicts the work principle of DSSCs. For DSSCs, solar energy is a driving force. In a green leaf, chlorophyll molecules harvest solar energy to generate electric charge, which are consumed by a redox reaction on a membrane to release oxygen from water and to reduce carbon dioxide to carbohydrates.[9] In general, a dye molecule, immobilized onto a transparent nanocrystalline semiconductor surface by an electrostatic or chemical reaction, is converted to an excited state with the absorption of incident light irradiation. The excited dye molecule sequentially injects an electron into the conduction band of the semiconductor. After the electron injection, a ground-state dye is regenerated with the reduced species of a hole-transport material, such as I^-, CuI, and NiO. After the dye regeneration, the oxidized species of the hole-transport materials appears. The injected electron diffuses towards a fluorine-doped tin oxide (FTO) glass and moves out from a photoanode as electric current to produce work, then accumulates at a photocathode, which was constructed with a FTO glass, coated with the film of Pt, a conducting polymer or carbon, to reduce the oxidized hole transport material. As a result, every material is revived, except for the conversion of light energy to a useful direct current of electricity.

1.2.2.2 Research progress of dyes in DSSCs

1.2.2.2.1 Research progress of metal complex dyes in DSSCs

Dyes, which serve as a light-absorber, are one of critical components of nanostructured DSSCs.[10] The performance of these cells mainly depends on the properties of dyes grafted on a TiO_2 surface, namely, the light response performance of cells is directly dependent on the light absorption of dyes. To enhance this performance, matching the absorption spectra of dyes with solar irradiation and extending the absorptions of the dyes into a near-infrared region are required. The well-positioned HOMO and LUMO of sensitizers are necessary to drive cell work well. To inject an electron, the LUMO level of dyes must be more negative than the conducting band edge of semiconductor electrodes. To accept an electron, the HOMO level of the dyes must be more positive than the redox potential of electrolytes. Thus, the proper molecular design of dyes is critical for DSSCs.

Dyes used in DSSCs can be divided in to two types, metal complex dyes and organic dyes. Metal complex dyes include poly(pyridine) complexes of Ru, Os, Pt, *etc*, metal porphyrin complexes, and metal phthalocyanine complexes, while organic dyes include natural and synthetic organic dyes. Comparing with organic dyes, metal complexes have higher chemical and thermal stabilities. In terms of their matched photo-absorption ability and chemical stability, poly(pyridine) Ru complexes are the most important sensitizers by far.[11] The outstanding efficiency of the Ru complexes can be attributed to a broad absorption range from visible to near-infrared region and to a directional electron transition from the ruthenium center to the anchor group of the dye by MLCT (metal-to-ligand charge transfer). Other than mononuclear ruthenium poly(bipyridine) complex

dyes, typically such as N3, N719, and black dye, polynuclear ruthenium complexes also have been investigated as dyes in DSSCs (Scheme 1.2.2.2.1).[12] Comparing with mononuclear ruthenium complexes, polynuclear ruthenium complexes possess higher absorption coefficiency. However, these bulky sensitizers occupy a larger surface area of TiO_2 particles, resulting in the reduction of the concentration of dyes on the TiO_2 surface. Therefore, the improved absorption coefficiency in a solution does not necessarily enhance the photo-absorption ability of the resulting polynuclear ruthenium complex dyes. Thus, it is proven that polynuclear ruthenium complexes are inefficient for DSSCs.

From a practical viewpoint, Ru, that is one of noble metals, is too expensive to be employed in a large scale in DSSCs. Moreover, the tricky synthesis and purification of Ru complexes are not suitable for industrial application. Similar drawbacks have been mentioned for other metal complexes adopted in DSSCs.

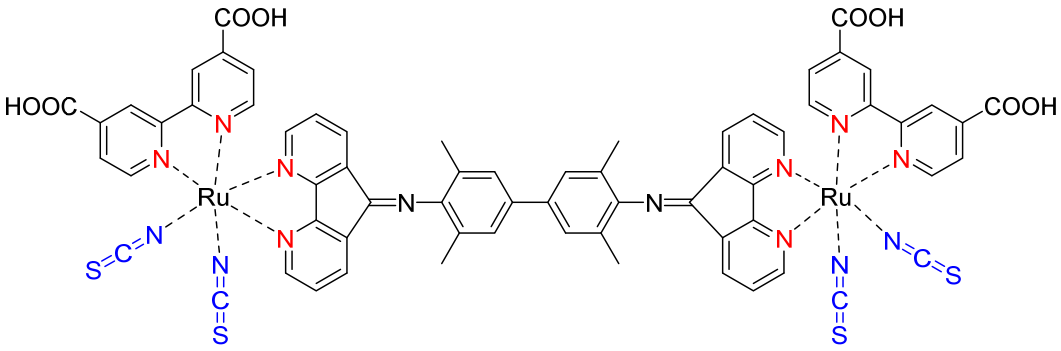

Scheme 1.2.2.2.1. Chemical structure of K20 dye[13]

Big progress has been made in the investigation of noble metal-free complex dyes (Scheme 1.2.2.2.2). Owing to their excellent photo-absorption ability in a range from 400 nm to 450 nm (Soret bands), as well as in a 500-700 nm region (Q bands), porphyrin

complexes have been extensively studied as molecular electronic and photo-electronic devices.[15] Given their primary role in photosynthesis, the use of chlorophylls as light harvesters in DSSCs is particularly attractive. Kay and Gräzel have firstly reported the utilization of copper porphyrin complexes as light absorbers in DSSC devices. The resulting DSSCs shown the incident photon-to-electricity conversion efficiency (IPCE) of up to 83%, along with the overall power conversion efficiency of 2.6%.[16] Since then, abundant attention has been focused on the preparation of optimal porphyrin derivative dyes for the further improvement of the performance of DSSCs. In 2011, by the elegant modification of a porphyrin dye and a tris(bipyridine)-based cobalt(II/III) redox electrolyte, the performance of the resulting DSSCs was boosted up to 12.3 %.[17] This is the first time that a non-ruthenium complex dye outputted the highest cell performance.

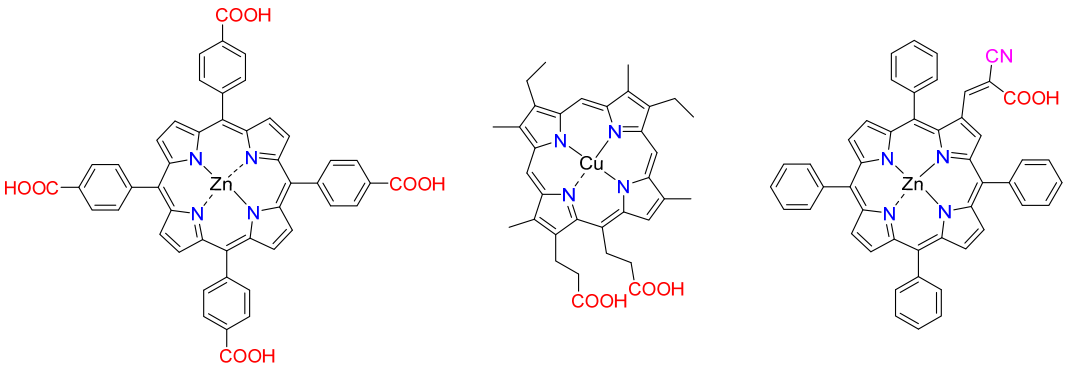

Scheme 1.2.2.2.2. Common metal porphyrin complex dyes reported in literatures[14]

1.2.2.2.2 Research progress of organic dyes in DSSCs

As metal-free sensitizers, organic dyes have been stimulating intensive research efforts because of their advantages as photosensitizers in DSSCs. 1) They have higher molar absorption coefficient than Ru complex dyes (for Ru complexes, $\varepsilon \leq 20000$ L mol^{-1} cm^{-1} for the longest wavelength of a MLCT (metal-to-ligand charge transfer) transition, owing

to an intramolecular π- π* transition, and have photo harvesting capability over a wider spectral range of sun light. 2) The photophysical and electrochemical properties of organic dyes, as well as their stereochemical structure can be easily tuned by facile synthesis and modification. 3) They can be easily synthesized and purified by well-established protocols. 4) There is no concern about resource limitation, because no metal was contained in the organic dyes. In the last ten years, a considerable effort has been made to synthesize various organic dyes to understand the relationship between the chemical structure of the dyes and the performance of the resulting DSSCs. Recently, a general design rule for organic dyes has been constructed: A donor-acceptor substituted π-conjugation bridge has been proven to be vital for the successful design of organic dyes (scheme 1.2.2.2.2.1).[18] Donor-acceptor π-conjugated dyes, possessing electron-donating and electron-accepting moieties linked by a π "bridge", have displayed broad and intensive photo-absorption spectral features. The spectral features of D-π-A dyes are associated with an intramolecular charge transfer (ICT).

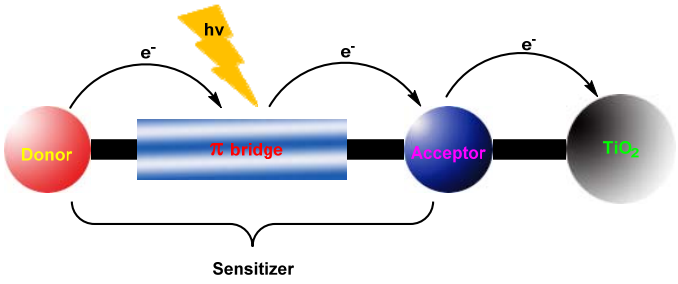

Scheme 1.2.2.2.2.1. Design principle of organic dyes for DSSCs

In D-π-A systems, electron-rich aryl amines, such as aminocoumarin, triphenylamine, indiline, and (difluorenyl)phenylamine derivatives, are popularly utilized as a donor. For π "bridge"s, which function as an electron transporter, oligo(thiophene)s,

thienylenevinylenes, dithienothiophenes, etc. have been investigated. There are rather small variations in acceptor moieties. So far, carboxylic acid, cyanoacrylic acid, phosphoric acid, and rhodanine-3-acetic acid derivatives have been reported as an acceptor moiety, as well as an anchoring group for the attachment of the dye molecule to a TiO_2 surface. Other than hydrophilic materials such as carboxylic acid, phosphorous acid, and cyanoacrylic acid derivatives, pyridine derivatives also have been reported as an electron-withdrawing anchoring group in DSSCs. Pyridine moieties were confirmed to coordinate with the Lewis acid sites (exposed Ti^{n+}) of a TiO_2 surface to efficiently facilitate electron injection.[19]

By the continuous optimization of D-π-A dyes in their photo harvesting ability, electron communication between the dye and a TiO_2 electrode, and between the dye and an electrolyte, and the molecular orientation and arrangement of the dye on a TiO_2 surface, the DSSCs devices based on D- π-A dyes (D205) afforded 9.52% overall power conversion efficiency, comparable to those of ruthenium complexes.[20] D205 is a derivative of indole (scheme 1.2.2.2.2.2). By substituting with an electron-withdrawing moiety on the benzene ring and introducing an electron-donating moiety onto the nitrogen atom, researchers could tune the properties of indole derivatives efficiently, making them suitable dyes in DSSCs.

Besides indole derivatives, coumarin derivatives are one class of well-explored organic dyes. coumarin is a natural compound, and can be found in not less than 24 plants families such as melilot species, woodruff, orchids species, and sweet-clover (scheme 1.2.2.2.2.3). Coumarin dyes have been explored as a sensitizer in DSSCs recently.[21] Although electron injection from excited coumarin dyes to the conducting band of a TiO_2

electrode proceeds much faster than that of ruthenium complexes, DSSCs based on coumarin dyes still present lower performance than that of DSSCs based on Ru complexes.

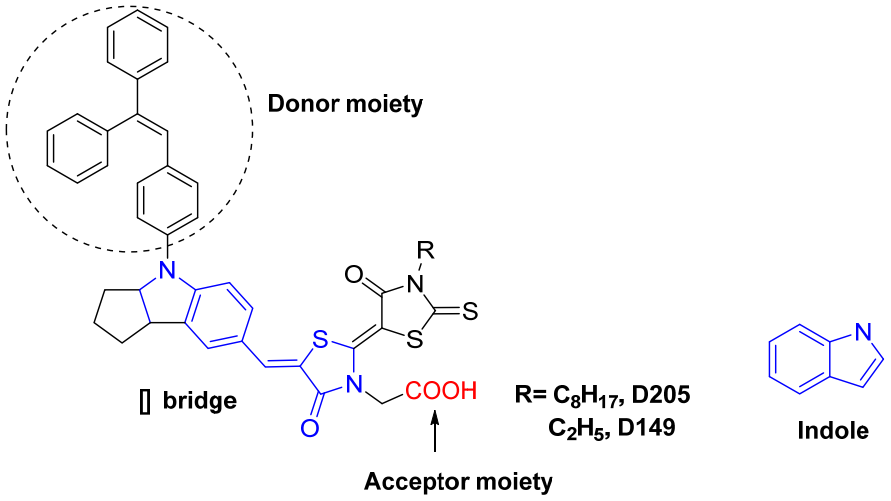

Scheme 1.2.2.2.2.2. Indole-based D- π-A dyes reported in DSSCs

Everything has pros and cons. The principal disadvantage for DSSCs based on organic dyes is their poor long-term stability and durability, comparing with those of inorganic dyes. Therefore, it will be urgent to enhance the stability of organic dye-based DSSCs. In addition, the shorter emission lifetime of excited-state organic dyes than that of Ru complexes impairs electron injection from the LUMO of the dyes to the conducting band of a TiO_2 electrode. Lastly, organic dyes commonly have a sharp absorption band in a visible region, which reduce the light harvesting performance of the dyes in whole solar radiation.

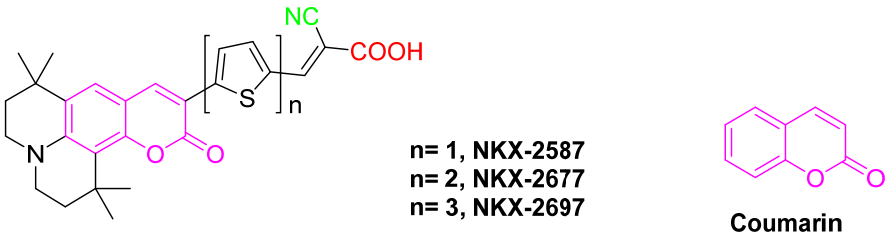

Scheme 1.2.2.2.2.3. Coumarin derivative dyes utilized in DSSCs

1.2.2.2.2 Research progress of natural dye in DSSCs

Because DSSCs mimic the primary process of photosynthesis in nature, it is quite fascinating to use natural dyes as a sensitizer in DSSCs. Owing to their low-cost, non-toxicity, complete biodegradability, and availability in a large scale, natural dyes have been actively studied and tested as sensitizers in DSSCs.[22] These dyes, found in flowers, leaves, fruits, can be collected by a simple extraction procedure.

Scheme 1.2.2.2.2.1. Natural dyes utilized in DSSC as a sensitizer

Several natural dyes have been used to prepare DSSC devices recently. However, DSSCs based on natural dyes output less than 1% overall photon-to-electricity conversion efficiency so far, due to poor grafting between natural dyes and a TiO_2 electrode, and poor photo harvesting ability for whole sun radiation. Until now, DSSCs based on natural dyes are exclusively used for an education purpose.

1.3. Introduction to the applications of conducting polymers in dye-sensitized solar cells

As the polymeric materials for third generation solar cells – "metallic polymers" defined by Heeger in his lecture at the Nobel Symposium in 2000, conducting polymers, especially poly(thiophene) derivatives, have been attracting much interest.[23] Because they are soluble in conventional solvents such as chloroform and even fusible at a relatively low temperature, and have high thermal and environmental stabilities both in neutral and doped states, poly(3-alkylthiophene)s have been found to be applicable to DSSCs research and other research fields.

1.3.1. Application of conducting polymers as an electron transfer mediator in DSSCs

An electron transfer mediator, also referred as a hole transport material, presented in an electrolyte plays a very critical role in the stable operation of DSSCs.[24] It transports electrons between the photoanode and photocathode of DSSCs by a redox reaction. After electron injection from excited dyes to the conducting band of a semiconductor (typically TiO_2, ZnO), the reduction of oxidized dyes to their neutral state by an electron donor in an electrolyte (reduced species of a redox couple such as I^-) should occur as fast as possible to continue the cycle of photon-to-electricity conversion. So there are some requirements for the choice of an electron transfer mediator: (1) To regenerate dyes, the redox potential of an electron transfer mediator should be more negative than that of a ground-state dye. (2) To prolong the long-term lifetime of DSSCs, an electron transfer mediator should be fully reversible. (3) To maximize the energy utilization in DSSCs, an electron transfer mediator should not present a significant absorption in the work wavelength range of a dye. (4) To revive an electron transfer mediator itself after the

reduction of a dye, a high diffusion coefficient of electron transfer materials is expected. So far, I^{3-}/I^{-} is the most successful redox couple as an electron transfer mediator. This can be attributed to the ultra-rapid regeneration (on a nanosecond scale) of a neutral dye from the corresponding oxidized dye by the action of I^{-}. Different from the mono-electronic reduction of an oxidized dye by I^{-}, in the reduction of I^{3-}, multistep reactions are involved. In other respects, the I^{3-}/I^{-} couple is also imperfect: (1) I_2, produced from I^{3-} under equilibrium, is volatile, destroying the long-term stability of the resulting DSSCs. (2) To catalyze the reduction of I^{3-} to I^{-}, Pt is needed. This results in the rise of cell cost. (3) Darkly colored I^{3-} limits the improvement of DSSCs in light harvesting performance. (4) The corrosivity of the I^{3-}/I^{-} couple towards metals leads to serious inhibition for the industrialization of DSSCs. Recently, two classes of materials, coordination complexes and conducting polymers, have been reported to replace the I^{3-}/I^{-} couple as an electron transfer mediator in DSSCs.

Scheme 1.3.1.1. Chemical structures of cobalt (II)/(III) and copper (I)/(II) electron transfer mediators used in DSSCs

Ease in tuning properties of coordination complexes by the rational choice of a metal center and a ligand may provide necessary flexibility to construct an electron transfer mediator capable of meeting the kinetic requirements. To date, octahedral cobalt(II)[25] and

tetrahedral copper(I) complexes[26] are the most successful alternatives to the conventional I^{3-}/I^- couple (scheme 1.3.1.1).

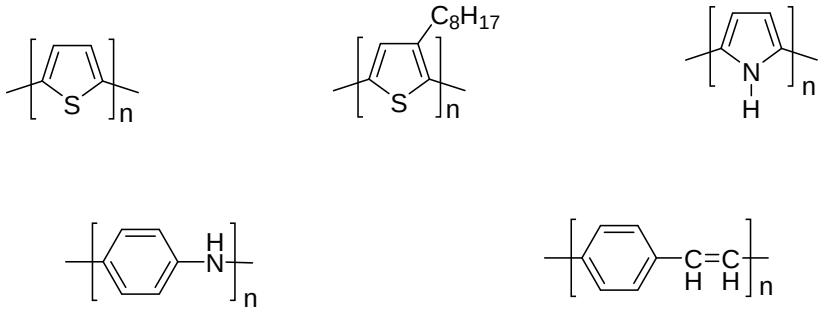

Scheme 1.3.1.2. Common conducting polymers that present hole transport properties

Intrinsically, conducting polymers are well-known as hole transport materials in various research fields (scheme 1.3.1.2). Conducting poly(thiophene)s and poly(pyrrole)s are interesting candidates to replace the conventional I^{3-}/I^- redox couple to construct solar cells, in the light of their optimal electro-conductivity, thermal stability, and low-cost.[27] To some extent, electron transfer between a TiO_2 electrode and hole transfer materials determines the power conversion performance of DSSCs. Some critical requirements for conducting polymers that act as hole transport materials are listed below: (1) Conducting polymers should be wettable to penetrate into the pores of TiO_2, ensuring good contact with adsorbed dyes. (2) Polymers should be transparent enough in the absorption range of dyes. (3) The hole mobility of polymers should be high enough to prevent electron recombination. Poly(thiophene) derivatives have been applied as hole transfer materials successfully in DSSCs. Although the resulting solar devices have presented Jsc (short circuit current density) of 450 μA cm^{-2} and Voc (open circuit voltage) of 0.6 v at 80 mW cm^{-2}, the overall performance of these DSSCs are quite inferior.[28] Some researchers have also reported the preparation and application of conducting poly(pyrrole)s as an electron

transfer mediator in DSSCs. With an oxidized ruthenium complex dye produced by electron injection on TiO_2 as an initiator, poly(ethylenedioxypyrrole)s (PEDOP) have been in situ prepared and grafted onto a ruthenium complex sensitized TiO_2 electrode surface chemically.[29] The chemical bonding may be beneficial for electron coupling and electron transfer rates between dye molecules and electron transfer mediators. However, solar cells, assembled by the method mentioned above, just afford about 2.6% overall photon-to-electricity conversion efficiency, due to serious electron recombination, dark current and incomplete filling of TiO_2 pores by the hole transport polymers. In fact, undoped conducting polymers such as poly(thiophene)s and poly(phenylene-vinylene)s have excellent light harvesting capability.[30] Thus, it is attractive to incorporate the function of sensitizers and hole transport materials into conducting polymers in DSSCs.

1.3.2. Application of conducting polymers in counter electrodes of DSSCs

A counter electrode, which collects electrons from an external circuit and regenerate a redox couple by catalyzing the reduction of I^{3-} to I^-, is one of critical component of DSSCs. Usually, a Pt film is vapor-deposited onto a conducting glass to construct a platinized counter electrode of DSSCs. Owing to its high conductivity and catalytic activity for the reduction of I^{3-} to I^-, the platinized counter electrode has been extensively studied in DSSCs.[31] However, platinum is too expensive to apply in a large scale in DSSCs. It is desirable to develop more economical alternatives to replace a Pt film. Recently, carbon-based materials, including carbon black, carbon nanotube, graphite, and mesoporous carbon, have been proposed as an alternative to Pt in DSSCs.[32] In comparison to Pt, carbon-based materials have poor catalytic activity towards a I^{3-}

reduction reaction in DSSCs. In addition, the mechanical instability of carbon-based materials on a conducting glass substrate is still in concerned.

Conducting polymers and conducting polymer/Pt composites are promising to replace Pt and carbon-based materials to form a counter electrode of DSSCs, in view of their excellence in conductivity and catalytic activity for the reduction of I^{3-} to I^-.

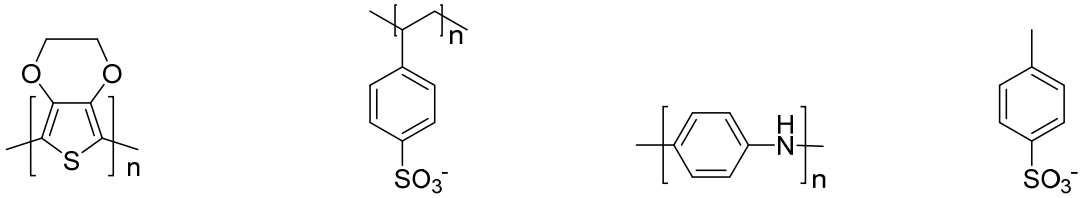

PEDOT PSS PANI TSO

Scheme 1.3.2.1. Chemical structures of PEDOT, PSS, PANI and TSO

Poly(3,4-ethylenedioxylthiophene) (PEDOT) and poly(aniline) (PANI) have found applications as the alternatives of Pt in DSSCs (scheme 1.3.2.1). In 1998, Johas *et al* have reported the application of PEDOT as a counter electrode in DSSCs.[33] They found that PEDOT, prepared by electropolymerization, showed optimal conductivity, transparency, and stability. PEDOT-poly(styrenesulfonic acid) (PSS) paste also have been prepared and applied in DSSCs as a counter electrode.[34] The introduction of PSS into a PEDOT main chain can improve the solubility and electrical conductivity of PEDOT. Hayase *et al* utilized PEDOT-PSS as a counter electrode in DSSCs, discovering that PEDOT-PSS performed better than Pt in an ionic liquid electrolyte. Generally, 1% to 5% iron impurity in PEDOT-TSO, prepared by a chemical oxidation method, leads to the loss of power conversion efficiency of DSSCs.[35] So, it is necessary to explore novel methods to prepare PEDOT-TSO without iron impurity. PANI also have been explored as a counter electrode. By a SEM analysis, the mesoporous structure of PANI has been found, which is

preferable for catalytic activity.[34] By a lot of optimizations, DSSCs based on a PANI counter electrode output the overall photo-to-electricity conversion efficiency of up to 7.15%.[36] Up to now, the stability of these DSSCs based on a conducting polymer counter electrode is still unknown.

1.4 Statement on the problems of dye, electrolyte and counter electrode in dye-sensitized solar cells

Electron-responsive materials are attracting a lot of attention from the viewpoint of their importance in fundamental research and practical applications. As excellent electron-responsive materials, ruthenium poly(bipyridine) complexes and poly(3-alkylthiophene)s have been investigated and applied in dye-sensitized solar cells (DSSCs) in the past two decades. Because of their premium photophysical and photochemical properties, ruthenium poly(bipyridine) complexes have been extensively explored as sensitizers in DSSCs. In most cases, ruthenium complex dyes were immobilized onto a semiconductor surface (typically TiO_2) by using a functional group in the complexes, such as carboxyl, phosphono, and thio groups, to construct the photoanodes of DSSCs. Up to now, Ru complexes without these functional groups cannot be candidates in DSSC research due to impossibility of immobilization; this drawback has limited the development of effective photosensitizers. On the other hand, poly(3-alkylthiophene)s have been used as an feasible alternative of a Pt film in the photocathodes of DSSCs to assist electron exchange between an electrolyte and the photocathode. For the large-scale application of poly(3-alkylthiophene)s in DSSCs and other research fields, it is essential that the polymerization of 3-alkylthiophenes proceeds with a simple route and in high yield. To date, the $FeCl_3$ oxidative method is the most popular in the synthesis of poly(3-

alkylthiophene)s. Unfortunately, detailed knowledge on their polymerization mechanism is still unavailable.

1.5 Objective of the project

In the light of these drawbacks pointed out above, the author initiated his effort to develop a new method for immobilizing a ruthenium complex with vinyl groups onto a TiO_2 electrode surface and to measure the incident photon-to-current conversion efficiency of a DSSC device fabricated with the resulting TiO_2 electrode. Moreover, the author made his effort to carry out detailed investigation on the mechanism for the polymerization of 3-alkylthiophenes.

1.6 references to chapter 1

1. Clifford, J. N.; Planells, M.; Palomares, E., *J. Mater. Chem*. **2012**, *22*, 24195-24201.
2. Nogueira, A. F.; Longo, C.; De Paoli, M. A., *Coord. Chem. Rev.* **2004**, *248*, 1455-1468.
3. http://rredc.nrel.gov/solar/spectra/am 1.5
4. Zhang, S.; Yang, X.; Numata, Y.; Han, L., *Energy Environ. Sci*., **2013**, *6*, 1443-1464.

   Hagfeldt, A.; Boschloo, G.; Sun, L.; Kloo, L.; Pettersson, H., *Chem. Rev.* **2010**, *110*, 6595-6663.
5. Tributsch, H., *Photochem. Photobiol*. **1972**, *16*, 261-269.

6. Tsubomura, H.; Matsumura, M.; Nomura, Y.; Amamiya, T., *Nature*, **1976**, *261*, 402-403.
7. O'Regan, B.; Gratzel, M., *Nature*, **1991**, *353*, 737-740.
8. Burschka, J.; Pellet, N.; Moon, S.-J.; Humphry-Baker, R.; Gao, P.; Nazeeruddin, M. K.; Gratzel, M., *Nature,* **2013**, *499*, 316-319.
9. Mobius, K., *Chem. Soc. Rev*. **2000**, *29*, 129-139.
10. Zervaki, G. E.; Roy, M. S.; Panda, M. K.; Angaridis, P. A.; Chrissos, E.; Sharma, G. D.; Coutsolelos, A. G., *Inorg. Chem*, **2013**, In press.
11. Kinoshita, T.; Dy, J. T.; Uchida, S.; Kubo, T.; Segawa, H., *Nat Photon,* **2013**, *7*, 535-539.
12. Bozic-Weber, B.; Constable, E. C.; Figgemeier, E.; Housecroft, C. E.; Kylberg, W., *Energy Environ.* Sci, **2009**, *2*, 299-305.
13. M. Ryan.; *Platinum Metals Rev*., **2009**, *53*,216-218.
14. Lingamallu, G.; Ravi-Kumar, K.; *Curr. Sci*, **2013**, *104*, 847-855.
15. Lu, J.; Xu, X.; Li, Z.; Cao, K.; Cui, J.; Zhang, Y.; Shen, Y.; Li, Y.; Zhu, J.; Dai, S.; Chen, W.; Cheng, Y.; Wang, M., *Chem. Asian J*, **2013**, *8*, 956-962.
16. Kay, A.; Graetzel, M., *J. Phys. Chem*, **1993**, 97, 6272-6277.
17. Ozawa, H.; Shimizu, R.; Arakawa, H., *RSC Adv*, **2012**, *2*, 3198-3200.
18. Mishra, A.; Fischer, M. K. R.; Bäuerle, P., *Angew. Chem. Int. Ed*, **2009**, 48, 2474-2499.
19. Ooyama, Y.; Ohshita, J.; Harima, Y., *Chem. Lett*. **2012**, *41*, 1384-1396.
20. Ito, S.; Miura, H.; Uchida, S.; Takata, M.; Sumioka, K.; Liska, P.; Comte, P.; Pechy, P.; Gratzel, M., *Chem. Commun*, **2008**, *41*, 5194-5196.

21. Hara, K.; Sato, T.; Katoh, R.; Furube, A.; Ohga, Y.; Shinpo, A.; Suga, S.; Sayama, K.; Sugihara, H.; Arakawa, H., *J. Phys. Chem. B*, **2002**, *107*, 597-606.

Hara, K.; Wang, Z.-S.; Sato, T.; Furube, A.; Katoh, R.; Sugihara, H.; Dan-oh, Y.; Kasada, C.; Shinpo, A.; Suga, S., *J. Phys. Chem. B*, **2005**, *109*, 15476-15482.

22. Chang, H.; Wu, H. M.; Chen, T. L.; Huang, K. D.; Jwo, C. S.; Lo, Y. J., *J. Alloys Compd*. **2010**, *495*, 606-610.

Sofyan A. Taya.; Taher M. El-Agez.; Hatem S. El-Ghamri.; Monzir S. Abdel-Latif., *I.J.M.S.A*, **2013**, *2*, 37-42.

23. Heeger, A. J., *Rev. Mod. Phys*, **2001**, *73*, 681-700.

24. Cazzanti, S.; Caramori, S.; Argazzi, R.; Elliott, C. M.; Bignozzi, C. A., *J. Am. Chem. Soc*. **2006**, *128*, 9996-9997.

25. Yum, J.-H.; Baranoff, E.; Kessler, F.; Moehl, T.; Ahmad, S.; Bessho, T.; Marchioro, A.; Ghadiri, E.; Moser, J.-E.; Yi, C.; Nazeeruddin, M. K.; Grätzel, M., *Nat Commun*, **2012**, *3*, 631-639.

26. Michele, B.; Stefano,C.; Silvia, C.; Luca, M.; Roberto, A.; Carlo A, B., *Int. J. Photoenergy*. **2007**, *2007*, 1-10.

27. Nogueira, A. F.; Longo, C.; De Paoli, M. A., *Coord. Chem. Rev*. **2004**, *248*, 1455-1468.

28. Gebeyehu, D.; Brabec, C. J.; Sariciftci, N. S.; Vangeneugden, D.; Kiebooms, R.; Vanderzande, D.; Kienberger, F.; Schindler, H., *Synth. Met*. **2001**, *125*, 279-287.

29. Caramori, S.; Cazzanti, S.; Marchini, L.; Argazzi, R.; Bignozzi, C. A.; Martineau, D.; Gros, P. C.; Beley, M., *Inorg. Chim. Acta,* **2008**, *361*, 627-634.

30. Spiekermann, S.; Smestad, G.; Kowalik, J.; Tolbert, L. M.; Grätzel, M., *Synth. Met.* **2001**, *121*, 1603-1604.

31. Zhang, B.; Wang, D.; Hou, Y.; Yang, S.; Yang, X. H.; Zhong, J. H.; Liu, J.; Wang, H. F.; Hu, P.; Zhao, H. J.; Yang, H. G., *Sci. Rep*. **2013**, 3, 1-7.

32. Cha, S. I.; Koo, B. K.; Seo, S. H.; Lee, D. Y., *J. Mater. Chem*. **2010**, *20*, 659-662.

Lee, B.; Buchholz, D. B.; Chang, R. P. H., *Energy Environ. Sci*, **2012**, 5, 6941-6952.

Gao, Y.; Chu, L.; Wu, M.; Wang, L.; Guo, W.; Ma, T., *J. Photochem. Photobiol., A*, **2012**, *245*, 66-71.

33. Groenendaal, L.; Jonas, F.; Freitag, D.; Pielartzik, H.; Reynolds, J. R., *Adv. Mater.* **2000**, *12*, 481-494.

34. Yohannes, T.; Inganäs, O., *Sol. Energy Mater. Sol. Cells*, **1998**, *51*, 193-202.

35. Gregg, B. A.; Pichot, F.; Ferrere, S.; Fields, C. L., *J. Phys. Chem. B*, **2001**, *105*, 1422-1429.

36. Li, Q.; Wu, J.; Tang, Q.; Lan, Z.; Li, P.; Lin, J.; Fan, L., *Electrochem. Commun*. **2008**, *10*, 1299-1302.

Chapter 2 General introduction to physical measurements

2.1 Cyclic voltammetry (CV)

As the most versatile electroanalytical technique, cyclic voltammetry (CV) has been becoming very popular in many research fields associated with the study on redox states.[1,2] CV is carried out by cycling the working potential between an initial potential and a switching potential. CV can be used to generate electroactive species in a positive potential scan and to monitor its fate with a reverse scan. If the electroactive species in the vicinity of an electrode are depleted by some components in the medium, CV will be irreversible.

In general, CV is performed in one compartment equipped with a working electrode, a counter electrode, and a reference electrode soaking in a solution containing a support electrolyte, under argon atmosphere. To avoid possible decomposition, the peak potential is usually lower than 2 v.

2.2 Gel permeation chromatography (GPC)

Gel permeation chromatography, also so-called size exclusion chromatography (SEC), is a well-defined technology to ascertain the relative molecular weight and molecular weight distribution of polymer samples.[3,4] Generally, a GPC system consists of a pump to push an eluent passing through the instrument, an injection port to charge a sample mixture onto a column, a column filled up with porous beads to separate the mixture, two detectors (UV detector and refractive index detectors) to monitor components eluted out

from the column, and a personal computer to control the instrument and to record spectra (Scheme 2.2.1).

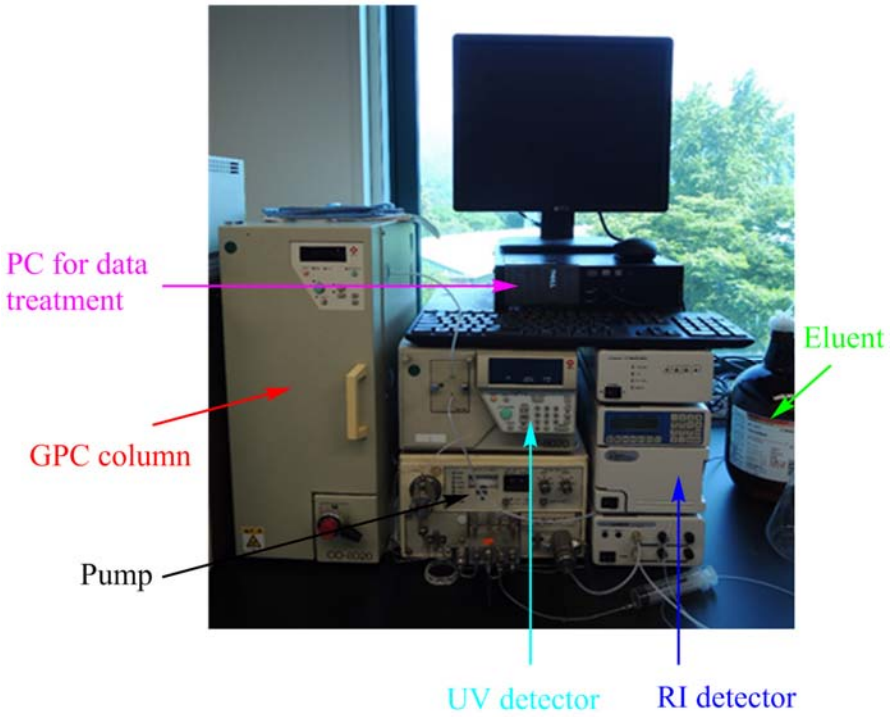

Scheme 2.2.1. GPC system

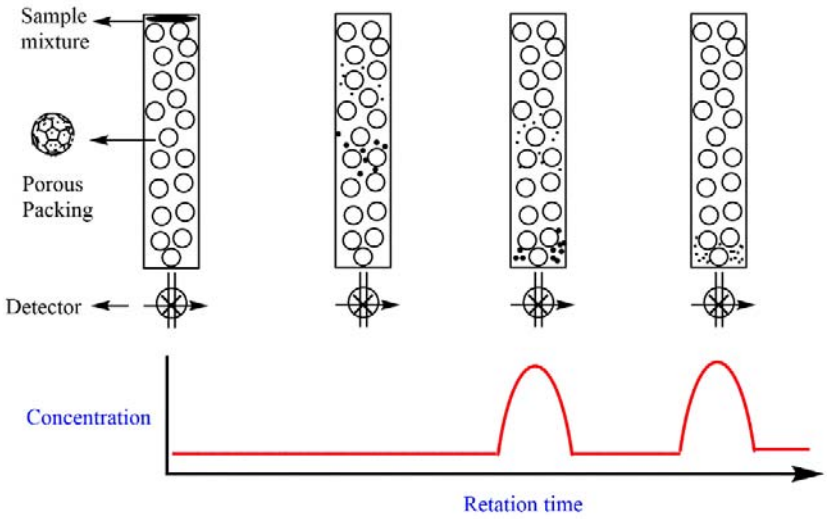

Scheme 2.2.2. Working principle of GPC

The work principle of GPC is based on the size exclusion by beads in a column.[5] Mostly, polymers, dissolved in a solvent, coils up themselves to form ball-like architectures, of which the diameters are fundamentally dependent on the molecular weights of the polymers. On the other hand, a polymer is actually a mixture of many species with a different molecular weight. Thus, when a polymer (mixture) solution travels down the column, the polymeric species with a different size pass through the porous beads with different pathways. When the sphere of a species is bigger than that of the biggest pore of the beads, the species will bypass them instantly, resulting in elution firstly. When the size of a species is smaller than that of the smallest pore of the beads, the species will enter all of the pores of the beads leading to elution lastly. A species with an intermediate size will occupy some pores of the beads (Scheme 2.2.2).

2.3 MALDI-TOF Mass

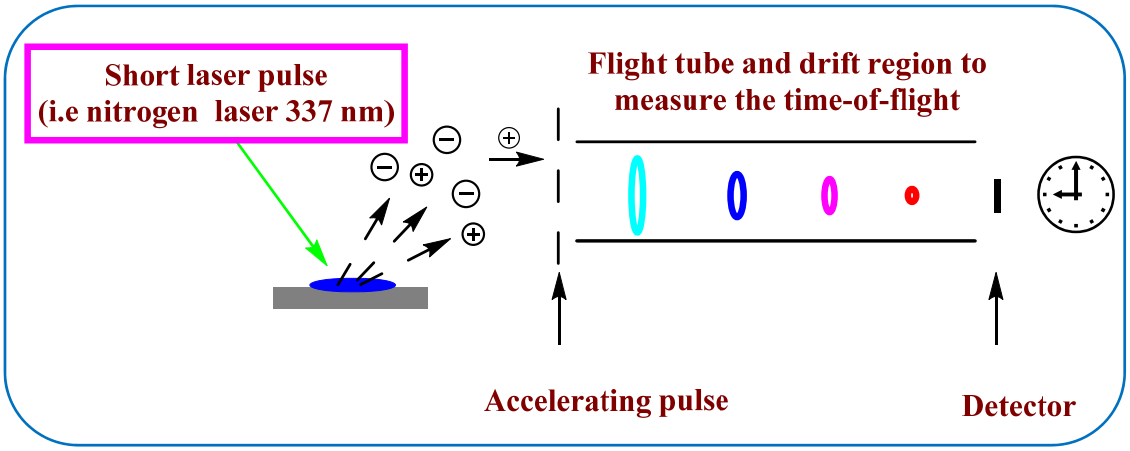

Scheme 2.3.1. Graph of MALDI-TOF MS

Matrix-assisted laser desorption/ionization time-of-flight mass (MALDI-TOF MS) is a relatively new technology to measure the molecular weight of samples including simple organic molecule, biomaterials,[6] and synthetic polymers.[7] Compared with GPC, which

just gives the relative molecular weight and molecular weight distribution of a polymer (Mn, Mw, Mz and PDT), MALDI-TOF MS has some distinguished advantages as below:

(1) The absolute molecular weights of polymers can be determined.

(2) MALDI-TOF MS has wider feasibility in the characterization of synthetic polymers. Generally, the GPC analysis of rigid-rod polymers such as tetrahydropyrene and homopolypeptides gives an overestimated molecular weight. However, MALDI-TOF MS is a viable tool to analyze these polymers.

(3) MALDI-TOF MS can provide information not only about molecular weight of a polymer, but also about the polymer structure such as the mass and composition of repeating units and end group(s).

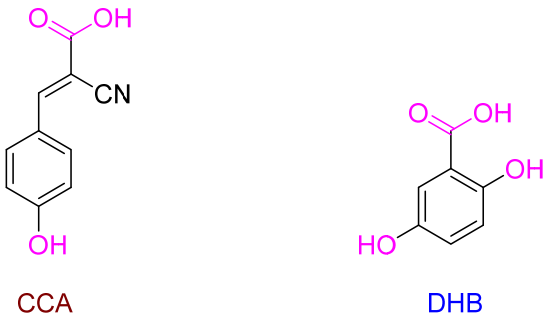

Scheme 2.3.2. Chemical structures of CCA and DHB

A matrix, which coats an analyte uniformly on a target, can promote the generation of sample ions by complex photoreactions between the excited matrix and the sample.[8] Usually organic acids such as α-cyano-4-hydroxycinnamic acid (CCA), 2,5-dihydroxybenzoic acid (DHB), which are excellent in ultraviolet-light absorption, are used as the matrix. In some cases, alkali metal salts (LiCl, NaCl, KCl) and silver salts such as silver trifluoroacetate (AgFTA) are utilized with a matrix to assist the ionization

of the analyte. In a positive mode, four type of sample ions, $[M + H]^+$, $[M - H]^+$, $[M]^+$, and $[M + Na \text{ or } Ag]^+$ are commonly observed.

2.4 References to chapter 2

1. Kissinger, P. T.; Heineman, W. R., *J. Chem. Educ*. **1983**, *60*, 702-706.
2. Queiroz, S. L.; de Araujo, M. P.; Batista, A. A.; MacFarlane, K. S.; James, B. R., *J. Chem. Educ*. **2001**, 78, 89-90.
3. He, H.; Zhong, M.; Adzima, B.; Luebke, D.; Nulwala, H.; Matyjaszewski, K., *J. Am. Chem. Soc*. **2013**, 135, 4227-4230.
4. Wang, Q.; Price, C.; Booth, C., *J. Chem. Soc., Faraday Trans*. **1992**, 88, 1437-1439.
5. Gorbunov, A. A.; Solovyova, L. Y.; Pasechnik, V. A., *J. Chromatogr. A*, **1988**, *448*, 307-332.
6. Sinz, A.; Kalkhof, S.; Ihling, C., *J. Am. Soc. Mass Spectrom*. **2005**, 16, 1921-1931.
7. Marie, A.; Fournier, F.; Tabet, J. C., *Anal. Chem*. **2000**, *72*, 5106-5114

   Liu, X. M.; Maziarz, E. P.; Heiler, D. J.; Grobe, G. L., *J. Am. Soc. Mass Spectrom*. **2003**, *14*, 195-202.
8. Hrabák, J.; Chudáčková, E.; Walková, R., *Clinical Microbiology Reviews*, **2013**, *26*, 103-114.

Chapter 3 Synthesis and Characterization of Di(isothiocyanato)bis(4-methyl-4'-vinyl-2,2'-bipyridine)Ruthenium(II)

3.1 Introduction

The design of efficient transition metal complexes is the critical first step in the development of novel materials for molecular-based devices, energy storage and conversion, and catalysts. Two requirements for the design of functionalized transition metal complexes lay in suitable bridging ligands and tuned transition metal ions. Bridging ligands, which capture a transition metal ion stably and efficiently, are viewed as the most important element in successful design. Bidentate ligands, 2,2'-bipyridine and its derivatives, which have ease in chemical modification and excellence in coordination ability towards central metal ions, are the most widely explored.[1] In recent years, these ligands have been successfully incorporated into a huge diversity of supramolecular inorganic architectures.[2] These investigations have expanded and enriched our knowledge on the structure-properties relationship of functionalized transition metal complexes. Other than outstanding coordination capability and facile structural modification, a large portion of recent interests in these ligands arises from their very fascinating photophysical and photochemical properties, exhibited by their transition-metal complexes (ruthenium, osmium, iridium, cobalt, *etc.*), especially those of ruthenium. Poly(bipyridine)ruthenium(II) complexes have been exploited in nanocrystalline TiO_2-based solar cells (dye-sensitized solar cells, DSSCs), biosensors, and molecular wires.[3,4,5] Ruthenium, one element of platinum group metals comprising of ruthenium, rhodium,

palladium, osmium, iridium, and platinum, has some intriguing properties such as high catalytic activity, advantageous resistance to chemical reactions, and electrical stability.

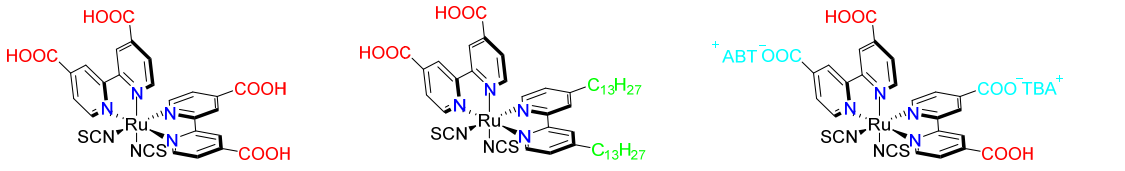

N3 N621 N719(TBA= tetrabutylammonium)

Scheme 3.1.1. Typical poly(bipyridine)ruthenium sensitizers adopted in DSSCs

The choice of ruthenium metal has a number of important reasons. 1) Because of the octahedral complex geometry, specific ligands can be introduced in a controlled manner. 2) The photophysical, photochemical, and electrochemical properties of these complexes can be fine-tuned in an expectable way. 3) Ruthenium possesses stable and accessible oxidation states ranging from I to III. Grätzel and coworkers have developed efficient photo-electrochemical cells by the use of sensitizers consisting of transition-metal complexes deposited on nanocrystalline titanium dioxide electrodes (Scheme 3.1.1).[6] Dye-sensitized solar cells (DSSCs) have attracted widespread academic and industrial interests for the conversion of sunlight into electricity, because of their low cost in manufacturing, flexibility, and high-energy conversion efficiency. The additional advantages of these cells are the availability and nontoxicity of the main component, that is, titanium dioxide, which is used in paints, cosmetics, healthcare products, and so on. The highest efficiency has been reported for nanocrystalline titanium dioxide coated with bis(4,4'-dicarboxyl-2,2'-bipyridine)dithiocyanatoruthenium(II) (N3 dye); the overall solar to electrical energy-conversion efficiency of up to 10% have been reported.[7] The high efficiency of this cell is owing to the significant overlap of the absorption spectrum with the emission spectrum, rapid charge separation, and efficient dye regeneration.

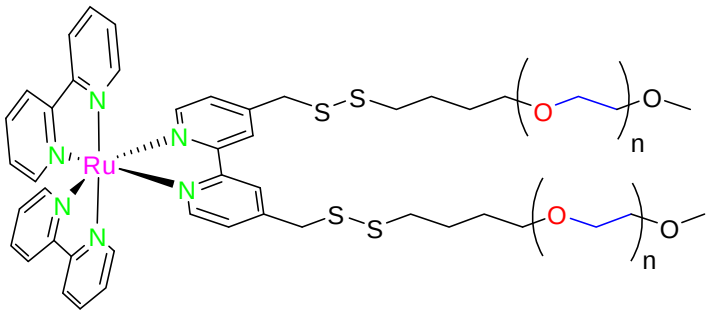

Scheme 3.1.2. Polymeric poly(bipyridine)ruthenium complex reported by Flore[8]

~~Interesting~~ Developments interesting from the viewpoint of polymer chemistry have been reported in polymeric metal complexes (PMCs).[9] PMCs are a class of materials, which feature with site-isolated metal centers in well-defined synthetic macromolecules. Transition metals, especially d^8 transition metal ions, have been widely utilized in PMCs, taking their premium properties into consideration (Scheme 3.1.2). The advantage of polymeric ruthenium complexes over single- or di-nuclear ruthenium complexes is the relatively stronger interaction between the ruthenium moieties in the polymeric ruthenium complexes, giving much better photo-physical properties such as an improved photo-absorption ability (extended responsive wavelength and increased molar extinction coefficient), the prolonged life time of the excited state of the ruthenium complexes, and processability. Polymeric poly(bipyridine)ruthenium(II) complexes also have been reported to undergo energy transfer and light-harvesting as an antenna. The preparation of polymeric ruthenium complexes has been investigated during the last two decades. Sumi *et al* have reported the synthesis and photochemical and photo-physical properties of a tris(bipyridine)ruthenium(II)-containing polymer in 1984 (Scheme 3.1.3).[10] They have demonstrated that a polymer with a ruthenium complex, modified with 4-methyl-4'-vinyl-2,2'-bipyridine and 2,2'-bipyridine as ligands, can act as an efficient sensitizer in

photochemical reactions. A similar ruthenium complex also has been prepared by an electrochemical polymerization method, especially by applying cyclic voltammetry.[11]

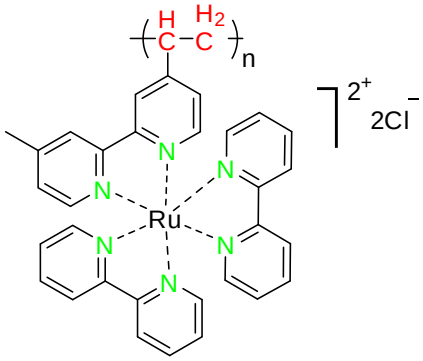

Scheme 3.1.3. Chemical structure of polymeric $(bpy)_2$(4-methyl-4'-vinyl-2,2'-bipyridine)ruthenium(II)

Another approach has been described by Schultze *et al*.; they have reported a copolymer consisting of functionalized coumarin and 2,2'-bipyridine moieties, onto which a bipyridine ruthenium complex was coordinated.[12] Furthermore, the copolymerization of a tris(vinyl-substituted bipyridine)ruthenium complex with a functionalized coumarin monomer has been described. These new polymer systems display very high energy transfer efficiencies and are therefore potentially interesting for applications in photovoltaics devices,[13] luminescence-based sensors for gases such as oxygen,[14] and PH,[15] temperature[16] and metal ion sensors.[17]

The polymeric films of electro-polymeriable ruthenium complexes with vinyl-substituted bipyridines, which are excellent in photo-absorption, can be deposited on a TiO_2 electrode surface to act as a dye in a DSSC device. To the best of our knowledge, there are only a few reports on the application of the polymeric film of ruthenium complexes in DSSCs as a sensitizer. So, the author embarked his efforts on the synthesis of a

ruthenium complex with a vinyl-substituted bipyridine, and on the exploration of the utility of its polymeric film in DSSCs as a sensitizer.

3.2 Experiment Section

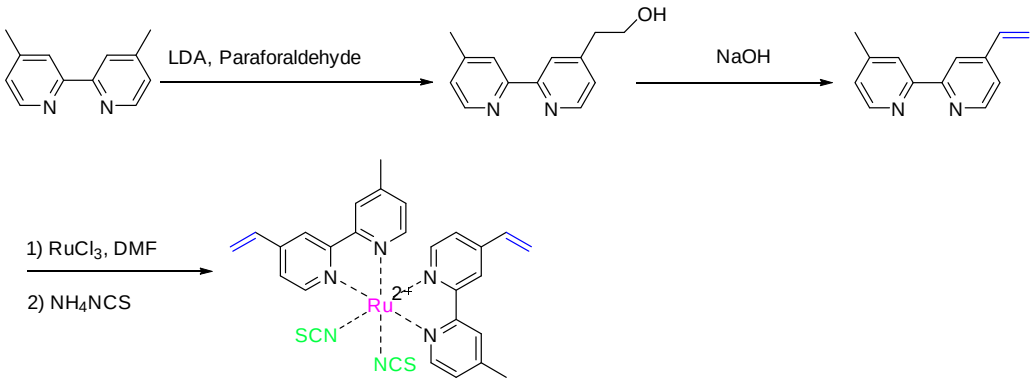

$NCS_2(mvbpy)_2Ru(II)$ (m = methyl, v = vinyl, bpy = bipyridine)

Scheme 3.2.1. Synthesis of $NCS_2(mvbpy)_2Ru(II)$

All reactions were performed under argon atmosphere. All reagents were purchased from Wako Pure Chemical Industries Ltd except for NH_4SCN and sodium 4-vinylbenzenesulfonate, which were purchased from Nacac Tesque, Inc. The reagents were used as received, except for 4,4'-dimethylbipyridine which was recrystallized from methanol prior to use. Dry tetrahydrofuran (THF) was distilled over Na and benzophenone. 2-(4'-Methyl-(2,2'-bipyridin-4-yl)ethanol[18,19] and 4-methyl-4'-vinyl-2,2'-bipyridine were synthesized according to the procedures in the literatures with some modifications. Di(isothiocyanato)bis(4-methyl-4'-vinyl-2,2'-bipyridine)ruthenium(II) was prepared by a method similar to that of bis(2,2'-bipyridine)di(isothiocyanato)ruthenium(II).[20] Chromatographic purifications were carried

out on neutral alumina gel, and thin-layer chromatography (TLC) was performed on Merck alumina gel F_{254}, otherwise noted.

2-(4'-Methyl-2,2'-bipyridin-4-yl)ethanol

4,4'-Dimethyl-2,2'-bipyridine (6.8 g, 36.91 mmol) was dissolved in dry THF (400 mL), and the solution was cooled down to 0 ℃ by ice/water. Lithium diisopropylamide (20.3 mL, 2 M in THF, 40.60 mmol) was added dropwise to the solution. The purple solution was stirred at 0 ℃ for 2 h, and then a large excess amount of dry paraformaldehyde (5.5 g, 183 mmol as formaldehyde) was added all at once to the solution. The mixture was allowed to warm to room temperature and stir for 24 h. The color of the solution gradually turned from purple to light yellow. The reaction was quenched with distilled water (200 mL), and the solution was concentrated to about 50 mL under reduced pressure. The residue was extracted with dichloromethane (3×50 mL), and the extracts were concentrated under reduced pressure. The yellow viscous liquid remained was purified on neutral alumina gel column chromatography; after washing off unreacted 4,4'-dimethyl-2,2'-bipyridine with hexane/ethyl acetate (19:1, v/v), the yellow-colored fraction eluted with hexane/ethyl acetate (2:1, v/v) was collected. The fraction was condensed under reduced pressure to afford a light-yellow oil (2.27 g, 29%).

^{1}H NMR (400 MHz, $CDCl_3$) δ (ppm): 8.56 (d, 1H, J = 5.0 Hz, PyH), 8.50 (d, 1H, J = 5.0 Hz, PyH), 8.25 (s, 1H, PyH), 8.20 (s, 1H, PyH), 7.18 (dd, 1H, J_1 = 5.0 Hz, J_2 = 1.6 Hz, PyH), 7.13 (d, 1H, J = 4.9 Hz, PyH), 3.96 (t, 2H, J = 6.5 Hz, CH_2CH_2OH), 2.95 (t, 2H, J = 6.4 Hz, CH_2CH_2OH), 2.44 (s, 3H, CH_3).

4-Methyl-4'-vinyl-2,2'-bipyridine (mvbpy)

2-(4'-Methyl-2,2'-bipyridin-4-yl)ethanol (2.27 g, 10.7 mmol), 4-*tert*-butylpyrocatechol (0.1 g, 0.6 mmol) and finely powdered sodium hydroxide (4.28 g, 107 mmol) were successively added to benzene (5 mL). The blue mixture was then heated at 115 °C for 2 h under reduced pressure (<1 mmHg). The crude product was purified on silica gel column chromatography by using dichloromethane/methanol (100:1, v/v) as an eluent. The corresponding fractions were concentrated under reduced pressure to yield a colorless solid (1.0 g, 48%).

^{1}H NMR (400 MHz, $CDCl_3$) δ (ppm): 8.62 (d, 1H, J = 5.0 Hz, PyH), 8.55 (d, 1H, J = 5.0 Hz, PyH), 8.40 (s, 1H, PyH), 8.24 (s, 1H, PyH), 7.30 (dd, 1H, J_1 = 5.1 Hz, J_2 = 1.8 Hz, PyH), 7.14 (d, 1H, J = 4.9 Hz, PyH), 6.80–6.73 (dd, 1H, J_1 = 14.32 Hz, J_2 = 6.8 Hz, PyH), 6.09 (d, 1H, J =17.7 Hz, CH=CH_2), 5.53 (d, 1H, J = 10.9 Hz, CH=CH_2), 2.44 (s, 3H, CH_3).

Di(isothiocyanato)bis(4-methyl-4'-vinyl-2,2'-bipyridine)ruthenium(II) [$(NCS)_2(mvbpy)_2Ru(II)$]

4-Methyl-4'-vinyl-2,2'-bipyridine (0.400 g, 2.04 mmol) was added to a solution of $RuCl_3$ (0.211 g, 1.01 mmol) in DMF (20 mL). After the mixture was refluxed for 8 h in the dark, NH_4NCS (6.367 g, 8.36 mmol) was added all at once at room temperature. The solution was refluxed again for 12 h and cooled down to room temperature. Upon adding methanol (200 mL) to the reaction mixture, a purple red powder was deposited, which was collected by filtration over a G4 glass filter. The purple powder was thoroughly washed with cold methanol (20 mL) and diethyl ether (15 mL), and dried for 12 h under reduced pressure to give $(NCS)_2(mvbpy)_2Ru(II)$ (0.24 g, 38%).

ν_{max} (KBr, cm^{-1}): 2104 (CN, s), 1400 (CH_3, s).

MALDI-TOF MS: calculated for $C_{28}H_{24}N_6S_2Ru$: $[M]^+$ = 610.0548; found 610.0517 with isotope peaks in agreement with those obtained by a calculation.

3.3 Results and discussion

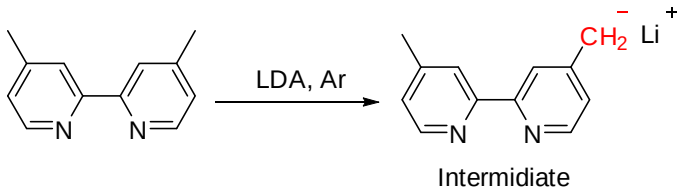

Scheme 3.3.1. Lithiation of 4,4'-dimethylbipyridine

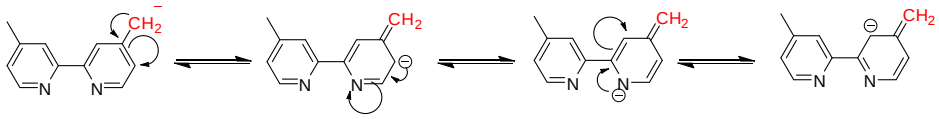

Scheme 3.3.2. Electron-donating effect of the carbanion on the bipyridine ring

Upon adding lithium diisopropylamide (LDA) into a THF solution of 4,4'-dimethylbipyridine, a color change from colorless to dark purple was observed. This phenomenon can be explained as follows: A strong base (pKa=40), LDA, eliminated the methyl proton of 4,4'-dimethylbipyridine to form a carbanion (Scheme 3.3.1). The carbanion can push electrons onto the bipyridine ring by a resonance effect to make the energy gap between the π and π* smaller. As a result, the maximal absorption wavelength (λ_{max}) was shifted to a visible region (scheme 3.3.2).

The apparatus for the synthesis of 4-methyl-4'-vinyl-2,2'-bipyridine is demonstrated in Scheme 3.3.3.

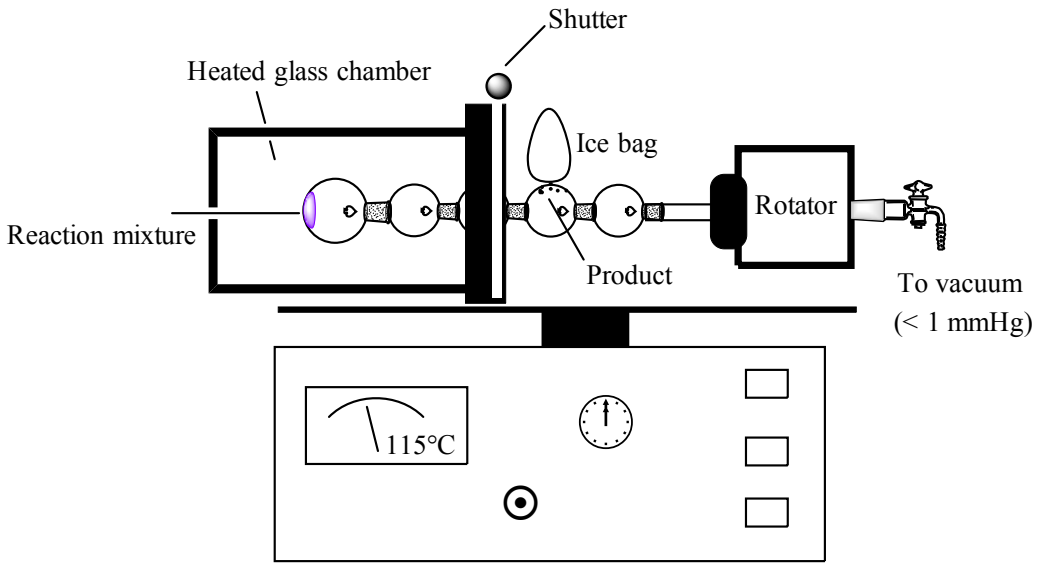

Scheme 3.3.3. Preparation of 4-methyl-4'-vinyl-2,2'-bipyridine in a kugelrohr bulb-to-bulb distillation apparatus

When finely powdered sodium hydroxide particles were poured into a solution of 2-(4'-methyl-2,2'-bipyridin-4-yl)ethanol and 4-tert-butylcatechol (TBC) in benzene, the solution turned from colorless to blue. This color change may arise from the deprotonation of TBC by NaOH. The phenoxide ions of the deprotonated catechol donate electrons to the aromatic ring with the help of a resonance effect. As a result, the electron density of the aromatic ring was increased, and the maximal ultraviolet-visible absorption (λ_{max}) was moved toward a longer wavelength (Scheme 3.3.4).

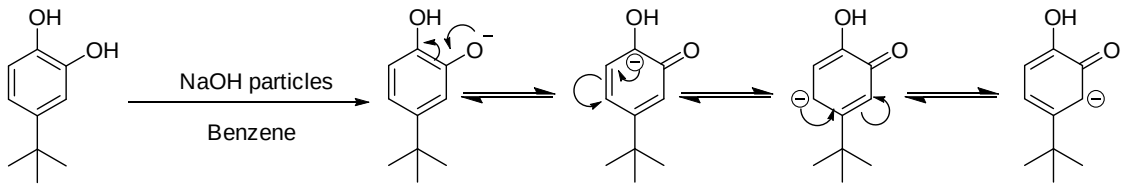

Scheme 3.3.4. Deprotonation of 4-tert-butylcatechol by NaOH powder

Because sodium hydroxide (NaOH) has no solubility in benzene, the dehydration reaction of 2-(4'-methyl-2,2'-bipyridin-4-yl)ethanol just occurred on the surface of NaOH particles. To improve the yield of the dehydration, it was necessary to make very fine NaOH particles by grinding NaOH pellets in a mortar with a pestle. Alternatively, the use of methanol or ethanol as the solvent in place of benzene also worked well. In light of the serious damage of benzene on researchers' health (long-term exposure to benzene causes a harmful effect on bone marrows and red blood cells), the alcohols are more favorable.

By dehydration, 4-methyl-4'-vinyl-2,2'-bipyridine was synthesized successfully. As we know, most of organic compounds with vinyl group(s) easily polymerize via a radical initiated polymerization mechanism, when exposed to light or heat, etc. (scheme 3.3.5).[21]

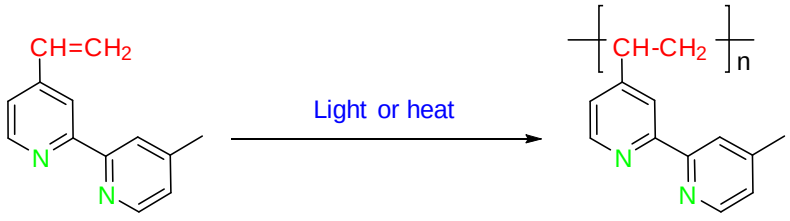

Scheme 3.3.5. Possible polymerization of 4-methyl-4'-vinyl-2,2'-bipyridine

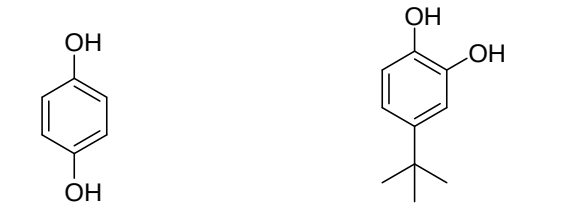

hydroquinone 4-tert-butylcatechol(TBC)

Scheme 3.3.6. Chemical structures of hydroquinone and 4-tert-butylcatechol

To overcome this drawback, an inhibitor like hydroquinone[22] and 4-tert-butylcatechol[23] (Scheme 3.3.6), which can eliminate radical species and prevent a polymerization process,

is usually added into a reaction system. On the other hand, removal of desired organic compounds with vinyl group(s) from a high-temperature reaction system is also critical. With these two factors in mind, Kugelrohr sublimation is a wise choice for the preparation of 4-methyl-4'-vinyl-2,2'-bipyridine.

Because our target ruthenium complex, di(isothiocyanato)bis(4-methyl-4'-vinyl-2,2'-bipyridine)ruthenium(II), suffered from solubility in common organic solvents (only soluble in DMF and DMSO), it was extremely hard to purify by recrystallization, chromatography separation and other purification techniques. The solubility problem may be attributed to the intimate intermolecular π-π stacking, which is a common phenomenon for ruthenium complexes.[24] Up to now, the author just could determine the structure of this compound with IR, MALDI-TOF MS; NMR and X-ray crystallography were unsuccessful. To get full characterization of the ruthenium complex, it is urgent to explore a successful purification method.

3.4 References to Chapter 3

1. (a) Ramos Sende, J. A.; Arana, C. R.; Hernandez, L.; Potts, K. T.; Keshevarz-K, M.; Abruna, H. D., *Inorg. Chem*, **1995**, *34*, 3339-3348.

   (b) Grätzel, M., *Inorg. Chem*. **2005**, *44*, 6841-6851.

   (c) Yu, Z.; Najafabadi, H. M.; Xu, Y.; Nonomura, K.; Sun, L.; Kloo, L., *Dalton Trans*. **2011**, *40*, 8361-8366.

2. (a) Robson, K. C. D.; Koivisto, B. D.; Yella, A.; Sporinova, B.; Nazeeruddin, M. K.; Baumgartner, T.; Grätzel, M.; Berlinguette, C. P., *Inorg. Chem*. **2011**, *50*, 5494-5508.

(b) Nazeeruddin, M. K.; Kay, A.; Rodicio, I.; Humphry-Baker, R.; Mueller, E.; Liska, P.; Vlachopoulos, N.; Graetzel, M., *J. Am. Chem. Soc.* **1993**, *115*, 6382-6390.

(c) Hanson, K.; Brennaman, M. K.; Luo, H.; Glasson, C. R.; Concepcion, J. J.; Song, W.; Meyer, T. J., *ACS Appl. Mater. Interfaces.* **2012**, *4*, 1462-1469.

(d) Abruna, H. D.; Bard, A. J., *J. Am. Chem. Soc.* **1981**, *103*, 6898-6901.

3. (a) Tetreault, N.; Gratzel, M., *Energy Environ. Sci*, **2012**, *5*, 8506-8516.

(b) Willinger, K.; Fischer, K.; Kisselev, R.; Thelakkat, M., *J. Mater. Chem.* **2009**, *19*, 5364-5376.

4. Yang, H.; Wang, Y.; Qi, H.; Gao, Q.; Zhang, C., *Biosensors and Bioelectronics.* **2012**, *35*, 376-381.

5. (a) Insung Choi.; Junghyun Lee.; Gunho Jo.; Kyoungja Seo.; Nak-Jin Choi.; Takhee Lee.; Hyoyoung Lee.; *Appl. Phys. Express.* **2009**, *2*, 015001-3.

(b) VI Grosshenny.; A. Harriman.; M. Hissler.; R. Ziessel.; *Platinum Metals Rev.* **1996**, *40*, 26-35.

6. Gräzel, M.; *Nature*, **2001**, *414*, 338-344.

7. O'Regan, B.; Gratzel, M., *Nature*, **1991**, *353*, 737-740.

8. Fiore, G. L.; Goguen, B. N.; Klinkenberg, J. L.; Payne, S. J.; Demas, J. N.; Fraser, C. L., *Inorg. Chem*. 2008, 47, 6532-6540.

9. (a) Rivas, B. L.; Seguel, G. V.; Ancatripai, C., *Polym. Bull.* **2000**, *44*, 445-452.

(b) Raja Shunmugam.; Gregory N. Tew.; *Macromol. Rapid Commun.* **2008**, *29*, 1355–1362.

10. Sumi, K., Furue, M. and Nozakura, S.-I., *J. Polym. Sci. Polym. Chem. Ed.*, **1985**, *23*, 3059–3067.

11. (a) Aranyos, V.; Hjelm, J.; Hagfeldt, A.; Grennberg, H. *Dalton Trans*, **2001**, *8*, 1319-1325.

(b) Elliott, C. M.; Baldy, C. J.; Nuwaysir, L. M.; Wilkins, C. L., *Inorg. Chem.* **1990**, *29*, 389-392.

12. Schultze, X.; Serin, J.; Adronov, A.; Fre´chet, *Chem Commun.* **2001**, *13*,1160-1161.

13. Marin, V.; Holder.; E. and Schubert.; *J. Polym. Sci. A Polym. Chem.*, **2004**, *42*, 374–385.

14. Payne, S. J.; Fiore, G. L.; Fraser, C. L.; Demas, J. N., *Anal. Chem.* **2010**, *82*, 917-921.

15. (a) Clarke Y.; Xu W.; Demas JN.; DeGraff BA.; *Anal. Chem.* **2000**, *75*, 3468-3475.

(b) Jason M. Price.; Wenying Xu.; J. N. Demas.;B. A. DeGraff.; *Anal. Chem.* **1998**, *70*, 265-270.

16. Baleizão, C.; Nagl, S.; Schäferling, M.; Berberan-Santos, M. r. N.; Wolfbeis, O. S., *Anal. Chem.* **2008**, *80*, 6449-6457.

17. (a) Heather M. Rowe, Wenying Xu, J. N. Demas, and B. A. DeGraff.; *Applied Spectroscopy*, **2002**, *56*, 167-173.

(b) Schmittel, M.; Lin, H., *J. Mater. Chem.* **2008**, *18*, 333-343.

18. Furue, M.; Yoshidzumi, T.; Kinoshita, S.; Kushida, T.; Nozakura, S.-i.; Kamachi, M., *Bull. Chem. Soc. Jpn*, **1991**, *64*, 1632-1640.

19. Terbrueggen, R. H.; Johann, T. W.; Barton, J. K., *Inorganic Chemistry*, **1998**, *37*, 6874-6883.

20. Yu, Z.; Najafabadi, H. M.; Xu, Y.; Nonomura, K.; Sun, L.; Kloo, L., *Dalton Transactions*. **2011**, *40*, 8361-8366.

21. Bengough, W. I.; Henderson, W., *Trans. Faraday Soc*., **1965**, *61*, 141-149.

22. Yassin, A. A.; Rizk, N. A.; Ghanem, N. A., *Eur. Polym. J.* **1973**, *9*, 677-685.

23. Usami Y.; Landau AB.; Fukuyama K.; Gellin GA.; *J THROMB THROMBOLYS*. **1980**, *6*, 559-567.

24. (a) Ishow, E.; Gourdon, A., *Chem. Commu.* **1998**, *17*, 1909-1910.

(b) Reger, D. L.; Derek Elgin, J.; Pellechia, P. J.; Smith, M. D.; Simpson, B. K., *Polyhedron*, **2009**, *28*, 1469-1474.

Chapter 4 Immobilization of di(isothiocyanato)bis(4-methyl-4'-vinyl-2,2'-bipyridine) Ruthenium(II) onto a TiO_2 electrode surface by a novel separated electrolysis method

4.1 Introduction

Dye-sensitized solar cells (DSSCs) have been attracting abundant attention as technically and economically credible alternatives to traditional silicon-based solar cells.[1-5] As a key component of DSSCs, photosensitizers that can absorb sunlight and inject electrons into the conducting band of a nanocrystalline semiconductor (mostly TiO_2 and ZnO) from their excited state have been mainly focused in DSSC research. To design an optimal dye for DSSC devices, there are two main requisites: (i) Dye molecules should present excellent abilities of photo-absorption (broad light absorption band combined with high molar extinction coefficient), and of transferring absorbed light energy towards a molecular component center (an antenna effect). (ii) Dye molecules should be bound to a semiconductor surface to facilitate electron injection from the dye in an excited state into the semiconductor particle. The modification of a dye is an important strategy to improve solar cell performance. Although abundant organic dyes and inorganic dyes based on transition metals such as iron(II), iridium(III) and copper(I) have been investigated in DSSC research, ruthenium-based dyes are still highlighted in dye research. Ruthenium-based photosensitizers having a general structure of $RuL_2(X)_2$, where L stands for functionalized 2,2'-bipyridine such as 4,4'-dicarboxyl-2,2'-bipyridine (Scheme 4.1.1) and

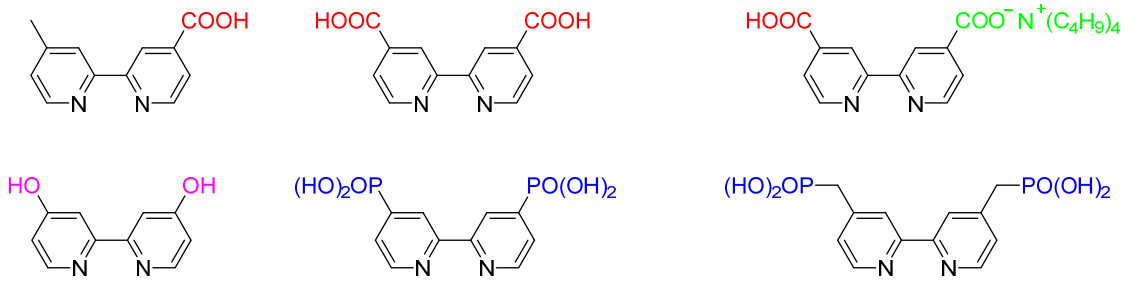

Scheme 4.1.1. Functionalized 2,2'-bipyridine ligands used in DSSCs

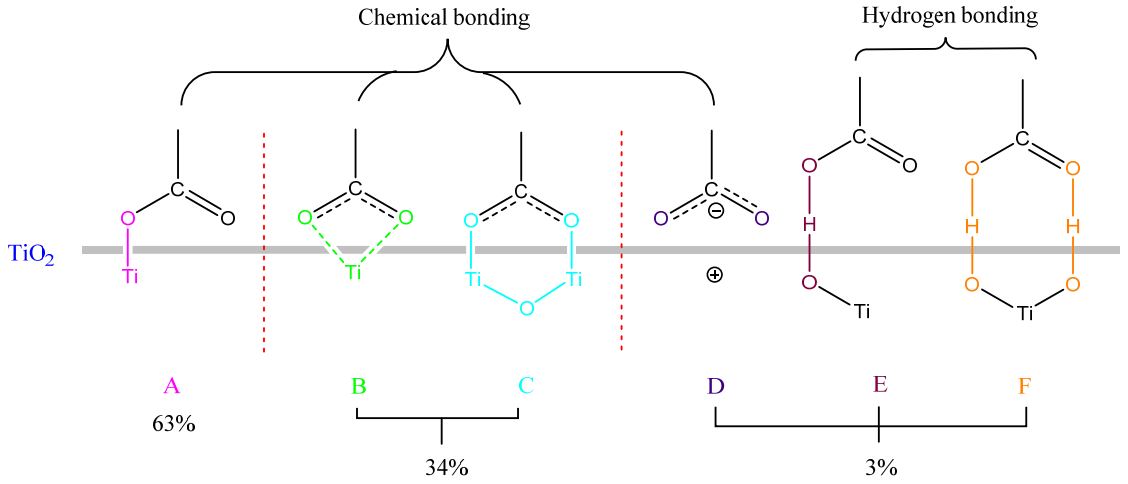

Scheme 4.1.2. Six possible graft modes of a carboxylic group on TiO_2 reported in literatures

X presents halide, cyanide, thiocyanate, thiolate, thienyl or ancillary water, have been extensively investigated as a photo absorber in DSSCs over the past two decades.[6-13] $RuL_2(NCS)_2$ (L indicates 4,4'-dicarboxyl-2,2'-bipyridine), known as N3 dye, has achieved a certified overall efficiency of more than 7%. The enhanced properties can be attributed to the improved overlap of its absorption with solar irradiation spectrum, the favorable positioning of both the ground-state and excited-state potentials of the dye relative to a redox couple in a solution and to the TiO_2 conduction band edge, and the facile interfacial electron injection dynamics relative to the back-reaction rates in the

cell.[14]

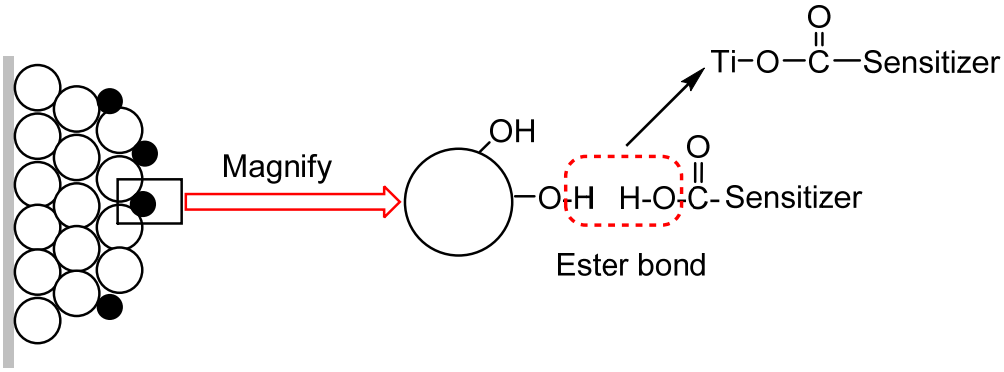

Scheme 4.1.3. Immobilization of carboxylic dyes by an esterification reaction

Dyes are commonly immobilized onto a semiconductor (typically TiO_2) surface with functional group(s), such as carboxyl, phosphono or thio group in the dyes. These special groups work as a linker between the semiconductor particles and the dye molecules, and provide an electronic coupling between the conducting band of the conductor (conductor CB) and the excited state of the dye molecules. It is well known that electron injection kinetics is affected obviously by an electronic coupling between a dye and TiO_2. The efficiency of electron injection from the excited-state (approximately LUMO) of a sensitizer to the conducting band (near to the Femi level) of a semiconductor is also highly determined by two factors; (1) an energy gap between the LUMO level of the dye and the Femi level of the semiconductor (the LUMO must be sufficiently negative with respect to the conducting band of TiO_2 to ensure electron injection effectively), (2) an electronic coupling between the LUMO of the dye and the conducting band of TiO_2 (a substantial and tight coupling improves injection efficiency).[15] By far, a carboxylic acid group is the most frequently employed for the attachment of sensitizers to a semiconductor surface. There reported six binding modes for dyes, which were grafted

onto TiO_2 with carboxylic group(s) (-COOH) (Scheme 4.1.2). These modes can be divided into two categories: chemical bonding (A, B, C, D) and hydrogen bonding (E, F). Comparing with hydrogen bonding modes, chemical bonding modes are expected to provide more robust linkages to semiconductor particle surfaces. By employing various analytical techniques including an interface-sensitive transient triplet-state probe, X-ray photoemission spectroscopy (XPS), and vibrational spectroscopy, as well as theory calculation, researchers have confirmed that among these six binding modes, mode A is predominant.[16] Moreover, some researchers have pointed out that the ester bond may be formed by an esterification reaction between the carboxyl group of dye molecules and the hydroxy group of TiO_2 particles as shown in Scheme 4.1.3.

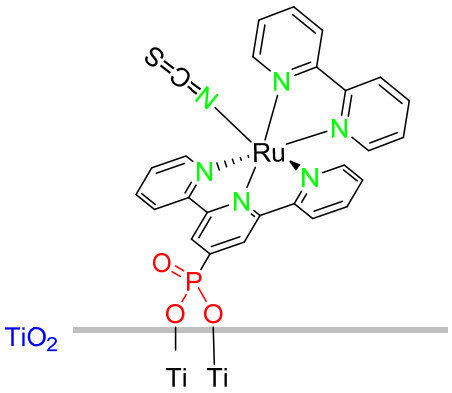

Scheme 4.1.4. Possible graft mode for phosphoric acid dyes immobilized onto a TiO_2 surface

Besides a carboxylic group, a phosphoryl group is also well-studied as a graft group in DSSC research. A phosphoryl group is known to afford stronger bonds onto a metal oxide surface than a carboxyl group.[17,18] In 2001, Gillaizeau-Gauthier *et al* reported that the adduct formation constant (K_{addut}) of a phosphoric acid-containing sensitizer formulated as $[Ru(bpy)_2(4,4'\text{-}(PO(OH_2)_2bpy))^{2+}$ is approximately one order bigger in

magnitude (K_{adduct}= (4.9 ± 0.8) ×10^5 M^{-1}) than that of the corresponding carboxylic acid analogous complex (K_{adduct} =2.2 ± 0.1) × 10^4 M^{-1}], indicating that a phosphoric acid moiety provide stronger and more stable linkages onto TiO_2 than a carboxylic acid moiety does. Here, worth to note is that the rate of electron injection from $[Ru(bpy)_2(4,4'\text{-}(PO(OH)_2)_2bpy)]^{2+}$ is just one half of that from carboxylic acid-anchored $[Ru(bpy)_2(4,4'\text{-}(COOH))_2bpy]]^{2+}$. However, owing to the higher stability of the phosphoric acid-anchored dye under actual operation conditions for DSSCs, compared with that of carboxylic acid-anchored dye, phosphoric acid-containing dyes are still expected to have a promising future in DSSC research. Unfortunately, compared with the knowledge of carboxylic acid-containing dyes, the nature of phosphoric acid-containing dyes immobilized onto a TiO_2 surface is less understood.[19] Some researchers have claimed that phosphoric acid-containing dyes may be grafted onto a titanium oxide surface with ester bonds, similar to graft mode A for carboxylic acid-type dyes mentioned above (Scheme 4.1.4).[20]

Up to now, Ru(II) complexes without these functional groups cannot be candidates in DSSC research due to the impossibility of immobilization; this drawback has limited the development of effective photosensitizers.

IPCE (incident photon-to-current conversion efficiency), sometimes referred to also as external quantum efficiency (QCE), is one of key parameters to evaluate the performance of DSSC devices.[21,22] IPCE corresponds to the number of electrons measured as photocurrent in an external circuit divided by monochromatic photon flux that strikes a cell. This key parameter can be given by the following equation.

$$IPCE(\lambda) = LHE(\lambda)\phi_{inj}\eta_{col} \qquad \textbf{Equation 4.1.1}$$

$$LHE = 1 - T = 1 - 10^{-A} \qquad \textbf{Equation 4.1.2}$$

In Equation 4.1.1, LHE (λ) indicates the light-harvesting efficiency for the photons of wavelength λ, ϕ_{inj} is the quantum yield for electron injection from an excited sensitizer to the conduction band of a semiconductor, and η_{coll} is the efficiency of electron collection at the back contact of a transparent conducting oxide (TCO).

IPCE also can be represented by the following equation:

$$IPCE(\%) = 1240(ev \cdot nm)\frac{J_{SC}(\mu Acm^{-2})}{\lambda(nm) \times \Phi(\mu Wcm^{-2})} \times 100 \qquad \textbf{Equation 4.1.3}$$

Where J_{SC} is the short-circuit photocurrent density for monochromatic irradiation, λ is the wavelength of monochromatic irradiation, and Φ is the monochromatic light intensity.

Among solar cells developed so far, that fabricated with the N3 dye (cis-(dcbpy)$_2$(NCS)$_2$ruthenium(II): dcbpy = 4,4'-dicarboxyl-2,2'-bipyridine) shows IPCE of about 80% in a visible light region. The N3 dye responds to a light from 400 nm to 800 nm with high extinction coefficient. In the view of the loss of light due to substrate absorption and light reflection, IPCE value of more than 90% is attained.

Electropolymerization, which can deposit conductive polymers on electrodes effectively, has been applied in the fabrication of counter electrodes of DSSCs.[23,24,25] A counter electrode is one of indispensable components in DSSCs. In general, a Pt film was deposited onto conducting substrates to construct counter electrodes, which assist an electron transfer between a counter electrode and an electrolyte solution with an excellent electrocatalytic activity for the I^{3-}/I^{-} redox couple. However, Pt as a noble metal is too

expensive to be used in a large scale in DSSCs. Only limited success has been reported for the replacement of Pt with carbon materials as cathode materials, due to their poor electrocatalytic ability in the reduction of I^{3-} to I^-.[26] Conducting polymers, especially poly(3-alkylthiophene), are promising alternatives to Pt and carbon materials as coating materials of counter electrodes, because of their excellence in low cost, high conductivity, and high catalytic activity for the regeneration of I^- from I^{3-}. [27, 28]

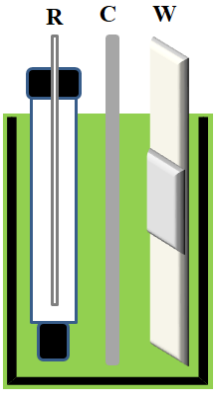

Scheme 4.1.5. Electropolymerization performed in a three-electrode cell (R: reference electrode; C: counter electrode; W: working electrode)

In general, electropolymerization is performed in one chamber equipped with a working electrode (Pt, TiO_2, or carbon electrode), a counter electrode (Pt wire) and a reference electrode commonly referred to a Ag/AgCl electrode (saturated calomel electrode (SCE), normal calomel electrode (NCE) etc.). Working potentials applied are undoubtedly less than the decomposition potentials of materials (commonly < 2 V). Upon the progress of electrode scanning, polymers were substantially generated and deposited onto an electrode surface. To some extent, the increase in scanning times results in the increase of the quantity of the polymer formed. Although polymers, especially conducting polymers, deposited on conducting substrates by electropolymerization, have been used as potential

alternatives to Pt- and carbon materials-coated counter electrodes in DSSCs, there is no report on the application of these polymers, deposited on semiconductor electrodes by electropolymerization, as dyes in DSSC research, primarily attributable to their ease of peeling off from the electrode surface.

To overcome these drawbacks in dye design, the author concentrated his efforts to the explorations of a new, electrochemically induced film formation method, which can immobilize di(isothiocyanato)bis(4-methyl-4'-vinyl-2,2'-bipyridine)ruthenium(II), and of a novel type of dye-sensitized solar cells with sufficient IPCE.

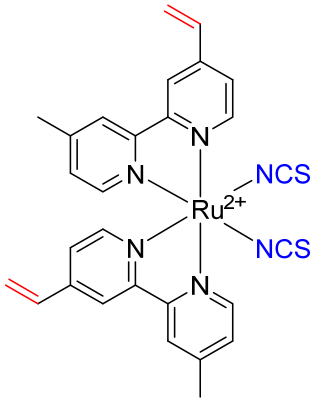

Scheme 4.1.6. Depositable ruthenium complex by a separated electrolysis method

4.2 Preparation of a TiO_2 electrode

Commercial conducting glasses, covered with fluorine-doped tin oxide (FTO, 7 Ω cm^{-2}), were employed as substrates for the fabrication of DSSCs. FTO glasses were firstly cleaned with a detergent, followed by rinsing twice with deionized water, flushed with acetone, and finally dried in air. The TiO_2 electrodes used for DSSCs were prepared by coating FTO glasses with single layered TiO_2 nanoparticles. The diameter of the nanoparticles was about 100 nm. The nanoparticles were spread on clean FTO glasses by

the doctor-blade method using an adhesive tape as the spacer, followed by air-drying at room temperature to obtain a transparent TiO_2 film on the glasses, and then calcined at 420 ˚C for 4 h in a muffle furnace under air (Scheme 4.2.1).

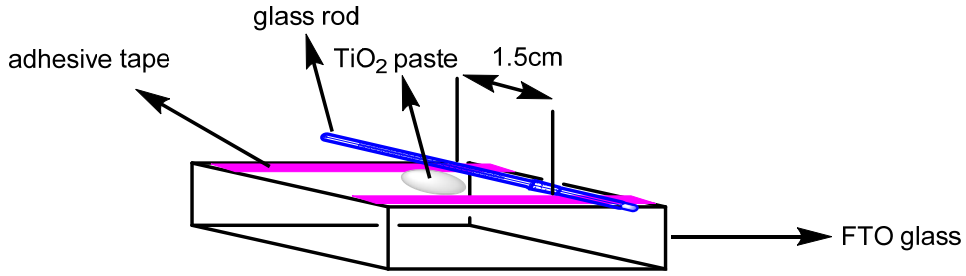

Scheme 4.2.1. Preparation of a TiO_2 film on FTO by the doctor-blade method

4.3 Immobilization

The immobilization of di(isothiocyanato)bis(4-methyl-4'-vinyl-2,2'-bipyridine)ruthenium(II) [$(NCS)_2(mvbpy)_2Ru(II)$] was performed in three steps under argon atmosphere. All solvents used were purged with argon for 15 min.

Step 1: The electrochemical treatment of an electrode was performed in a one-compartment cell according to the three-electrode method (TiO_2-coated, fluorine-doped tin oxide (TiO_2/FTO) as a working electrode, Pt wire as a counter electrode, and Ag/AgCl as a reference electrode) by using a CH instrument 701 electrochemical analyzer. These electrodes were dipped in an electrolytic solution containing 0.1 M of TBAP, and swept between 0-n-0 V (n = 2, 4, 6, 8, and 10) at a rate of 100 $mV \cdot s^{-1}$ with bubbling with argon during the electrolysis.

Step 2: After the electrolysis, the working electrode was soaked in a washing solvent for several seconds to remove adsorbents on the TiO_2/FTO surface.

Step 3: The electrode was dipped into a solution of $(NCS)_2(mvbpy)_2Ru(II)$ (1 mM) or the

Ru complex/sodium 4-vinylbenzenesulfonate (1 mM and 1 mM) in DMF (30 mL), and kept for appropriate hours in the dark under argon atmosphere. Then, the electrode was taken out, washed with acetone (30 mL), and dried at room temperature in air to afford the corresponding Ru complex film.

4.4 Measure of incident photon-to-current conversion efficiency (IPCE) of DSSCs

A fluorometer (Horiba Jobin Yvon-Spex fluorolog, Horiba Inc.) equipped with a xenon lamp (Fluorolog instruments S.A., Inc.) was used in order to generate monochromatic lights from 350 nm to 750 nm with a width of 5 nm. The photon number was counted by an optometer (Photometer S370 UDT, Gamma Scientific Inc.). The electrical quantities were measured with an electrometer (Keithley 6514 system electrometer, Keithley Instruments Inc.). The DSSC was fabricated from TiO_2/FTO coated with the Ru (II) complex film (photoanode), FTO (photocathode), and LiI/I_2 (0.5 M/1.1×10^{-3} M) in CH_3CN (mediator).

4.5 Results and discussion

4.5.1 Formation of Di(isothiocyanato)bis(4-methyl-4'-vinyl-2,2'-bipyridine)ruthenium(II) film on the surface of a titanium oxide-coated, fluorine-doped tin oxide electrode

Because the present Ru(II) complex, di(isothiocyanato)bis(4-methyl-4'-vinyl-2,2'-bipyridine)ruthenium(II) [$(NCS)_2(mvbpy)_2Ru(II)$], has no functional group reactive with TiO_2 such as carboxyl, phosphono or thio group, this complex cannot be immobilized onto the surface of TiO_2-coated, fluorine-doped tin oxide (TiO_2/FTO) electrode with conventional film formation methods that have been adopted in the

fabrication of DSSCs.

Paying his attention to the fact that the Ru complex has vinyl groups, the author at first tried to immobilize the Ru complex onto a TiO_2-coated, fluorine-doped tin oxide (TiO_2/FTO) surface by the electrolysis of a solution of the Ru complex. However, the attempt resulted in failure, most likely due to the decomposition of the Ru complex during the electrolysis. After numerous trials, the author finally found a stepwise, electrochemically induced film formation method to give a film-like deposit of the Ru complex on the surface of TiO_2/FTO. This method is composed of three steps: Step 1, the electrolysis of a TiO_2/FTO electrode only; Step 2, the washing of the electrode with a solvent; Step 3, the immobilization of the Ru complex upon immersing the washed electrode in a solution of the Ru complex. Scheme 4.5.1.1 schematically represents the immobilization procedure.

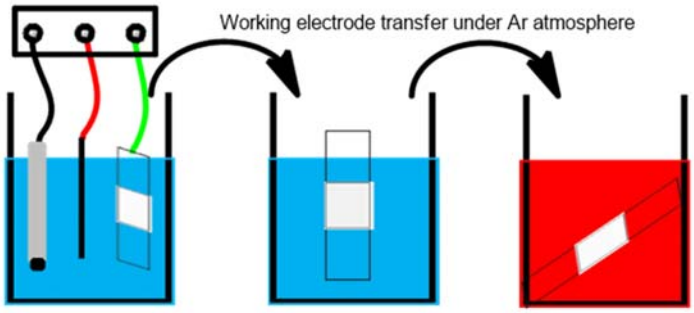

Scheme 4.5.1.1. Schematic representation of the immobilization procedure

The immobilization was found to be very sensitive to the history of the potential scanned onto a TiO_2/FTO electrode (Step 1). Figures 4.5.1.2 and 4.5.1.3 show the cyclic voltammograms during the electrolysis of the electrodes in ranges of 0-n-0 V (n = 2, 4, 6, 8, and 10) at a rate of 100 $mV \cdot s^{-1}$ and the UV-vis spectra of the resultant

electrodes. As shown in Figure 4.5.1.3, an irregular trace in the cyclic voltammograms was observed in a range of 1–3.5 V independent on the potential applied, which would correspond to irreversible oxidation. Moreover, it is clear from Figure 4.5.1.3 that the electrochemically initiated film deposition of the Ru complex took place only when the electrode, potentially swept between 0-8-0 V at a rate of 100mV·s^{-1}, was used.

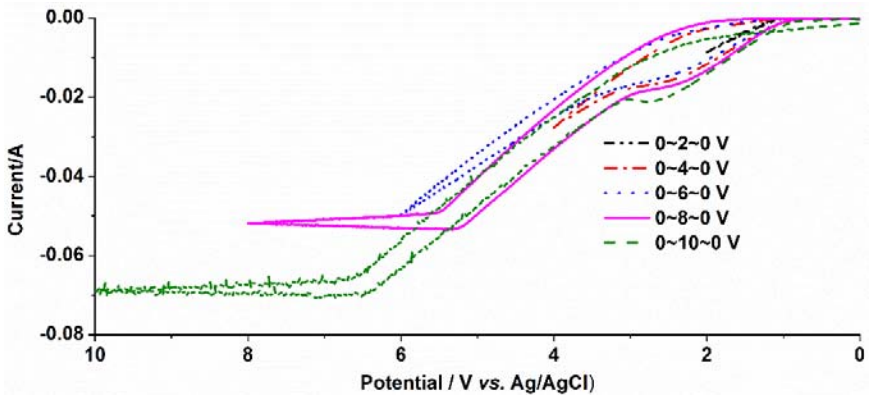

Figure 4.5.1.2. Cyclic voltammograms of TiO_2/FTO electrodes at a scan rate of 100 mV·s^{-1} in Step 1

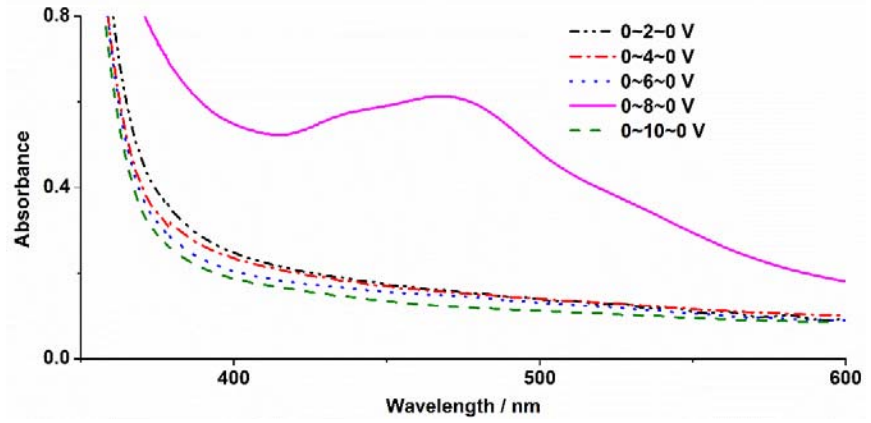

Figure 4.5.1.3. Uv-vis spectra of the resultant TiO_2/FTO electrodes

As shown in Figure 4.5.1.4, the electrode was colored after Step 3, undoubtedly indicating the film deposition. Moreover, the film deposited was insoluble in any

solvents including aprotic polar solvents such as DMF and DMSO. These changes strongly support the deposition of the Ru complex through some reaction. The electrochemically initiated film deposition method was also affected by solvents used in Steps 1-3. Different organic electrolyte solvents, namely CH_2Cl_2, CH_3CN, and CH_3OH, were applied in the electrolysis process. As shown in Figure 4.1.5.5, the solvent used in Step 1 influenced, to a considerable extent, the quantity of the Ru complex which finally immobilized on the surface of a TiO_2/FTO electrode; although dichloromethane gave a better result than acetonitrile or methanol did, it was very hard to maintain steady conditions for the electrolysis due to the evaporation of dichloromethane upon bubbling argon during the electrolysis. Then, acetonitrile, which was better than methanol, was used in Step 1.

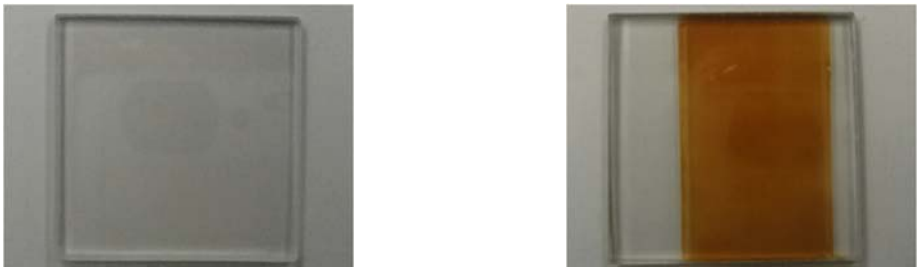

Before film deposition After film deposition

Figure 4.5.1.4. Electrodes before and after film deposition. (The electrodes were potentially swept between 0-8-0 V at a rate of 100 mV•s-1 in Step 1)

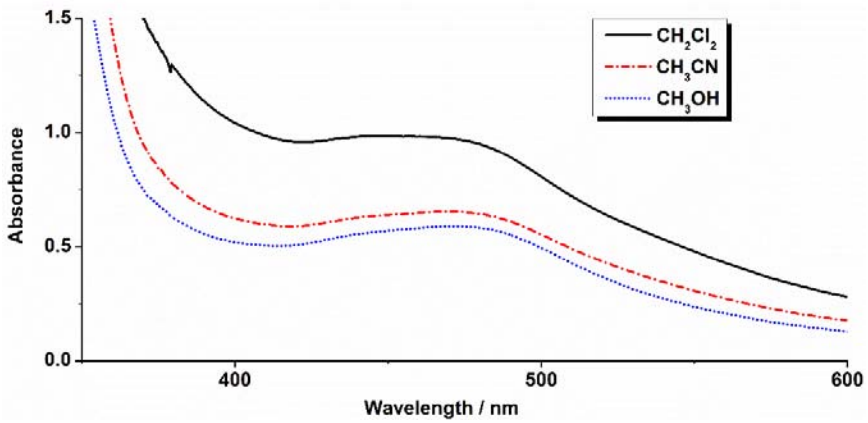

Scheme 4.1.5.5. Effect of electrolytic solvents on the formation of Ru complex deposit

The author speculated that some active species on a TiO_2 surface, originated from the decomposition of the solvent, a trace amount of an impurity, and/or the TiO_2 thin-film on the electrode itself treated at an extremely high voltage, can initiate some reactions with the ruthenium complexes to deposit the film onto the electrode surface. Some factors, like the electrolyte solvent and the working potential, influenced evidently the activity and quantity of active species, substantially the amount of the immobilized ruthenium complex.

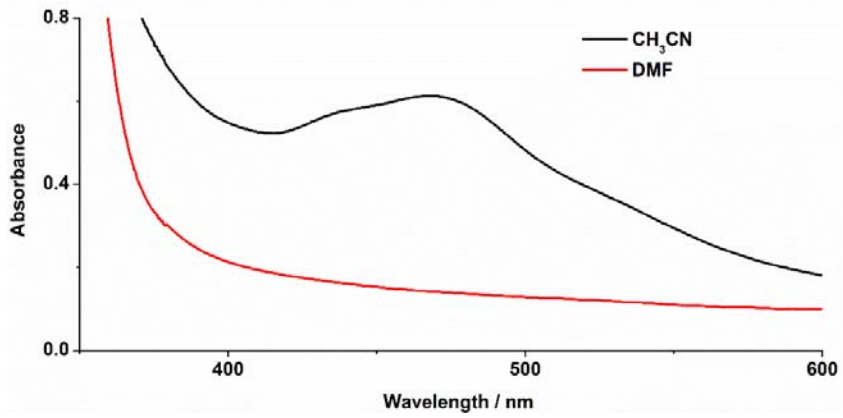

Scheme 4.1.5.6. Effect of washing solvents on the formation of the Ru complex deposit

In Step 2, no film was formed on the surface of TiO_2/FTO, when the electrode was washed with DMF instead of acetonitrile (Scheme 4.1.5.6).

Because the Ru complex is soluble only in DMF and DMSO among common organic solvents, the immobilization, Step 3, was carried out by using DMF or DMSO. To our surprise, the film was just formed on a TiO_2/FTO surface, only when DMF was used as the solvent (Scheme 4.1.5.7). Secondarily produced active species in DMF, transformed from primary active species existed on a TiO_2 surface, may also initiate some reaction and deposit the ruthenium complex film onto a TiO_2 surface

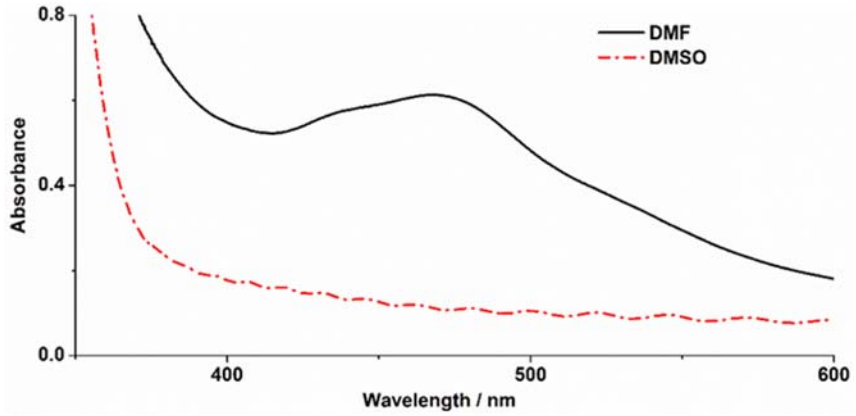

Scheme 4.1.5.7. Effect of immobilization solvents on the formation of the Ru complex deposit

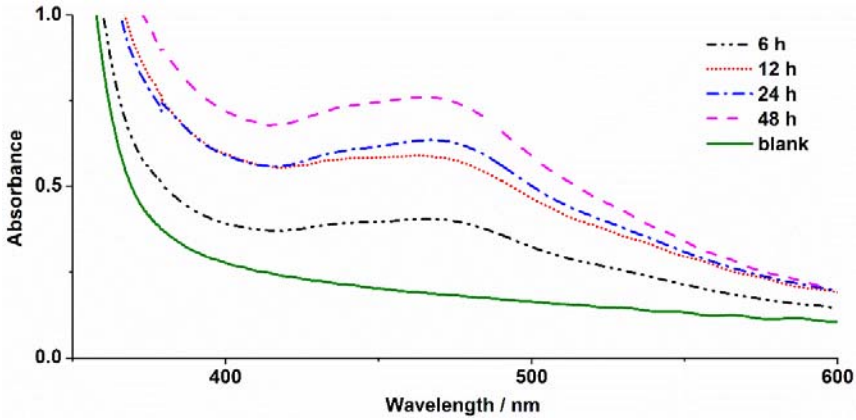

Figure 4.1.5.8. Dependency of the dipping time on the film deposition

Figure 4.1.5.8 shows the effect of the dipping time in Step 3 on the electrochemically initiated film deposition. The absorption arising from the Ru complex on the surface of TiO_2/FTO increased continuously with prolonging the dipping time. In sharp contrast, when a TiO_2/FTO electrode without any electrochemical treatment was directly dipped into a DMF solution of the Ru complex for 24 h, no absorption of the Ru complex was observed, indicating that the film was not formed at all on the TiO_2/FTO surface without electrochemical treatment.

4.5.2 Active species generated on the surface of TiO_2/FTO by the electrochemical treatment

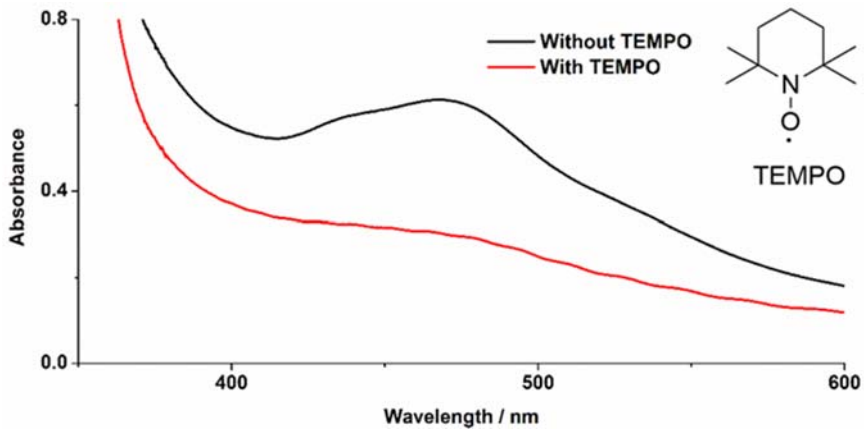

Figure 4.5.2.1. Effect of TEMPO on the deposition of the Ru complex

In order to know the active species generated on the TiO_2/FTO surface by the electrochemical treatment (Step 1), 2,2,6,6-tetramethylpiperidine-1-oxyl (TEMPO), a typical radical capture, was added to the washing solvent in Step 2 (acetonitrile); after the electrolysis in Step 1, the electrode was soaked in acetonitrile containing TEMPO (50 mM) for 2 h in Step 2. Then, the electrode was immersed into a DMF solution of the Ru

complex for 24 h (Step 3). As shown in Figure 4.5.2.1, the deposition of the Ru complex was considerably inhibited by TEMPO. On the basis of this result, the author supposed the formation of a radical species, which may react with the vinyl group in the Ru complex. The radical formation would be consistent with the fact that irreversible oxidation took place during the electrolysis of a TiO_2/FTO electrode.

To study the surface condition of TiO_2 in the electrolysis, the quartz crystal microbalance (QCM) method was used. QCM, which can monitor a small change of mass (down to 1 ng cm^{-2} per Hz), has broad applications in polymer chemistry.[30]

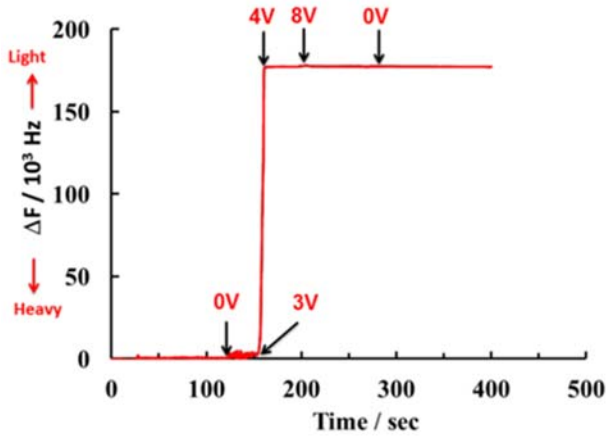

Fig 4.5.2.2. Quartz crystal microbalance (QCM) chart during the electrolysis (10^3 Hz ≈ 1 μg cm^{-2}; scan rate, 100 mV s^{-1}; solution, CH_3CN with 0.1M TBAP; F=8793775.1 Hz at ΔF=0 Hz; electrode, TiO_2 on Pt/Quartz)

As shown in Figure 4.5.2.2, from 3 V to 4 V, the mass of the electrode (TiO_2-coated Pt/quartz electrode) decreased evidently, but during 4-8-0 V, a constant mass was maintained. This phenomena would be valuable for the explaination of the formation of radicals during the electrolysis. Between 3V and 4V, some species (such as the adsorbed solvent and/or the supporting electrolyte) attached on a TiO_2 surface decomposed to give oxidized species, so that the loss of mass was observed, and the quantity of the oxided

species did not increse due to the saturation of the reaction. During 8-0 V, the current flow direction was opposite to that from 0 V to 8 V. As a result, the oxidized species may get electrons and would be reduced to neutral radicals. So, the obvious change of the mass was not observed. The real character of the active species on the TiO_2/FTO surface and the reaction mechanism for the deposition of the Ru complex are not clear at present; the author should continue to clarify them in a near future.

4.5.3 Incident photon-to-current conversion efficiency of the Ru complex film

Incident photon-to-current conversion efficiency (IPCE), which defines light to electricity conversion efficiency at a certain wavelength (λ), is one of important parameters for the evaluation of a dye-sensitized solar cell (DSSC) performance. IPCE was plotted as a function of the wavelength of incident light. Solar cells, sensitized with the present ruthenium complex film deposited by the newly developed method, were fabricated to measure their conversion efficiency of a monochromatic light to current (1.1 mM LiI/I_2 in CH_3CN as a mediator, a platinized FTO glass as a photocathode, and the present ruthenium complex film-coated TiO_2/FTO electrode as a photoanode).

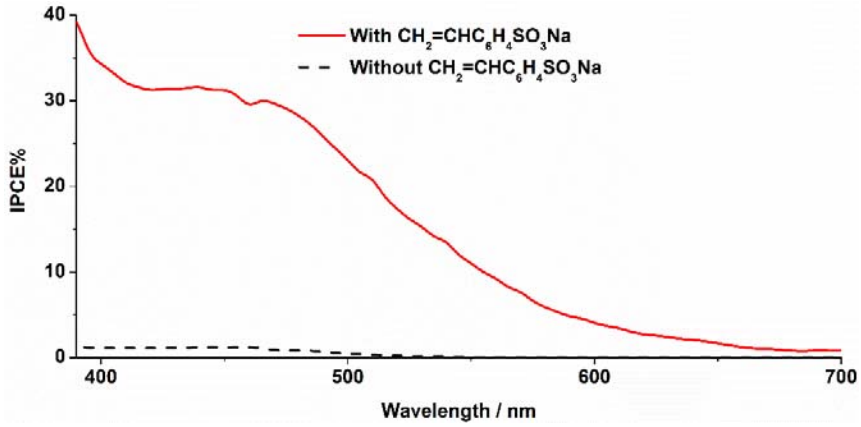

Scheme 4.5.3.1. Spectral response curve of photocurrent for a DSSC consisting of the

ruthenium complex film deposited without sodium 4-vinylbenzenesulfonate (---) and with sodium 4-vinylbenzenesulfonate (−)

The maximum IPCE of the Ru complex film, obtained by the present method, was disappointedly only 1.2% at 440 nm. The low efficiency would arise from a fast back electron transfer. In general, electron transport through films takes place in association with a successive electron transfer between neighboring redox centers.[31] After an electron transfer from an excited dye to a neighboring ground-state dye, two kinds of charged moieties, positively and negatively charged moieties, were formed. Strong electrostatic interaction between the two charged dyes can accelerate electron recombination and decrease the IPCE (Scheme 4.5.3.2).

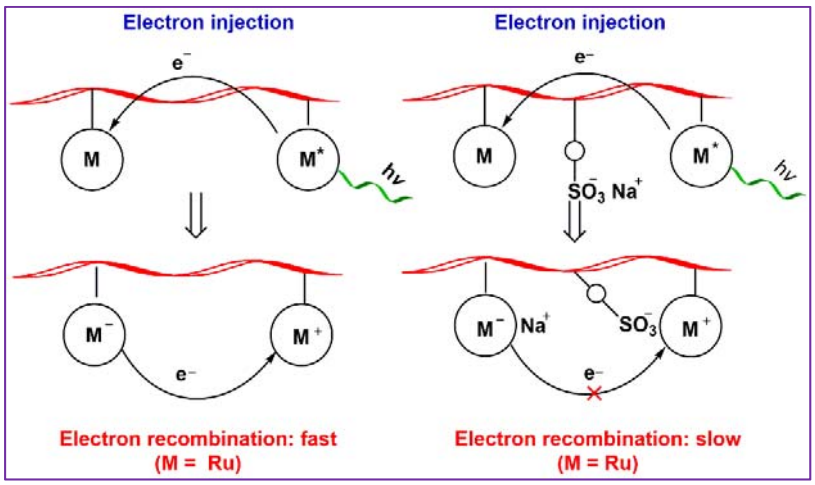

Scheme 4.5.3.2. Possible electron transfer process occurred in the film

Then, the author conversely considered that IPCE would be improved when the electron recombination between the layers is blocked. On the basis of the consideration, the author coexisted sodium 4-vinylbenzenesulfonate with the Ru complex for the immobilization (Step 3) with an expectation that the sodium cations and the sulfonate groups would partially stabilize electron-accepting dye moieties and electron-donating dye moieties,

respectively. Composite films consisting of the Ru complex and sodium 4-vinylbenzenesulfonate were similarly deposited by using a DMF solution containing the Ru complex and sodium 4-vinylbenzenesulfonate (1:1 molar ratio) in the immobilization (Step 3). Although the UV-vis absorption of the composite film decreased with the addition of sodium 4-vinylbenzenesulfonate, the IPCE of the composite film was dramatically increased to show maximum IPCE of 31.7% at 438 nm. The highly improved IPCE would arise from the electronic neutrality of the composite even after charge separation, which was secured by sodium 4-vinylbennzenesulfonate, that is, sodium cations would neutralize electron-accepting dyes while sulfonate groups would neutralize electron-donating dyes. Thus, the composite film could provide much higher IPCE by the inhibition of a back electron transfer.

Until now, the cause of the ruthenium complex deposition and the nature of the corresponding film are still unknown. So, tremendous efforts should be devoted to push this research ahead.

4.6 References to Chapter 4

1. O'Regan O'Regan, B.; Gratzel, M., *Nature*. **1991**, *353*, 737-740.
2. Robson, K. C. D.; Koivisto, B. D.; Yella, A.; Sporinova, B.; Nazeeruddin, M. K.; Baumgartner, T.; Grätzel, M.; Berlinguette, C. P., *Inorg. Chem*. **2011**, *50* (, 5494-5508.
3. Yella, A.; Lee, H.-W.; Tsao, H. N.; Yi, C.; Chandiran, A. K.; Nazeeruddin, M. K.; Diau, E. W.-G.; Yeh, C.-Y.; Zakeeruddin, S. M.; Grätzel, M., *Science*. **2011**, *334*, 629-634.

4. Argazzi, R.; Murakami Iha, N. Y.; Zabri, H.; Odobel, F.; Bignozzi, C. A., *Coord. Chem. Rev*, **2004**. *248*, 1299-1316.
5. Koumura, N.; Wang, Z.-S.; Mori, S.; Miyashita, M.; Suzuki, E.; Hara, K., *J. Am. Chem. Soc*, **2006**, *128*, 14256-14257.
6. Bae, E.; Choi, W., *J. Phys. Chem. B*. **2006**, *110*, 14792-14799.
7. Liska, P.; Vlachopoulos, N.; Nazeeruddin, M. K.; Comte, P.; Graetzel, M., *J. Am. Chem. Soc*. **1988**, *110*, 3686-3687.
8. Hanson, K.; Brennaman, M. K.; Luo, H.; Glasson, C. R.; Concepcion, J. J.; Song, W.; Meyer, T. J., *ACS Appl. Mater. Interfaces*. **2012**, *4*, 1462-1469.
9. Dittrich, T.; Neumann, B.; Tributsch, H., *J. Phys. Chem. C.* **2007**, *111*, 2265-2269.
10. Li, G.; Bomben, P. G.; Robson, K. C. D.; Gorelsky, S. I.; Berlinguette, C. P.; Shatruk, M., *Chem. Commun*. **2012**, *48*, 8790-8792.
11. Xie, P. H.; Hou, Y. J.; Wei, T. X.; Zhang, B. W.; Cao, Y.; Huang, C. H. *Inorg. Chim. Acta*. **2000**, *308*, 73-79.
12. Nazeeruddin, M. K.; Kay, A.; Rodicio, I.; Humphry-Baker, R.; Mueller, E.; Liska, P.; Vlachopoulos, N.; Graetzel, M., *J. Am. Chem. Soc*.**1993**, *115*, 6382-6390.
13. Robson, K. C. D.; Koivisto, B. D.; Yella, A.; Sporinova, B.; Nazeeruddin, M. K.; Baumgartner, T.; Grätzel, M.; Berlinguette, C. P., *Inorg. Chem*. **2011**, 50, 5494-5508
14. Kilså, K.; Mayo, E. I.; Brunschwig, B. S.; Gray, H. B.; Lewis, N. S.; Winkler, J. R., *J. Phys. Chem. B*. **2004**, *108*, 15640-15651.
15. (a) Jae-Joon Lee.; Md. Mahbubur Rahman.; Subrata Sarker.; N.C. Deb Nath.; A.J. Saleh Ahammad.; Jae Kwan Lee.; “Advances in Composite Materials for

Medicine and Nanotechnology," ed by Brahim Attaf, Intech, **2011**, 182-185.

(b) Hara, K.; Arakawa, H.; "Handbook of Photovoltaic Science and Engineering," ed by A. Luque and S. Hegedus, John Wiley & Sons, Ltd, Chichester, **2005**, 670-672.

16. (a) Finnie, K. S.; Bartlett, J. R.; Woolfrey, J. L., *Langmuir*. **1998**, *14*, 2744-2749.

(b) Weng, Y.-X.; Li, L.; Liu, Y.; Wang, L.; Yang, G.-Z., J. Phys. Chem. B. **2003**, *107*, 4356-4363.

(c) Oprea, C. I.; Panait, P.; Lungu, J.; Stamate, D.; Dumbrav; Cimpoesu, F.; *Int. J. Photoenergy*. **2013**, *2013*, 1-15.

17. Gillaizeau-Gauthier, I.; Odobel, F.; Alebbi, M.; Argazzi, R.; Costa, E.; Bignozzi, C. A.; Qu, P.; Meyer, G. J., *Inorg. Chem*. **2001**, *40*, 6073-6079.

18. Liu, Y.; Jennings, J. R.; Wang, X.; Wang, Q., *Phys. Chem. Chem. Phys.* **2013**, *15*, 6170-6174.

19. Wang, P.; Klein, C.; Moser, J.-E.; Humphry-Baker, R.; Cevey-Ha, N.-L.; Charvet, R.; Comte, P.; Zakeeruddin, S. M.; Grätzel, M., *J. Phys. Chem. B*. **2004**, *108*, 17553-17559.

20. Galoppini, E., *Coord. Chem. Rev*. **2004**, *248*, 1283-1297.

21. Grätzel, M., *Inorg. Chem*. **2005**, *44*, 6841-6851.

22. Yuancheng Qin and Qiang Peng, *Int. J. Photoenergy*, **2012**, *2012*, 1-21.

23. Xiao, Y.; Lin, J.-Y.; Tai, S.-Y.; Chou, S.-W.; Yue, G.; Wu, J., *J. Mater. Chem*. **2012**, *22*, 19919-19925.

24. Li, Z.; Ye, B.; Hu, X.; Ma, X.; Zhang, X.; Deng, Y., *Electrochem. Commun*. **2009**, *11*, 1768-1771.

25. Yuan, C.; Guo, S.; Wang, S.; Liu, L.; Chen, W.; Wang, E., *Ind. Eng. Chem. Res*. **2013**, *52*, 6694-6703.

26. Roy-Mayhew, J. D.; Bozym, D. J.; Punckt, C.; Aksay, I. A., *ACS Nano.* **2010**, *4*, 6203-6211.

27. Kwon, J.; Ganapathy, V.; Kim, Y. H.; Song, K.-D.; Park, H.-G.; Jun, Y.; Yoo, P. J.; Park, J. H., *Nanoscale*. **2013** (in press).

28. (a) He, J.; Duffy, N. W.; Pringle, J. M.; Cheng, Y.-B., *Electrochim. Acta.* **2013**, *105,* 275-281.

(b) Muto, T.; Ikegami, M.; Miyasaka, T., J. Electrochem. Soc. 2010, 157, B1195-B1200.

(c) Fan, B.; Mei, X.; Sun, K.; Ouyang, J., *Appl. Phys. Lett*. **2008**, *93*, 143103-143103-3.

(d) Tan, S.; Zhai, J.; Xue, B.; Wan, M.; Meng, Q.; Li, Y.; Jiang, L.; Zhu, D., *Langmuir*, **2004**, *20*, 2934-2937.

29. David Martineau, "Dye Solar Cells for Real- The assembly guide for making your own Solar cells", Solaronix.

30. (a) Marx, K. A., *Biomacromolecules*. **2003**, *4*, 1099-1120.

(b) Bruckenstein, S.; Shay, M., *Electrochim. Acta*. **1985**, *30*, 1295-1300.

31. Aranyos, V.; Hjelm, J.; Hagfeldt, A.; Grennberg, H., *Dalton Trans*. **2001**, 8, 1319-1325.

Chapter 5 Polymerization of 3-alkylthiophenes with transition metal complexes

5.1 Introduction

Conducting polymers, which are distinguished in high strength-to-weight ratio, toughness, ease of processing into a film and ease of the molecular design of desired properties, are extremely attractive for applications in the area of solar energy collection and storage,[1,2] advanced communication,[3] robotic system[4] and so on. The synthesis and properties of conjugated polymers have attracted significant interest over the past twenty years.[5,6] Among various conducting polymers, poly(3-alkylhiophene)s are one of the most thoroughly investigated linear conjugated polymers. Generally, the polymerization of 3-alkylthiophenes can be carried out by many different methods. These methods can be classified into three categories: (i) metal-catalyzed coupling reactions, (ii) electropolymerizations, and (iii) chemical oxidative polymerizations. Yamamoto *et al* have reported the nickel-catalyzed polycondensation of 2,5-dibromothiophene to afford 2,5-coupled polythiophene in 1980.[7] Unfortunately, the extremely poor solubility and infusibility of the unsubstituted poly(thiophene) obstructed its application. In the quest of soluble and processable poly(thiophene)s, 3-alkylthiophenes were used as the monomer. In 1985, Elsenbaumer and his co-workers synthesized a poly(3-alkylthiophene) using the nickel-catalyzed polycondensation of a 2,5-harogenated 3-alkylthiophene to obtain a 2,5-coupled poly(thiophene).[8] Electropolymerization is a widely used method for the preparation of insoluble films of poly(3-alkylthiophene)s on an electrode surface.[9] Usually, polycondensation and electropolymerization just afford poly(thiophene)s with

low molecular weight. Contrarily, the $FeCl_3$ oxidative polymerization of 3-alkylthiophenes, reported by Sugimoto *et al* in 1986, produces much higher polymers with polydispersity ranging from 1.3 to 5.[10]

Poly(3-alkylthiophene)s have an orthorhombic crystal structure, and the conformation of the alkyl chains is mostly *transoid* at RT.[11] Regardless of poly(3-alkylthiophene)s being crystalline polymers, practical poly(3-alkylthiophene)s consist of polycrystalline regions and large amorphous regions which arise from the dissymmetry of the thiophene ring.

The dissymmetry of the thiophene ring resulting from the 3-substitution on the thiophene ring leads to three different coupling modes along the polymer main chain; thereby three types of dyads and furthermore four types of triads. The chemical structures of dyads and triads are exhibited in Scheme 5.1.1.

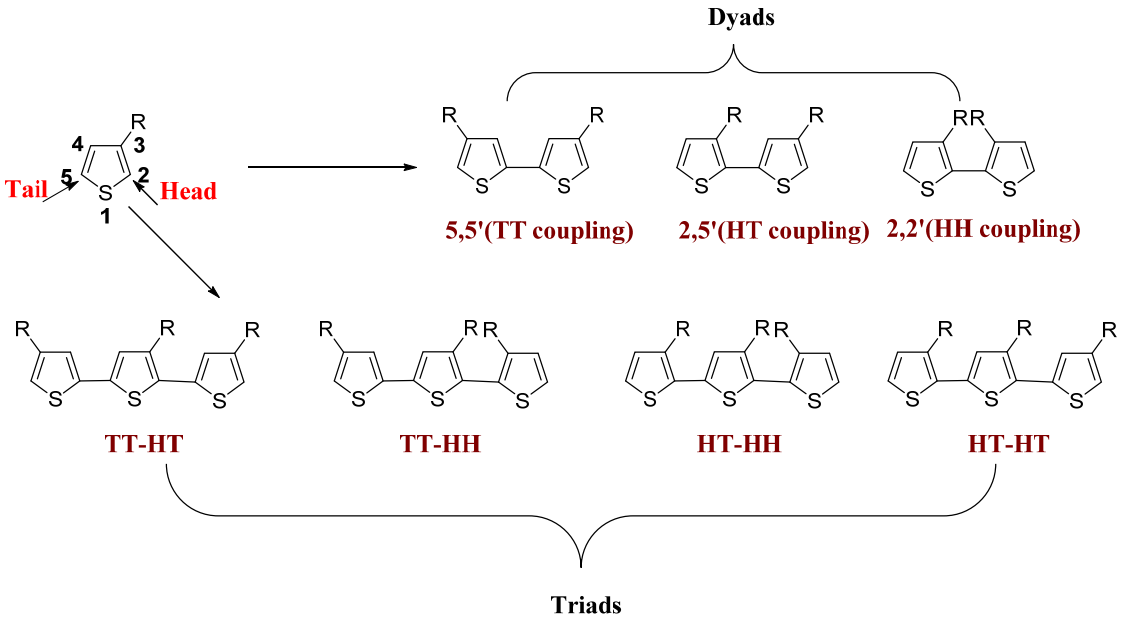

Scheme 5.1.1. Coupling regiochemistry in the polymerization of 3-alkylthiophenes

Generally, both chemical oxidative polymerization and metal-catalyzed polycondensation afford all types of dyads and triads presented above to form regio-random poly(3-

alkylthiophene)s. The presence of 2,2'-dyad (HH coupling) and 5,5'-dyad (TT coupling) in regio-random poly(3-alkylthiophene)s causes an increased twist between the thiophene units (due to steric repulsion) with the concomitant loss of conjugation. This structural feature results in an increased band gap energy between the bottom edge of the conducting band and the top edge of the valence band (blue shift in absorption and luminescence) to decrease electrical conductivity and to bring other undesired changes in electrical properties.

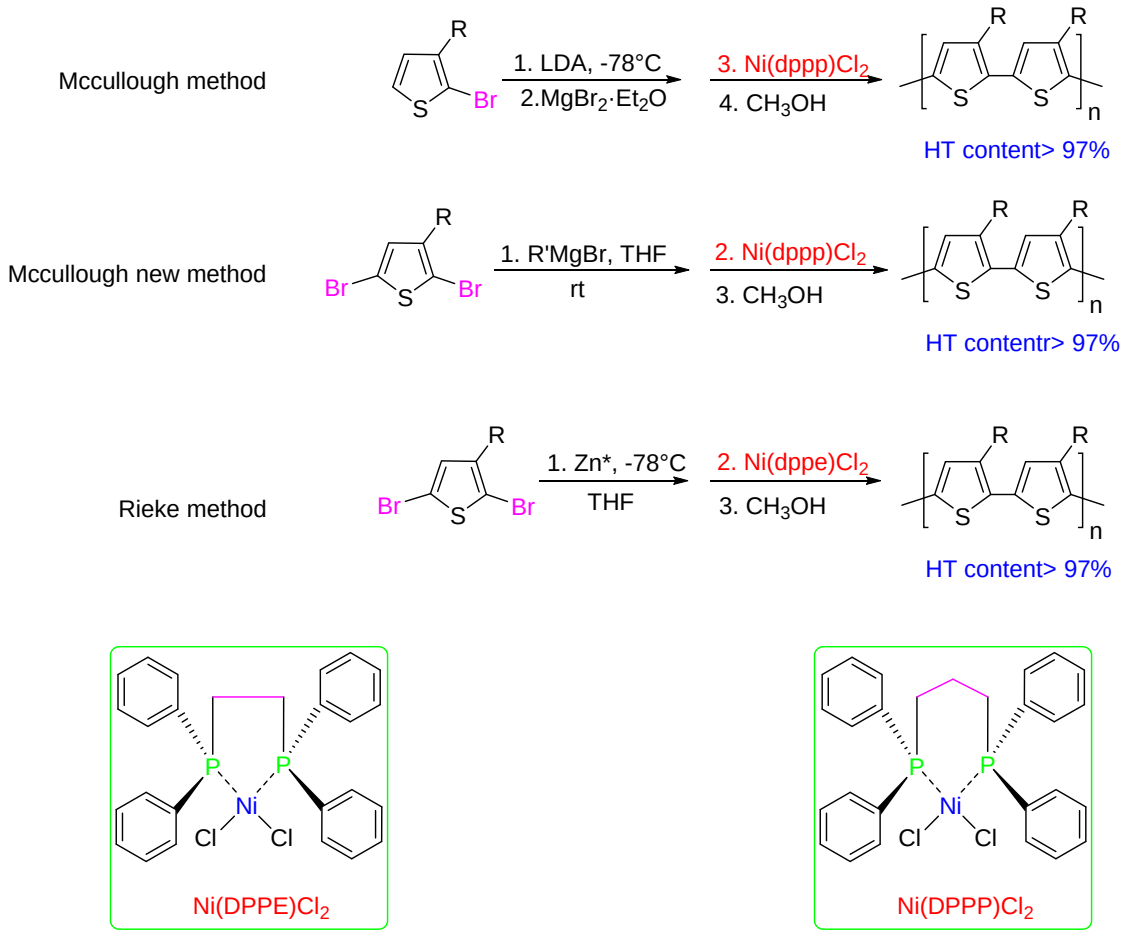

Scheme 5.1.2. The Mccullough and Rieke methods for the synthesis of regioregular HT-poly(3-alkylthiophene)s

Therefore, synthetic methodologies have been evolved to prepare regioregular poly(3-alkylthiophene)s. Several approaches have been proposed to synthesize sterically least congested HT-poly(3-alkylthiophene)s which have desirable physicochemical properties, compared with those of other poly(3-alkylthiophene)s. Mccullough *et al* have developed two approaches to efficiently synthesize poly(3-alkylthiophene)s with high HT regioregularity. In these two methods, 2-bromo-3-alkylthiophen-5-ylmagnesium bromides, generated by regiospecific metallation of 2-bromo-3-alkylthiopnenes with lithium diisopropylamide (LDA) or 2,5-dibromo-3-alkylthiophene with methylmagnesium or vinylmagnesium polymerized in the presence of a small amount of $Ni(dppp)Cl_2$ applying the Kumada cross-coupling method to yield almost 100% regioselective HT-poly(3-alkylthiophene).[11] In the Rieke method, highly active "Rieke Zinc" (Zn*) was utilized to form bromo-substituted thiophene-based zinc intermediates which polymerized with a catalytic amount of $Ni(dppe)_2$ to afford almost 100% regioselective poly(3-alkylthiophene)s (Scheme 5.1.2).[12]

Other than regioselectivity, molecular weight and molecular weight distribution (PDI) are important parameters influencing the properties of poly(thiophene) derivatives. Although the Mccullough methods, the Rieke method, and other newly developed approaches can lead the formation of regioregular poly(3-alkylthiophene)s with relatively low molecular weight, the complexity of these reactions and reaction conditions make the reactions inapplicable in a large scale.

On the contrary, the $FeCl_3$ oxidative method has advantages in relative simplicity of experimental set-up and mild reaction conditions; this method has become extremely prevalent for the laboratory- and industrial-scale syntheses of poly(alkylthiophene)s and

their derivatives.

Andersson *et al.* found a high degree of regioregularity (HT content was 94±2%) when $FeCl_3$ was added to the monomer mixture slowly.[12]

Although three possible polymerization mechanism of 3-alkylthiophenes with $FeCl_3$ in $CHCl_3$ have been proposed (radical initiated polymerization,[13] carbocation polymerization,[14] and radical carbocation polymerization[15]), its reaction mechanism is still remained under intense and controversial discussion. The heterogeneity of a reaction for the polymerization of 3-alkylthiophenes with $FeCl_3$ in $CHCl_3$ makes studies on reaction mechanisms difficult. Then, the author investigated the effect of oxidants, additives, solvents etc. on the oxidative polymerization of 3-hexylthiophenes. The study will provide beneficial insight on its reaction mechanism.

5.2 Polymerization and characterization of poly(3-alkylthiophene)s prepared by the chemical oxidative method

Materials: 3-Hexylthiophene, 2-bromo-3-hexylthiophene, 2,5-dibromo-3-hexylthiophene, $FeCl_3$ and 2,2,6,6-Tetramethyl-1-piperidinyloxy (TEMPO) were used as received from Tokyo Chemical Industry Co., Ltd. $FeBr_3$ was purchased from Sigma-Aldrich Co., Ltd. $CHCl_3$, benzene, toluene, xylene, mesitylene were dried by standing over 4A molecular sieves 1 day and bubbled with argon for 15 min prior to use. The weighing of dehydrated $FeCl_3$ and $FeBr_3$ was performed in a dry vacuum box (UNICO UN 650F) under argon. α-Cyano-4-hydroxycinnamic Acid (CCA) was purchased from Tokyo Chemical Industry Co., Ltd and used as the matrix in the MALDI-TOF MS measurement of oligo(3-hexylthiophene)s and oligo(2, 5-dibromo-3-hexylthiophene)s.

Instruments: ^{1}H (400 MHz) and ^{13}C NMR (100 MHz) spectra were recorded on a Bruker Ascend 400 spectrometer. All chemical shifts are given in ppm downfield from the signal of internal tetramethylsilane. Gel permeation chromatography (GPC) was performed by using a system consisting of a Shimadzu LC-6A pump, Tow Shodex LF-804 columns connected in series, a Jasco RI-2031 plus intelligent RI detector, and a ChromNAV software to determine the molecular weight and distribution of the polymers relative to polystyrene standards. The elution solvent used was tetrahydrofuran (THF), and GPC was carried out with an injection volume of 100 μL at a flow rate of 1 mL min^{-1}. The MALDI-TOF MS spectra were acquired on a Bruker autoflex speed-KE in a reflector mode.

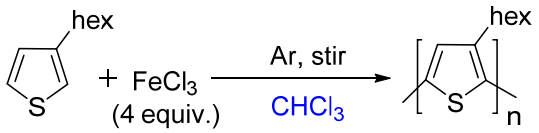

Scheme 5.2.1. Synthesis of poly(3-hexylthiophene) by using $FeCl_3$ in $CHCl_3$

Polymerization of 3-hexylthiophene with $FeCl_3$ in $CHCl_3$: Poly(3-hexylthiophene) was prepared by following the $FeCl_3$ oxidative polymerization procedure in the literature with some modifications. To a suspension of $FeCl_3$ (0.65 g, 4 mmol) in dry $CHCl_3$ (6.5 mL), 3-hexylthiophene (170 μL, 1 mmol) was added dropwise with a syringe under argon atmosphere. Stirring of the suspension was continued for an appropriate time. Then, 30 mL of methanol was added all at once to the reaction mixture to quench the reaction. After complete removal of the solvents under vacuum, the black residue was transferred into a thimble filter and extracted successively with methanol (100 mL) and acetone (100 mL) for several hours by the continuous Soxhlet extraction method. The resulting black purple solid was extracted with chloroform (100 mL) by using the same apparatus. The

light-red chloroform extract was concentrated to dryness on a rotary vacuum evaporator to afford poly(3-hexylthiophene). The methanol extract was also condensed to dryness. The resulting residue was treated with a mixture of chloroform (50 mL) and distilled water (50 mL), and then the chloroform solution was washed with distilled water (3 × 50 mL) to remove unreacted $FeCl_3$ and other iron salts, dry over Na_2SO_4 and filtered. After removal of chloroform, the brown oil-like residue was purified by distillation using a kugelrohr (103 ℃, 7.5 mmHg). The acetone extract was concentrated to afford the acetone-soluble oligomer.

Polymerization of 3-hexylthiophene with $FeBr_3$ in $CHCl_3$ was performed with a procedure similar to that mentioned above, except that the quench of polymerization was realized by adding extremely cold methanol (-180℃) dropwise to the reaction mixture. It is worthy to note that this polymerization should be stopped by the dropwise addition of extremely cold methanol, in light of the release of a large amount of heat arising from the decomposition of $FeBr_3$ with methanol.

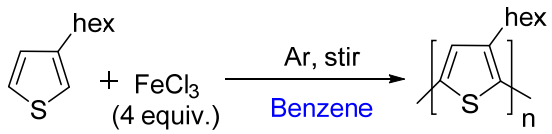

Scheme 5.2.2. Synthesis of poly(3-hexylthiophene) with $FeCl_3$ in benzene

Polymerization of 3-hexylthiophene with $FeCl_3$ in aromatic hydrocarbons: The polymerization of 3-hexylthiophene in benzene was performed with a procedure similar to that of the polymerization of 3-hexylthiophene with $FeCl_3$ in dry $CHCl_3$ mentioned above, except for the replacement of $CHCl_3$ with benzene.

The polymerization of 3-hexylthiophene with $FeCl_3$ in toluene, xylene and mesitylene were conducted with a similar procedure performed above.

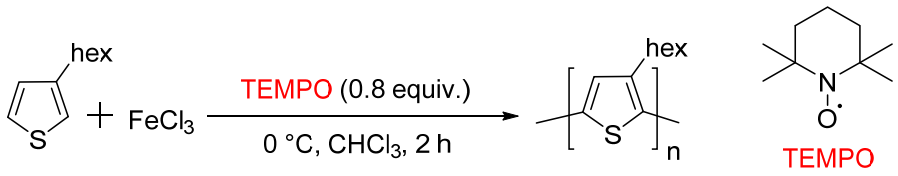

Scheme 5.2.3. Synthesis of poly(3-hexylthiophene) with $FeCl_3$ in the presence of TEMPO

Polymerization of 3-hexylthiophene with $FeCl_3$ in the presence of TEMPO: To a stirred suspension of $FeCl_3$ (0.65 g, 4 mmol) in 6.5 mL of $CHCl_3$, TEMPO (2,2,6,6-Tetramethylpiperidin-1-yl)oxyl (0.12 g, 0.8 mmol) was added all at once, and then the suspension was stirred for 1 h. A color change of the suspension from black to yellow occurred, when TEMPO was added. 3-Hexylthiophene (0.17 g, 1 mmol) was added dropwise to the yellow suspension, stirred for another 2 h under argon. The polymer was precipitated upon adding the reaction suspension in $CHCl_3$ into methanol (100 mL). Then, the solvents were removed by a rotary evaporator to afford a black residue, which was thoroughly filtered through a thimble filter. The polymer was further purified by extracting with methanol (100 mL), acetone (100 mL), and $CHCl_3$ (100 mL) by using a Soxhlet extractor. The $CHCl_3$ extract was concentrated, dried under vacuum to give a dark red solid with metallic luster.

Molecular weight of the $CHCl_3$-soluble fraction of poly(3-hexylthiophene): Mn=138500; Mw=1610800; PDI (Mw/Mn)=11

5.3 Results and discussion

5.3.1 Usefulness of Soxhet extraction in the isolation of poly(3-alkylthiophene) prepared with $FeCl_3$ in $CHCl_3$

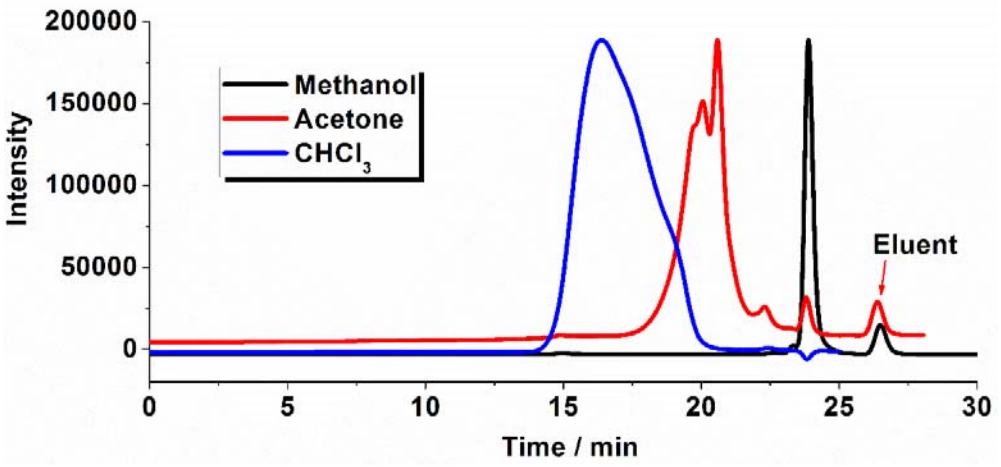

Figure 5.3.1.1. GPC profiles of three fractions of poly(3-hexylthiophene) prepared by the standard $FeCl_3$ method (reaction conditions : 0°C, 2 min)

Soxlet extraction is a benchmark technique in the extraction of compunds with low solubility in some solvents from the reaction mixtures.[16] This method for separation relies on the solubility characteristics of particular species involved. By rinsing with solvents with the different polarity (in the present experiments, methanol was used to eliminate unreacted $FeCl_3$, other iron salts and oligomer with low molecular weight; acetone was utilized to remove oligomers with middle molecular weight; $CHCl_3$ was used to collect polymer), poly(3-alkylthiophene)s can be separated into three fractions (methanol-soluble fraction, acetone-soluble fraction, and $CHCl_3$-soluble fraction). The usefulness of Soxhlet extraction has been was demonstrated by the GPC (gel permeation chromatography) analysis of the three fractions of poly(3-hexylthiophene)s. From Figure 5.3.1.1, it is clearly found that oligo(3-hexylthiophene) was effectively separated from poly(3-hexylthiophene) and that oligomers collected from the acetone solution have a molecular weight larger than that of oligomers recovered from the methanol solution.

5.3.2 Solubility of poly(3-hexylthiophene) at room temperature

CCl_4	◯	Benzene	◯	Hexane	Δ	Diethyl ether	Δ
$CHCl_3$	◯	Toluene	◯	Cyclohexane	Δ	Diisopropyl ether	x
$CH2Cl_2$	◯	Xylene	◯	Pyridine	Δ	Acetone	x
CH_2ClCH_2Cl	Δ	Mesitylene	◯	1,4-dioxane	Δ	Ethyl acetate	x
CH_3COOH	x	H_2O	x	DMSO	x	DMF	x

Scheme 5.3.2.1. Solubility of poly(3-hexylthiophene) in common organic solvents at room temperature (◯: Soluble; Δ: Slightly soluble; x: insoluble)

As well-known, the low solubility of unsubstituted thiophene polymers in organic solvents, resulting in poor processability and difficulty in structural characterization, has limited their potential applications. The introduction of an alkyl group (typically, hexyl and octadecyl) at the 3-position of the thiophene ring, breaking the symmetric structure of the thiophene polymer backbone and increasing interplanar spacing, imparts a premium solubility in common organic solvents such as CH_2Cl_2, $CHCl_3$, and aromatic solvents (benzene, toluene, xylene and mesitylene). The conformational difference of polymer main chains in different solvents may be the origin of the color difference in these solvents. The detailed study on the effect of solvents on the color of poly(alkylthiophene)s has been reported by Sugimoto *et al* in 1987.[17]

5.3.3 Influence of the molar ratio of 3-hexylthiophene to $FeCl_3$ on the polymer yield

The influence of the molar ratio of 3-hexylthiophene monomer to the oxidizing agent, $FeCl_3$, on the polymer yield was investigated, and the results are summarized in Table

5.3.3.1. When the ratio was reduced from 1:4 to 0.15:4, about two-fold increase in the resulting polymer yield was evidently observed.

Table 5.3.3.1. Conversion of the monomer to the polymer at different monomer-to-oxidizing agent ratios (All reactions were conducted at 0 ˚C).

Entry	Reaction Time (min)	Molar Ratio	Oligomer Yield (%)	Polymer Yield (%)	Gel Yield (%)	Total Yield (%)
1	2	1:04	3	16	0	19
2	2	0.15:4	5	31	0	36
3	3	1:04	2	22	0	24
4	3	0.15:4	5	46	0	51
5	5	1:04	3	30	0	33
6	5	0.15:4	6	62	0	68

*monomer versus $FeCl_3$

5.3.4 Effect of oxidants on the polymerization of 3-alkylthiophene

Other than $FeCl_3$, $FeBr_3$ and $FeCl_3 \cdot 6H_2O$ were also tried to use as the oxidant in the synthesis of poly(3-alkylthiophene)s. However, $FeCl_3 \cdot 6H_2O$ did not work as the oxidant in the polymerization of 3-hexylthiophene. On the other hand, $FeBr_3$, an analogue of $FeCl_3$, acted as the oxidizing agent for the polymerization of 3-alkylthiophene. Comparing with $FeCl_3$, under standard reaction conditions, $FeBr_3$ could offer poly(3-hexylthiophene) with higher molecular weight but lower polymer yield (Table 5.3.4.1). The covalent incorporation of the bromide atom(s) of $FeBr_3$ into the polymer backbone was observed by MOLDI-TOF MS spectrometry (Scheme 5.3.4.2). Although $FeBr_3$ is not

as convenient as $FeCl_3$ in usage, poly(3-alkylthiophene)s with bromine end group(s) are more fascinating than their chlorinated analogues, because further functionalization of brominated poly(3-alkylthiophene) is easy through the metallation of the bromo functionality.[18]

Table 5.3.4.1. Effect of oxidants on the polymerization of 3-hexylthiophene (the reaction was conducted with a standard procedure described in the literatures[10] (Reaction temperature, 0 ˚C; reaction solvent, $CHCl_3$; molar ratio of monomer/oxidant, 1:4)

Run	Reaction Time (h)	Oxidant	Oligomer Yield (%)	Polymer Yield (%)	Gel Yield (%)	Total Yield (%)	MW of Polymer	
							Mn	Mw
1	16	$FeCl_3$	4	71	0	75	33800	145000
2	16	$FeBr_3$	15	36	0	51	128900	297000

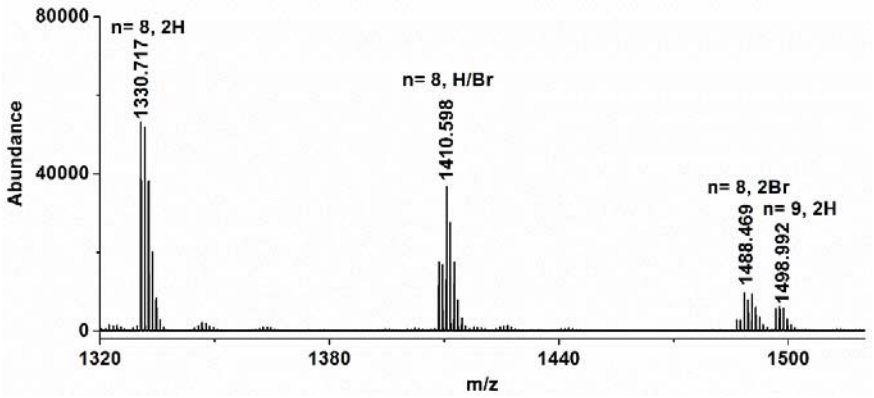

Scheme 5.3.4.2. MALDI-TOFF MS spectrum of the acetone-soluble fraction of poly(3-hexylthiophene) prepared by the $FeBr_3$ oxidative method (reaction temperature, 0 ˚C; time, 16 h; solvent, $CHCl_3$).

5.3.5 Effect of additives on the polymerization of 3-hexylthiophene with $FeCl_3$

Table 5.3.5.1. Effect of $FeCl_2$ on the polymerization of 3-hexylthiophene with $FeCl_3$ in dried $CHCl_3$ (star symbol indicates the molar ratio of $FeCl_3$/ $FeCl_2$)

Run	Temp (0 °C)	Reaction Time (min)	Molar Ratio	Oxidant	Oligomer Yield (%)	Polymer Yield (%)
1	0	5	1:4	$FeCl_3$	3	30
2	0	5	1:4	$FeCl_3$ + $FeCl_2$ (20:1)*	−−−	10

Table 5.3.5.2. Effect of TEMPO on the polymerization of 3-hexylthiophene with $FeCl_3$ in $CHCl_3$ (reactions were conducted at 0 °C in $CHCl_3$ with a 3-hexylthiophene/$FeCl_3$ ratio of 1:4)

Run	TEMPO	Yield for acetone part	Yield for polymer part	Yield for gel	MW for polymer	
					Mn	Mw
1	0	4.1%	67%	0	48400	161000
2	0.8 equiv.	4.6%	72%	0	138500	1611000

The effect of $FeCl_2$ and 2,2,6,6-tetramethylpiperidine-1-oxyl (TEMPO) as an additive on the polymerization of 3-hexylthiophene with $FeCl_3$ in dried $CHCl_3$ was determined. As a result, it was found that the addition of $FeCl_2$ evidently decreased the monomer-to-polymer conversion as shown in Table 5.3.5.1. However TEMPO brought a positive effect on the polymerization of 3-hexylthiophene. When the polymerization was performed in the presence of TEMPO, poly(3-hexylthiophene) was obtained in higher polymer yield and with higher molecular weight (Table 5.3.5.2). Poly(3-hexylthiophene)

synthesized in the presence of TEMPO showed a similar absorption spectrum to that of poly(3-hexylthiophene) prepared by the standard $FeCl_3$ oxidation, indicating the similar planarity of the two polymers (Scheme 5.3.5.3).

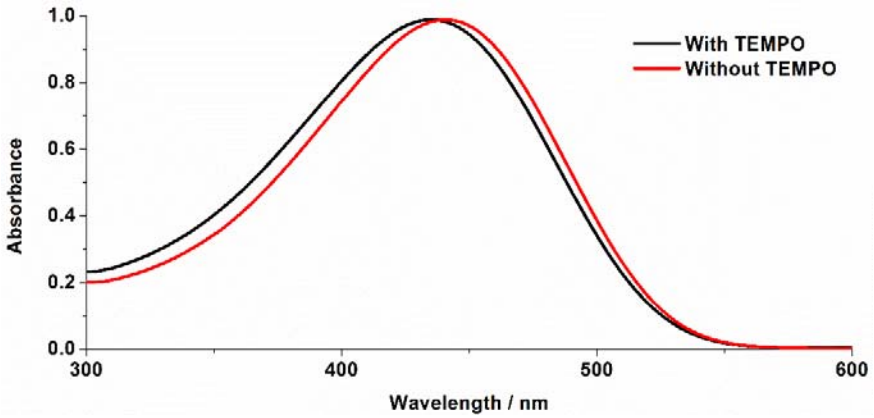

Scheme 5.3.5.3. Uv-vis spectra of poly(3-hexylthiophene) prepared in the presence (black solid) and absence (red solid) of TEMPO.

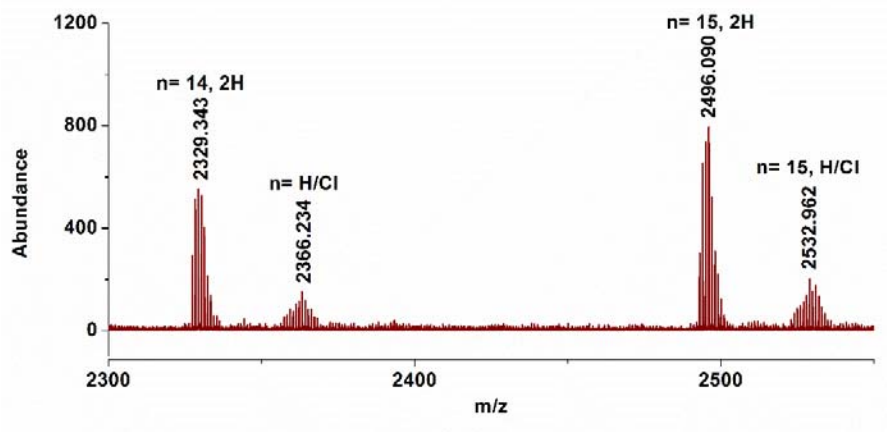

Scheme 5.3.5.4. MALDI-TOF MS spectroscopy of the acetone-soluble part of poly(3-hexylthiophene) prepared in the presence of TEMPO

To get more information about the effect of TEMPO on the resulting polymer, MALDI-TOF MS spectroscopy, popular in the structural analysis of polymers, was adopted. As shown in Scheme 5.3.5.4, only $[H + Cl]^+$ and $[H + H]^+$ ion series could be identified, different from the ion series of poly(3-hexylthiophene) synthesized in the absence of

TEMPO (besides $[H + Cl]^+$ and $[H + H]^+$ ion series, $[2Cl]^+$ and $[nCl]^+(n>2)$ were also observed in the latter sample). This finding may be helpful for the understanding the role of TEMPO on the polymerization, in view of serious deterioration of the polymerization activity by the halogenation of 3-alkylthiophene monomer and the resulting oligomer.[19]

In the area of the metal-free catalytic oxidative transformation of alcohols to aldehydes, TEMPO has emerged as a novel catalyst.[19] The mechanism of TEMPO-mediated oxidation of alcohols to aldehydes has been proposed as shown below (Scheme 5.3.5.5).[20] The secondary oxidants, such as bleach and $FeCl_3 \cdot 6H_2O$, oxidize TEMPO into its oxoammonium salt, which transform alcohols to the corresponding aldehydes as a primary oxidant. The transformation results in the generation of the corresponding hydroxylamine derivative that is oxidized to TEMPO by the secondary oxidant. Thus, one catalytic cycle completes.

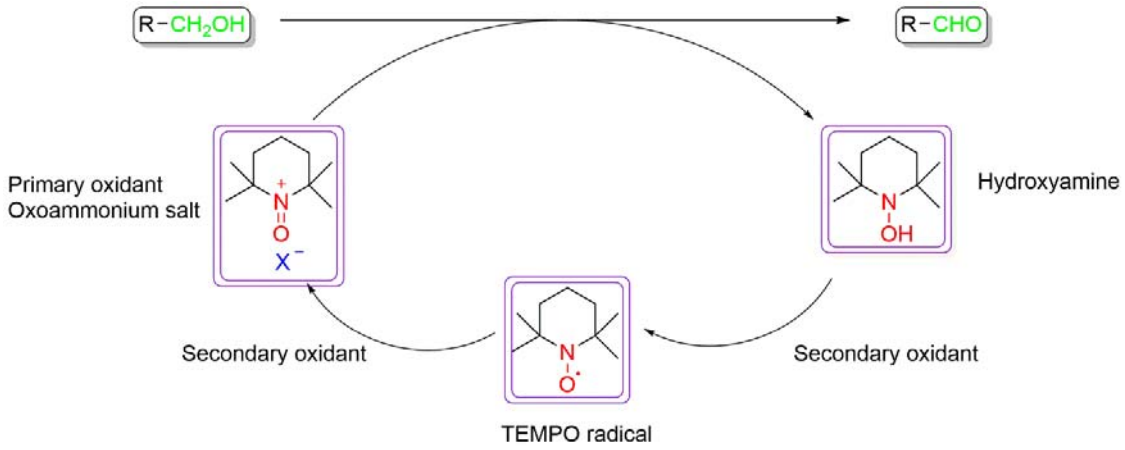

Scheme 5.3.5.5. Catalytic cycle of TEMPO-mediated oxidation of alcohols to aldehydes

In a similar manner, a possible mechanism for the polymerization of 3-hexylthiophene in the presence of TEMPO is proposed as shown in Scheme 5.3.5.6. As a mild oxidant, $FeCl_3$ oxidized TEMPO to its oxoammonium salt, which was evidenced by a color change of a $FeCl_3$ suspension in $CHCl_3$ from black to yellow. After dropwise addition of

the monomer to the yellow suspension, a color change of suspension occurred from yellow to black, implying the polymerization of 3-hexylthiophene with the oxoammonium salt of TEMPO proceeded. Along with polymerization, the oxoammonium salt of TEMPO is reduced to its hydroxylamine, which subsequently is oxidized to TEMPO radical by $FeCl_3$.

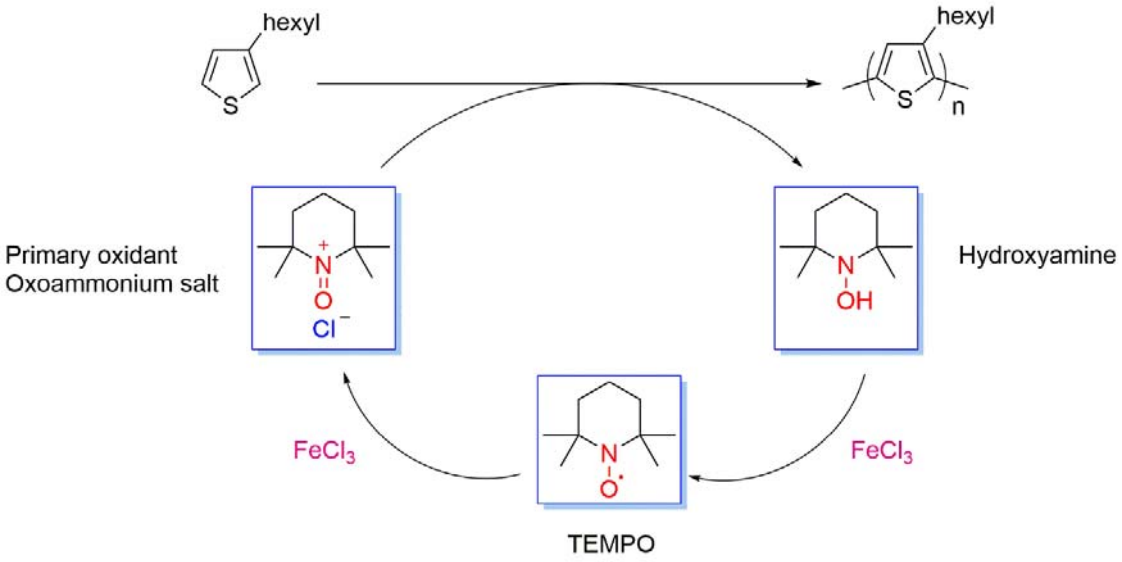

Scheme 5.3.5.6. A possible mechanism for the polymerization of 3-hexylthiophene in the presence of TEMPO

5.3.6 Solvent effect for the polymerization of 3-alkylthiophene with $FeCl_3$

5.3.6.1 Usefulness of Soxhet extraction in the isolation of poly(3-alkylthiophene) prepared with $FeCl_3$ in aromatic solvents

The solvent effect for the 3-alkylthiophene polymerization with $FeCl_3$ was studied in detail. Other than the reported chlorinated solvents (CH_2Cl_2, $CHCl_3$ and CCl_4), the polymerization was found to proceed in aromatic solvents (benzene, toluene, xylene and mesitylene) (Scheme 5.3.6.1.1).

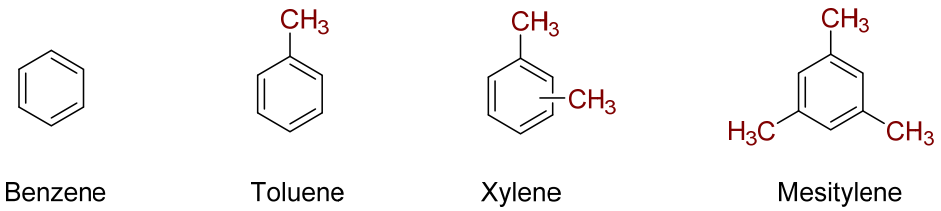

Scheme 5.3.6.1.1. Aromatic solvents adopted in this work

As described in 5.3.6.1.2, poly(3-hexylthiophene)s synthesized in aromatic solvents were also isolated from solid masses by continuous Soxhlet extraction (methanol, acetone and $CHCl_3$ in turn). The effectiveness of the extraction was verified by the GPC analysis of the corresponding extracts (Scheme 5.3.6.1.2).

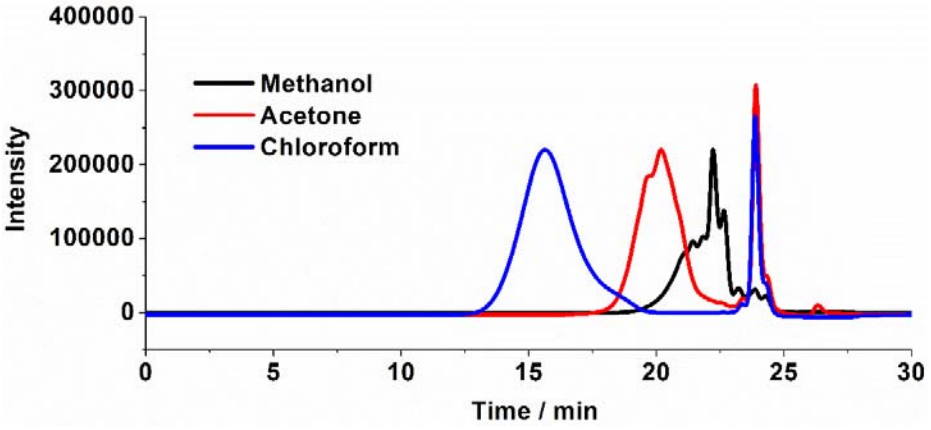

Scheme 5.3.6.1.2. GPC of CH_3OH-soluble, acetone-soluble, and $CHCl_3$-soluble fractions of poly(3-hexylthiophene) prepared in toluene

5.3.6.2 Temperature dependency of the polymerization of 3-hexylthiophene in aromatic solvents

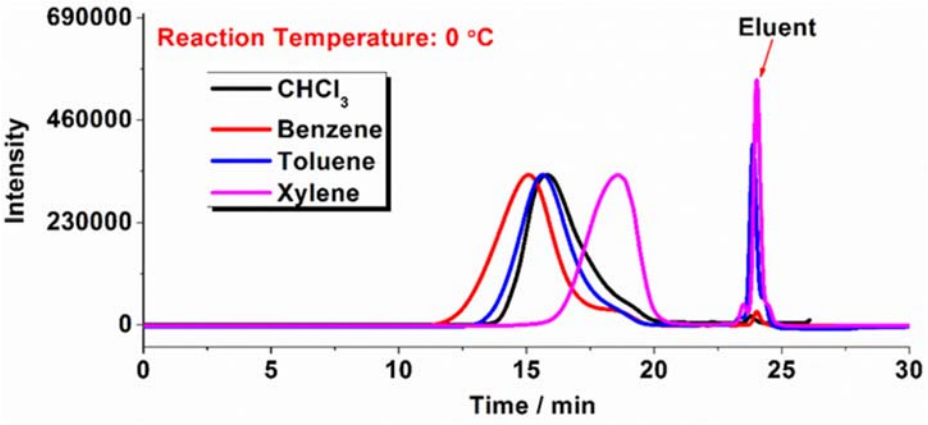

Scheme 5.3.6.2.1. GPC profiles of poly(3-hexylthiophene)s prepared in aromatic solvents at 0 ˚C (as frozen at 5 ˚C, the polymerization of 3-hexylthiophene in benzene was conducted at 6 ˚C)

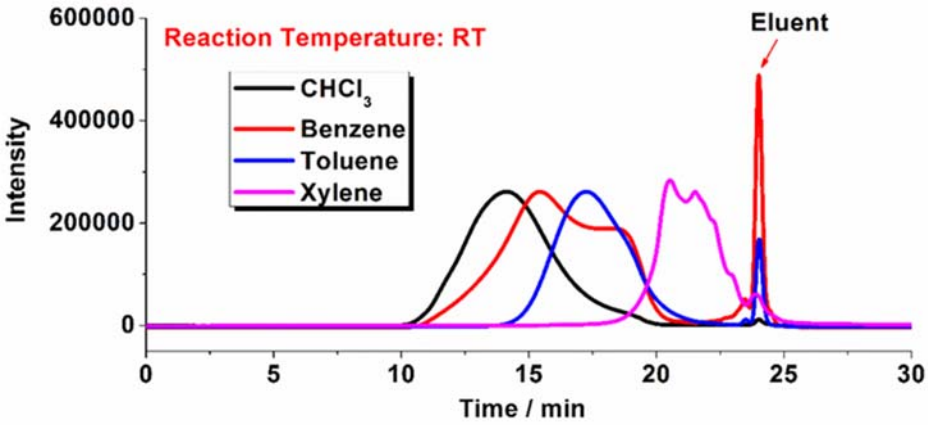

Scheme 5.3.6.2.2. GPC profiles of poly(3-hexylthiophene)s prepared in aromatic solvents at room temperature

The reaction of aromatic solvents with $FeCl_3$ has been reported by Wu *et al.*[21] However, the polymerization of 3-alkylthiophenes with $FeCl_3$ in an aromatic solvent has not been investigated. When conducting the polymerization reaction in aromatic solvents, rising the reaction temperature from 0 ˚C to room temperature (23 ˚C) resulted in the definite formation of oligomer in higher yield and that of polymer in slightly changed yield and with lower molecular weight (except for benzene, oligomer yield was hardly changed

when elevated the temperature), which is opposite to the observed results of the polymerization of 3-hexylthiophene in $CHCl_3$ (Scheme 5.3.6.2.1 and Scheme 5.3.6.2.2). These results suggest that the resulting oligomers formed in toluene, xylene and mesitylene show low polymerization activity at a higher temperature. Likewise, the solvent used imposes vast influence on polymer yield and polymer molecular weight. The molecular weight of poly(3-hexylthiophene) obtained in the aromatic solvents follows the following sequence: benzene > toluene > xylene. In mesitylene, only oligomer was generated, independent of the reaction temperature. These results can imply the inhibition of polymerization, due to the steric hindrance of the aromatic solvents, which increased from benzene to mesitylene. Comparing with the reaction in $CHCl_3$, the reaction in benzene provided poly(3-hexylthiophene) with much higher molecular weight and decreased polymer yield under the same reaction conditions.

5.3.6.3 Structure analysis of poly(3-hexylthiophene)s prepared in aromatic solvents

$CHCl_3$ Toluene Benzene

Scheme 5.3.6.3.1. Photos of poly(3-hexylthiophene)s prepared in different organic solvents at room temperature

As shown in Scheme 5.3.6.3.1, the appearance of poly(3-hexylthiophene)s synthesized in benzene presented dark gray color and non-metallic luster, which are quite different from those of poly(3-hexylthiophene)s synthesized in $CHCl_3$, indicating the difference in the

conjugation degree of the resulting polymer main chain between these two polymers. Although the reaction in toluene output poly(3-hexylthiophene)s (P3HTs) with similar appearance to that of P3HT produced in $CHCl_3$, the use of xylene just provided brown-colored, oily, low molecular P3HT.

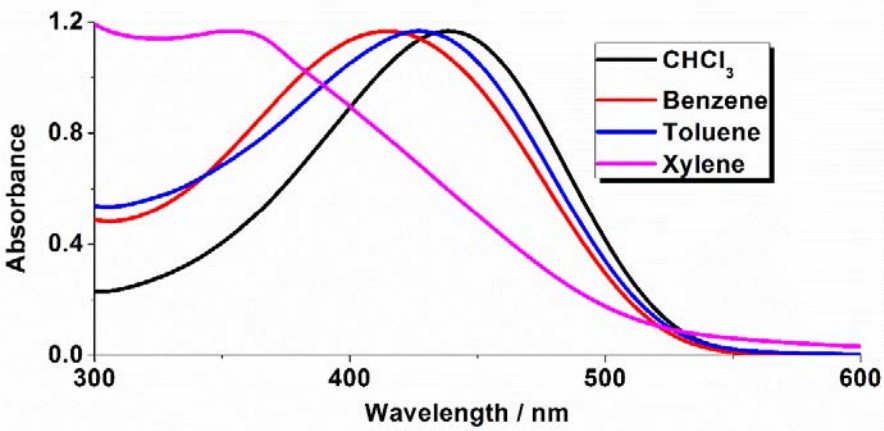

Scheme 5.3.6.3.2. UV-vis spectra of poly(3-hexylthiophene)s synthesized in $CHCl_3$, benzene, Toluene, and xylene at room temperature for 2 h.

The difference of the color of poly(3-hexylthiophene)s synthesized in different solvents were also recorded by UV-vis spectroscopy (Scheme 5.3.6.3.2). The blue shift of the maximal absorption wavelengths of P3HTs, polymerized in aromatic solvents, was clearly demonstrated, comparing with that of P3HTs obtained in $CHCl_3$ ($\lambda_{max}(CHCl_3)$ = 438 nm; λ_{max}(benzene) = 415 nm; λ_{max}(toluene) = 427 nm; λmax(xylene) = 355 nm). A blue shift of up to 23 nm may explain the color difference between polymers synthesized in benzene and $CHCl_3$. The completely different UV profile of P3HTs obtained in xylene may point out their nature of low molecular weight.

As a powerful tool for structural analysis, ^{1}H NMR has been widely used to characterize polymers. By comparing the ^{1}H NMR of P3HT synthesized in $CHCl_3$ with that of P3HT prepared in benzene, new peaks in a range from 7.7 ppm to 7.3 ppm were observed

(Scheme 5.3.6.3.3), which were designated to the protons of benzene rings. This means that benzene molecules may be incorporated into the polymer main chain by the copolymerization with 3-hexylthiophene monomer in the presence of $FeCl_3$.

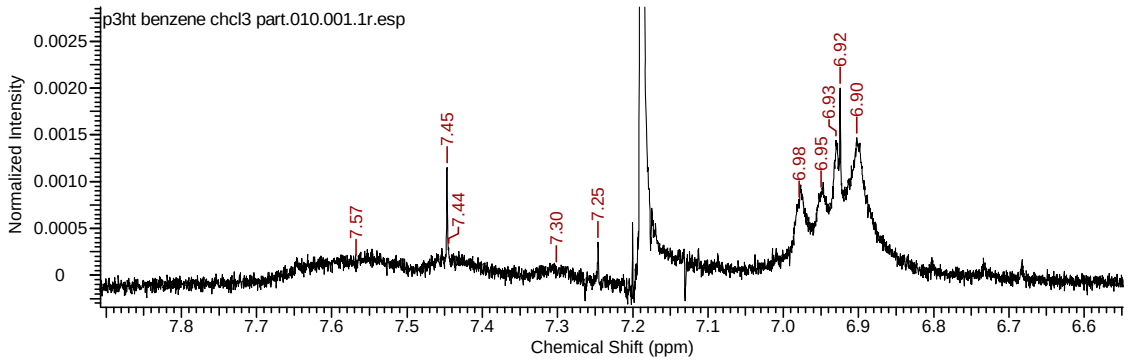

Scheme 5.3.6.3.3. ^1H NMR of poly(3-hexylthiophene) prepared by the standard $FeCl_3$ oxidative method in benzene

MALDI-TOF MS (Matrix-assisted laser desorption-ionization time-of-flight mass spectrometry) is becoming a vital tool for the analysis of many biopolymers and the characterization of synthetic polymers.[20] Advantages of MALDI-TOF MS over GPC for synthetic polymers can be summarized as follows:

(i) The absolute molecular weight of synthetic polymers can be determined as opposed to the relative molecular weight by GPC.

(ii) The end group of synthetic polymers can be monitored.

The structure of the acetone-soluble poly(3-hexylthiophene) attained in benzene was verified by MALDI-TOF MS by using α-cyano-4-hydroxycinnaminic acid (CCA) as the matrix (Scheme 5.3.6.3.4). To our surprise, common end groups like $[H+Cl]^+$, $[2Cl]^+$, and $[H+H]^+$, which were presented in poly(3-alkylthiophene)s synthesized by $FeCl_3$ in $CHCl_3$ were not found in this sample. In contrast, the presence of three novel end groups ([Ph + Cl], [Ph + H] and [2Ph]) were undoubtedly confirmed.

The characterization of the acetone-soluble fraction of poly(3-hexylthiophene) obtained in xylene was also conducted by MALDI-TOF MS. Different from the three end groups in the acetone-soluble fraction of poly(3-hexylthiophene) prepared in benzene, only [2 xylene] was found as the end group (Scheme 5.3.6.3.5). For P3HTs attained in toluene and mesitylene, similar results were obtained.

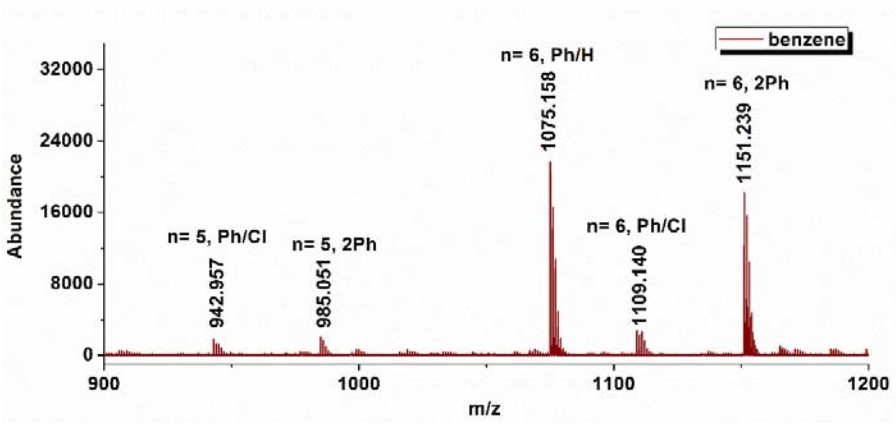

Scheme 5.3.6.3.4. MALDI-TOF MS spectrum of the acetone-soluble fraction of poly(3-hexylthiophene) prepared in benzene

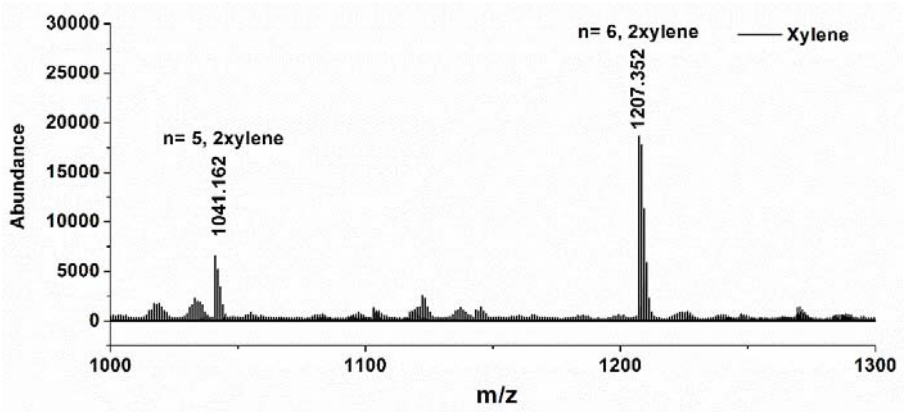

Scheme 5.3.6.3.5. MALDI-TOF MS spectrum of the acetone-soluble fraction of poly(3-hexylthiophene) prepared in xylene.

Other than chlorinated methane and aromatic solvents, diethyl ether, diisopropyl ether, and ethyl acetate were also adopted in the polymerization of 3-hexylthiophene with

$FeCl_3$. The results are summarized in Table 5.3.6.3.6.

Table 5.3.6.3.6. Polymerization of 3-hexylthiophene with $FeCl_3$ in diethyl ether, diisopropyl ether, and ethyl acetate at 0 ˚C for 2 h

Solvent	Yield of acetone part oligomer (%)	Yield of polymer (%)	Yield of gel (%)	Total Yield (%)	Mn of Polymer
Diethyl ether	0.6	0.6	0.2	1.4	17000
Diisopropyl ether	0.6	0	0	0.6	0
Ethyl acetate	0.2	2.8	1.9	4.9	10600

As presented in Table 5.3.6.3.6, only a trace amount of oligomer and polymer with low molecular weight were obtained, indicating a negative effect of the three solvents on polymerization. This obstruction can be explained by the coordination of the solvents to $FeCl_3$ to form the corresponding Lewis acid/Lewis base salts, which could not initiate the polymerization of 3-hexylthiophene, similar to that with $FeCl_3{\cdot}(H_2O)_6$ in $CHCl_3$ as mentioned in 5.3.4 (Scheme 5.3.6.3.7).

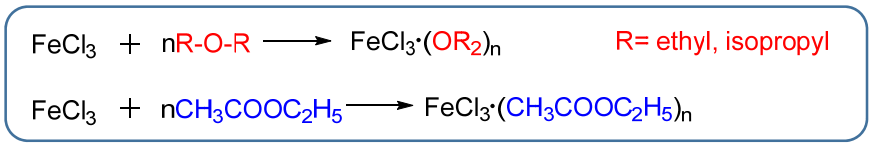

Scheme 5.3.6.3.7. Possible coordinations between $FeCl_3$ and several solvents

5.4 References to Chapter 5

1. Schultze, X.; Serin, J.; Adronov, A.; Frechet, J. M. J., *Chem. Commun*. **2001**, *13*, 1160-1161.

   Bundgaard, E.; Krebs, F. C., *Macromolecules*. **2006**, *39*, 2823-2831.

   Günes, S.; Neugebauer, H.; Sariciftci, N. S., *Chem. Rev*. **2007**, *107*, 1324-1338.

2. Marrocchi, A.; Lanari, D.; Facchetti, A.; Vaccaro, L., *Energy Environ. Sci*. **2012**,

5, 8457-8474.

Qian, D.; Ma, W.; Li, Z.; Guo, X.; Zhang, S.; Ye, L.; Ade, H.; Tan, Z. a.; Hou, J., *J. Am. Chem. Soc*. **2013**, *135*, 8464-8467.

3. Lendlein, A.; Shastri, V. P., *Adv. Mater*. **2010**, *22*, 3344-3347.

   Koike, Y.; Asai, M.,. *NPG Asia Mater*. **2009**, *1*, 22-28.

   Argyros, A., J. Lightw. Technol. **2009**, *27*, 1571-1579.

4. Hwang, S.-W.; Choi, G.; Bates, A.; Ench, R. M.; Lee, S. C.; Kwon, O. S.; Lee, D. H.; Mukherjee, S.; Park, S., *ECS Trans***. 2013**, 50, 805-815

   Kamamichi, N.; Yamakita, M.; Kozuki, T.; Asaka, K.; Luo, Z.-W., *Advanced Robotics*. **2007**, *21*, 65-85.

   Kolesar, E. S.; Reston, R. R.; Ford, D. G.; Fitch, R. C., *J. Robotic Syst*.**1992**, *9*, 37-63.

5. Shirakawa, H., *Angew. Chem. Int. Ed*. **2001**, *40*, 2574-2580.

   MacDiarmid, A. G., *Angew. Chem. Int. Ed***. 2001**, *40*, 2581-2590.

   Heeger, A. J*., Chem. Soc. Rev*. **2010**, *39*, 2354-2371.

   Kane-Maguire, L. A. P.; Wallace, G. G., *Chem. Soc. Rev*. 2010, *39*, 2545-2576.

   Roncali, J., *Chem. Rev.* **1992**, *92*, 711-738

6. Kim; Chen, L.; Gong; Osada, Y., *Macromolecules*. **1999**, *32*, 3964-3969.

7. Yamamoto, T.; Sanechika, K.; Yamamoto, A., *J. Polym. Sci. B Polym. Lett. Ed*. **1980**, *18*, 9-12.

8. Jen, K.-Y.; Miller, G. G.; Elsenbaumer, R. L., *J. Chem. Soc., Chem. Commun*. **1986**, *0*, 1346-1347.

9. Krische, B.; Zagorska, M., *Synth. Met*. **1989**, *33*, 257-267.

Takahashi, Y.; Taura, S.; Akiyama, T.; Yamada, S., *Langmuir*. **2012**, *28*, 9155-9160.

10. R. Sugimoto, S. Takeda, H. B. Gu, and K. Yoshino, *Chem. Express*. **1986**.*1*, 635-638.
11. Tashiro, K.; Ono, K.; Minagawa, Y. Kobatashi, M.; Kawai, T.; Yoshino, K., J. Polym. Sci. Polym. Phys., 1991, 29, 1223-1233.
12. Andersson, M. R.; Selse, D.; Berggren, M.; Jaervinen, H.; Hjertberg, T.; Inganaes, O.; Wennerstroem, O.; Oesterholm, J. E., *Macromolecules*. **1994**, *27*, 6503-6506.
13. McCullough, R. D.; Lowe, R. D., *J. Chem. Soc., Chem. Commun*. **1992**, *1*, 70-72.

    Loewe, R. S.; Ewbank, P. C.; Liu, J.; Zhai, L.; McCullough, R. D., *Macromolecules*. **2001**, *34*, 4324-4333.

    Loewe, R. S.; Khersonsky, S. M.; McCullough, R. D., *Adv. Mater.* **1999**, *11*, 250-253.
14. Chen, T. A.; Rieke, R. D., *J. Am. Chem. Soc*. **1992**, *114*, 10087-10088.
15. Niemi, V. M.; Knuuttila, P.; Österholm, J. E.; Korvola, *Polymer*, **1992**, *33*, 1559-1562.
16. Andersson, M. R.; Selse, D.; Berggren, M.; Jaervinen, H.; Hjertberg, T.; Inganaes, O.; Wennerstroem, O.; Oesterholm, J. E., *Macromolecules*. **1994**, *27*, 6503-6506.
17. Barbarella, G.; Zambianchi, M.; Di Toro, R.; Colonna, M.; Iarossi, D.; Goldoni, F.; Bongini, A., *J. Org. Chem*. 1996, *61*, 8285-8292.
18. Jensen, W. B. *J. Chem. Educ*. **2007**, *84*, 1913.

    Adam, D. J.; Mainwaring, J.; Quigley, M. N., *J. Chem. Educ.* **1996**, *73*, 1171.
19. Yoshino, K. N., Shigeaki; Gu, Hal Bon; Sugimoto, Ryu-ichi, *Jpn. J. Appl. Phys.,*

1987, *26*, 2.

20. Liu, Y.; Nishiwaki, N.; Saigo, K.; Sugimoto, R., *Bull. Chem. Soc. Jpn*. **2013**, in press.
21. Kovacic, P.; Wu, C., *J. Org. Chem*, **1961**, *26*, 762-765.

    Kovacic, P.; Brace, N. O., *J. Am. Chem. Soc*. **1954**, *76*, 5491-5494.
22. McCarley, T. D.; Noble; DuBois, C. J.; McCarley, R. L., *Macromolecules*. **2001**, *34*, 7999-8004.
23. Bolm, C.; Magnus, A. S.; Hildebrand, J. P., *Org. Lett*. **2000**, *2*, 1173-1175.

    Hoover, J. M.; Steves, J. E.; Stahl, S. S., *Nat. Protocols*. **2012**, *7*, 1161-1166.
24. Zhao, M.; Li, J.; Mano, E.; Song, Z.; Tschaen, D. M.; Grabowski, E. J. J.; Reider, P. J., *J. Org. Chem*. **1999**, *64*, 2564-2566.

Chapter 6 Kinetics of the polymerization of 3-alkylthiophene with $FeCl_3$

6.1 Introduction

The syntheses and properties of conjugated conducting polymers have attracted much interest over a quarter of a century. Since the $FeCl_3$ oxidative polymerization method has been firstly reported by Sugimoto *et al* in 1986,[1] this method with advantages in relative simplicity of experimental set-up and mild reaction conditions has become extremely prevalent for the laboratory- and industrial-scale syntheses of poly(alkylthiophene)s and their derivatives. Various types of substituted poly(thiophene)s prepared by the present method have been extensively studied, and a number of intriguing applications also have been proposed for these substituted poly(thiophene)s.[2-6] Even though the importance of poly(alkylthiophene)s as one of conducting polymers is well-known, systematic kinetics studies on the polymerization of substituted thiophenes by using $FeCl_3$ have not been reported until now, except for a fragmental report by Olinga and François that the polymerization of unsubstituted thiophene with $FeCl_3$ followed a first order *vs.* monomer at a very low initial concentration of the monomer.[7] In this chapter, the author describes kinetics of 3-hexylthiophene polymerization initiated by $FeCl_3$ and discusses the mechanism of the $FeCl_3$ oxidative polymerization. Although bromo-substituted 3-alkylthiophenes have been explored as blocks in the synthesis of HT-regioregular poly(3-alkylthiophene)s by metal-catalyzed polycondensation methods about twenty years ago, the possibility of the directive polymerization of these halogen-substituted 3-alkylthiophenes by chemical oxidative approaches has not been examined up to now. In

this chapter, the author also describes studies on the polymerization activity of these halogen-substituted 3-alkylthiophenes by chemical oxidative approaches.

6.2 Experimental section

Materials: 2-Bromo-3-hexylthiophene and 2,5-dibromo-3-hexylthiophene were purchased from Tokyo Chemical Industry Co., Ltd. and used as received. $CHCl_3$ was dried over 4A molecular sieves for 12 h and bubbled with argon for 10 min prior to use. To avoid hydrolysis, $FeCl_3$ was weighed in a glove box. All experiments mentioned below were conducted under argon atmosphere, unless otherwise noted.

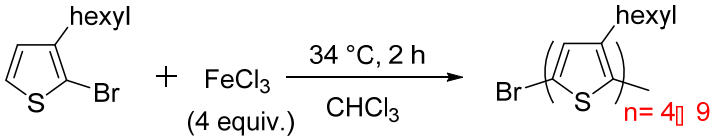

Scheme 6.2.1. Oligomerization of 2-bromo-3-hexylthiophene with $FeCl_3$ in $CHCl_3$

Oligomerization of 2-bromo-3-hexylthiophene with $FeCl_3$ in $CHCl_3$: To a stirred suspension of $FeCl_3$ (2.6 g, 16.2 mmol) in dry $CHCl_3$ (15 mL), 1.00 g (4.1 mmol) of 2-bromo-3-hexylthiophene was added dropwise under argon atmosphere at 34 °C. The stirring was continued for 2 h, and then the suspension was poured into 100 mL of methanol all at once to quench the polymerization reaction. Solvents were removed with a rotary vacuum evaporator to afford a brown oil. The resultant was transferred into a thimble filter by wiping with absorbent cotton, and then continuously extracted with methanol (100 mL) to remove off unreacted $FeCl_3$ and other iron salts. After the extraction, the solvent in the thimble filter became colorless, and then the resulting material in the thimble filter was extracted with 100 mL of acetone in a Soxhlet extractor.

The yellow acetone solution was concentrated to dryness to give 0.4 g of a brownish yellow oil. Yield: 39%.

The molecular weight of the acetone-soluble oligomer: Mn = 1100; Mw = 1300; PDI (Mw/Mn) = 1.1

The oligomerization of 2,5-dibromo-3-hexylthiophene with $FeCl_3$ in chloroform was carried out in a similar manner, except for the reaction temperature (0 ˚C).

The molecular weight of the acetone-soluble oligomer: Mn = 1100; Mw = 1200; PDI (Mw/Mn) = 1.1

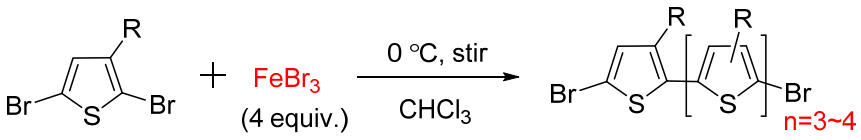

Scheme 6.2.2. Oligomerization of 2,5-dibromo-3-hexylthiophene with $FeBr_3$ in $CHCl_3$

Oligomerization of 2,5-dibromo-3-hexylthiophene with $FeBr_3$ in $CHCl_3$: 2,5-Dibromo-3-hexylthiophene (0.163 g, 0.5 mmol) was added with a syringe to a stirred suspension of $FeBr_3$ (0.591 g, 2 mmol) in dry chloroform (4 mL) under argon atmosphere at 0 °C. The suspension was continuously stirred at 0 °C for additional 2 h. Then, the suspension was cooled down to -78 °C by a dry ice/methanol bath, and methanol (100 mL) was added dropwise to the reaction mixture to quench the oligomerization reaction. The solvents were removed by a rotary vacuum evaporator to afford a brown oil. The brown oil was purified by washing with distilled water to remove unreacted $FeBr_3$ and other iron salts, and then dissolved in chloroform (100 mL). The yellow chloroform solution was dried over Na_2SO_4, filtered, and concentrated to dryness under reduced pressure to afford a light-yellow oil.

The molecular weight of the acetone-soluble oligomer: Mn = 810, Mw = 820, and PDI (Mw/Mn) = 1.01.

6.3 Results and discussion

6.3.1 Kinetics study on 3-hexylthiophene polymerization with iron(III) chloride

The profile of 3-hexylthiophene polymerization by $FeCl_3$ was obtained by monitoring the progress of the reaction. From Figure 6.3.1.1, it is clear that under the mild reaction conditions (0 °C), a high polymerization rate in the initial stage was realized, meaning that the polymerization smoothly took place without any induction period. With 3-hexylthiophene monomer being consumed during the polymerization, the rate of polymerization (Rp) was found to decline exponentially with the reaction time. After 4 h, Rp reduced to almost zero, implying the attainment of a stationary propagation stage. As a result, the monomer-to-polymer conversion reached over 60% within 30 min, and the increase of the polymer yield was significantly retarded along with the remarkable reduction of Rp; the polymer yield was only 70% even after 16 h.

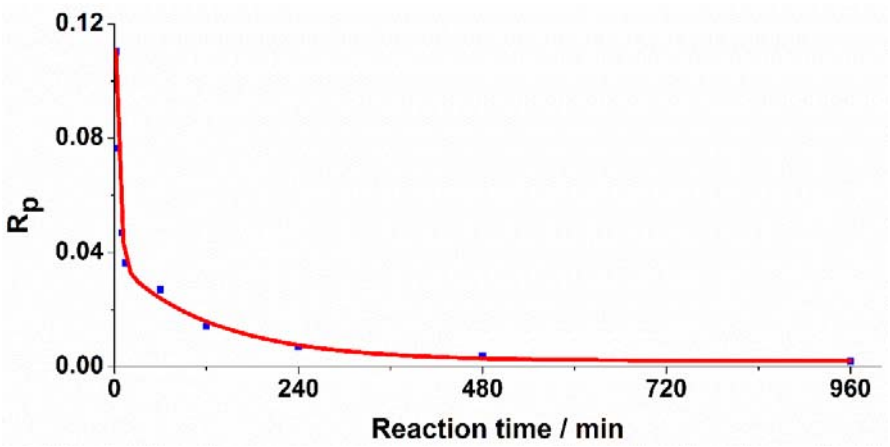

Figure 6.3.1.1. Time dependence of Rp (rate of polymerization).

The dependency of the z average molecular weight (Mz) and the polydispersity index (PDI = Mw/Mn) (Mw, weight-average molecular weight; Mn, number-average molecular weight) of poly(3-hexylthiophene) on the reaction time was also investigated (Figure 6.3.1.2). The Mz was found to increase monotonically with the polymerization time in the early stage of the reaction at 0 °C. After 4 h, the Mz was hardly changed, although the prolonged reaction time resulted in the increase of the overall yield. Upon reflecting the change in the Mz, the PDI was observed to rise from 2.9 to 3.9, when the reaction time was prolonged from 2 min to 16 h. In a similar manner, the number-average chain length of poly(3-hexylthiophene), calculated from Mn, changed from about 180 repeating units in the early stage (within 2 min) to about 280 repeating units after 4 h and gradually set. The author also confirmed that the regioselectivity did not change with reaction time. For the diads, the regioselectivity of HT (head-to-tail) to HH (head-to-head) was kept to about 4:1; for the triads, the ratio of HT-HT: HT-HH: TT-HH: TT-HT stayed about 6:1:1:1.

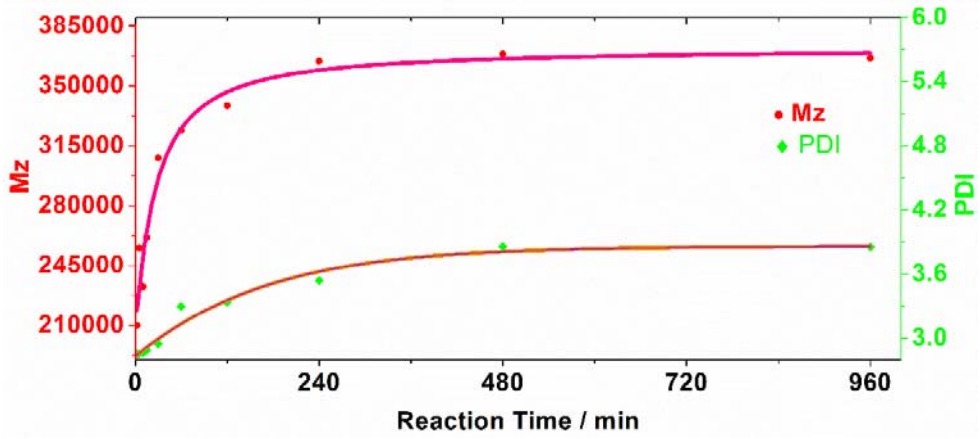

Figure 6.3.1.2. Time dependency of molecular weight of poly(3-hexylthiophene) (Mz: z average molecular weight)

The change of the UV-vis spectra of poly(3-hexylthiophene)s prepared at different times are shown in Scheme 6.3.1.3. The maximal absorption wavelength of poly(3-hexylthiophene) was shifted to longer wavelength from 434 nm to 440 nm, when reactions were carried out for 2 min and 8 h, respectively, indicating that prolonged reaction time resulted in the extension of the conjugation length of the resulting polymer main chain. This result is easy to understand, in terms of the rise in the polymer molecular weight with the reaction time.

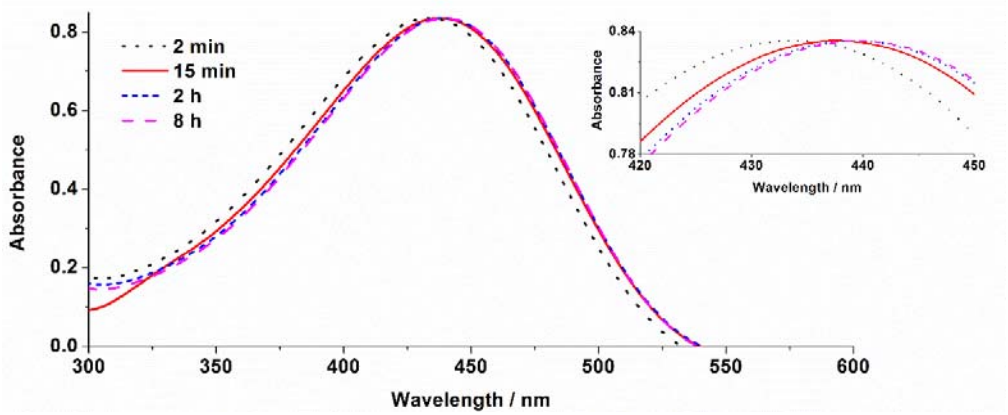

Scheme 6.3.1.3. UV-vis spectra of poly(3-hexylthiophene)s prepared at different reaction times

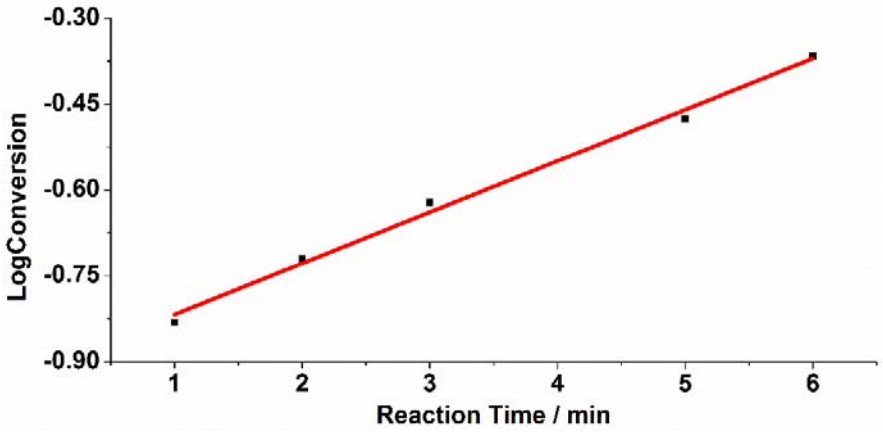

Figure 6.3.1.4. First order kinetics at the initial stage of the polymerization.

For the present polymerization of 3-hexylthiophene with $FeCl_3$ in $CHCl_3$ at 0 °C, the author confirmed that in the initial stage (within 6 min) of the polymerization, the initial reaction rate followed first-order kinetics (Figure 6.3.1.4). However, after 6 min, significant deviation from first order kinetics was observed.

Polymerization initiated by $FeCl_3$ was performed at temperatures from –45 to +50 °C. The results are summarized in Table 6.3.1.5 A partially gelated polymer was obtained, when the reaction was performed at ≥50 °C, probably ascribable to the cross-linking at the 4-position of the thiophene ring in the polymer.

Table 6.3.1.5. Conversion and regioselectivity for the 3-hexylthiophene polymerization for 0.5 h. The values in the parentheses indicate the conversion of the monomer to the gelated polymer. The content of HT diad was determined by ^1H NMR of poly(3-hexylthiophene). RT indicates the reaction temperature. Reaction time, 30 min; molar ratio of 3-hexylthiophene to $FeCl_3$, 1: 4

Run	RT (°C)	Polymer yield (%)	Diads		Triads			
			HH (%)	HT (%)	HT-HT (%)	HT-HH (%)	TT-HT (%)	TT-HH (%)
1	50	76 (15)	24	76	60	14	13	13
2	30	90 (0)	19	81	65	13	12	10
3	0	45 (0)	19	81	69	11	10	10
4	-15	25 (0)	33	67	63	12	13	12
5	-45	10 (0)	44	56	49	17	16	18

As can be seen from Table 6.3.1.5, the catalytic activity (A) was not so low at low temperatures; even when the polymerization was carried out at -45 ℃, the polymer yield of up to 10% was realized. Moreover, there was a linear correlation between the A values and the temperatures over an entire range of temperatures. The yield of poly(3-

hexylthiophene) per $FeCl_3$ (in mol), the monomer (in mol) and time (in h) followed the simple Arrhenius relationship (Figure 6.3.1.6). From Figure 6.3.1.6, the overall activation energy for the polymerization was estimated to be 15.4 kJ mol^{-1}.

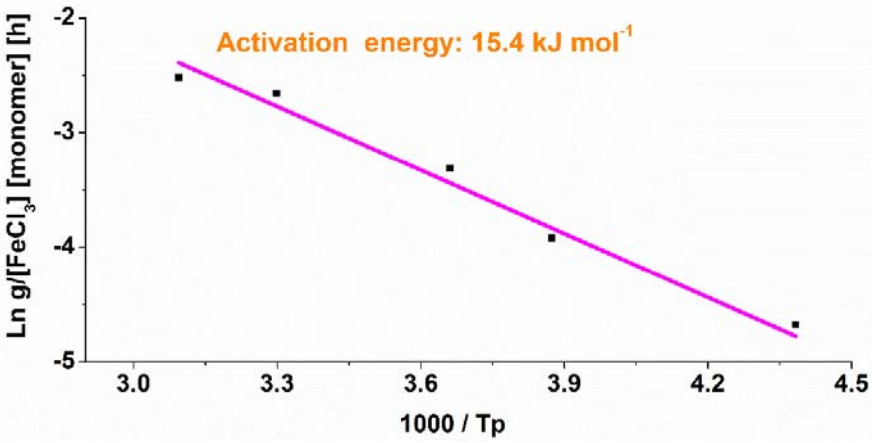

Figure 6.3.1.6. Arrhenius plot of 3-hexylthiophene polymerization by $FeCl_3$ in $CHCl_3$.

The change of the regioselectivity with the reaction temperature in the polymerization of 3-hexylthiophene is also presented in Table 6.3.1.5. There is a general tendency that in a temperature range from 30 °C to -45 °C, the content of HT decreases from 81% to 56% with lowering the temperature, different from the results reported,[8] and the exception of Run 1 is most likely due to the formation of a gel. Similar tendency is also found in HT-HT part. A lower reaction temperature results in the decrease of the content of HT-HT, from 69% at 0°C to 49% at -45°C. Because the 2-position is more reactive than the 5-position of the thiophene ring in 3-hexylthiophene and because the HH coupling is influenced by steric repulsion between two hexyl groups, the HH and HT couplings may be kinetically and thermodynamically controlled reactions, respectively. Therefore, the content of HT would decrease, when the polymerization was carried out at a low temperature.

To further understand the progress and mechanism of 3-hexylthiophene polymerization by $FeCl_3$ in $CHCl_3$, MALDI-TOF MS (matrix-assisted laser desorption/ionization mass spectroscopy), which is a useful tool for the characterization of synthetic polymers, was utilized.[9] The partial MALDI-TOF MS spectra of acetone-soluble oligo(3-hexylthiophene)s by using α-cyano-4-hydroxycinnamic acid (CCA) as the matrix are shown in Figure 6.3.1.7. The hydrogen end groups of the oligomer obtained by the reaction at 0 °C for 8 h, are substituted with chlorine atoms, which is consistent with the result reported by McCarley *et al.*[10] In contrast, the end groups of the oligomer obtained by the reaction at 0 °C for 3 min have no chlorine atom at all. This result indicates that no chlorination took place for the terminal proton in the early stage of the polymerization even though the molecular weight (Mn) reached to about 25,000.

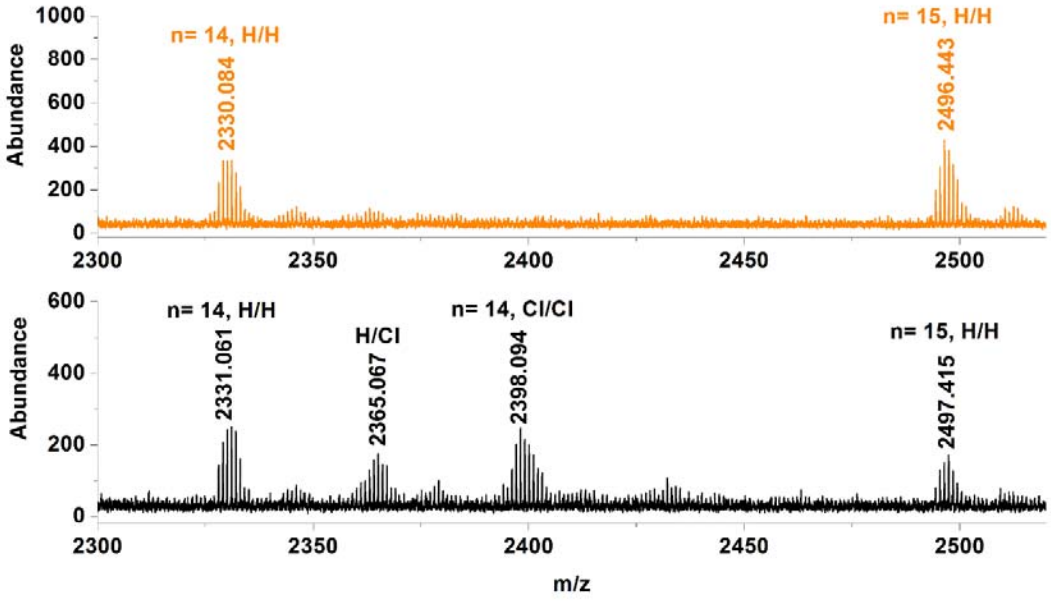

Figure 6.3.1.7. MALDI-TOF MS spectra of acetone-soluble 3-hexylthiophene oligomers (CCA as the matrix). A, the oligomer obtained by the reaction at 0 °C for 3 min; B, the oligomer obtained by the reaction at 0 °C for 8 h.

In the MS spectrum of the oligomer, which was collected after the reaction at 0 °C for 8 h, more than four ion series are presented: $[166n]^+$, $[166n + Cl]^+$, $[166n + 2Cl]^+$, and $[166n + 3Cl]^+$. This means that other than the substitution of terminal proton(s) with chlorine(s), some proton(s) at the 4-position of the thiophene ring in the oligomer was also substituted with chlorine(s) generated from $FeCl_3$. It is well-known that anhydrous $FeCl_3$ is one of chlorinating agents for aromatic compounds.[11] The chlorination of the thiophene ring likely occurs in a similar reaction mechanism.

To determine the change of the content of chlorine atom(s) in poly(3-hexylthiophene) synthesized by using $FeCl_3$ in $CHCl_3$ at different reaction times, energy-dispersive X-ray (EDX) analysis, which is a novel technology to determine the elemental distribution of a sample with several micrometers range,[12,13] was performed. As shown in Scheme 6.3.1.8, the TEM (transmission electron microscopes) image of poly(3-hexylthiophene) showed a rough surface. The EDX analysis indicated that the chlorine content in percentage in poly(3-hexylthiophene)s increased from 0.06% (reaction time, 2 min) to 0.15% (reaction time, 8 h) (Scheme 6.3.1.8 and 6.3.1.9) .

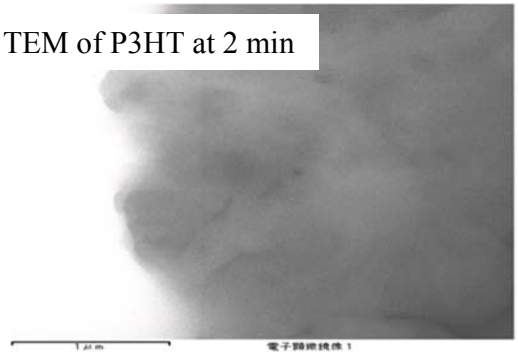

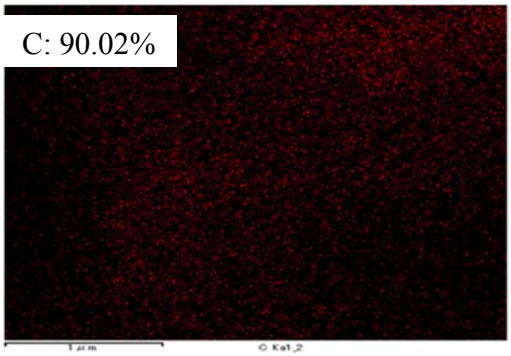

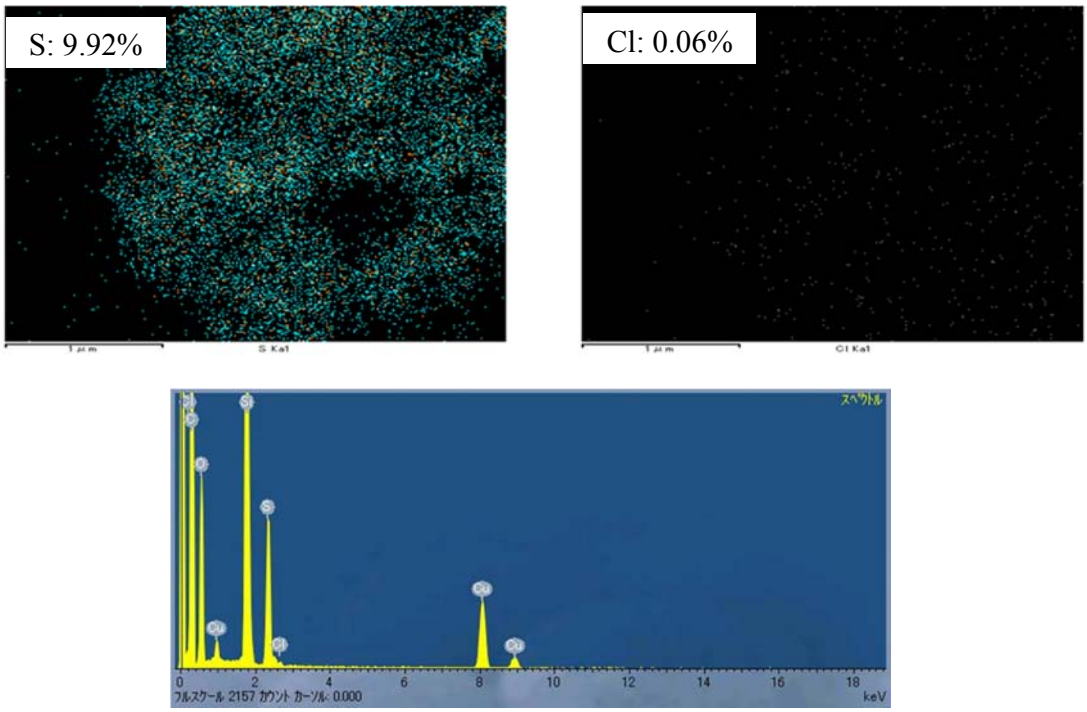

Scheme 6.3.1.8. EDX of poly(3-hexylthiophene) obtained by using $FeCl_3$ in $CHCl_3$ at 0 °C for 2 min

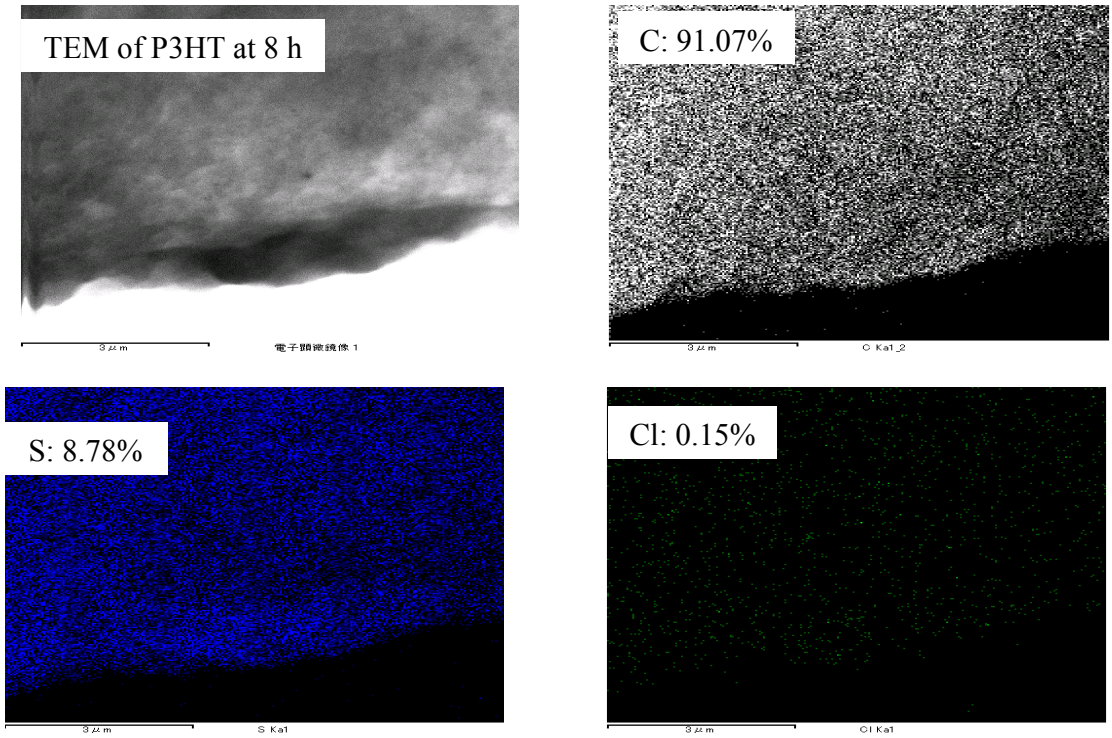

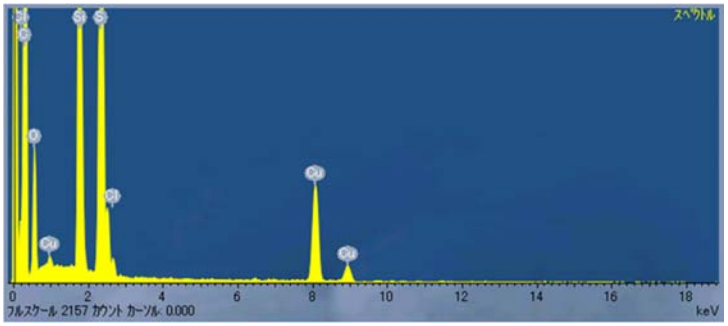

Scheme 6.3.1.9. EDX of poly(3-hexylthiophene) synthesized in $CHCl_3$ at 0 °C for 8 h

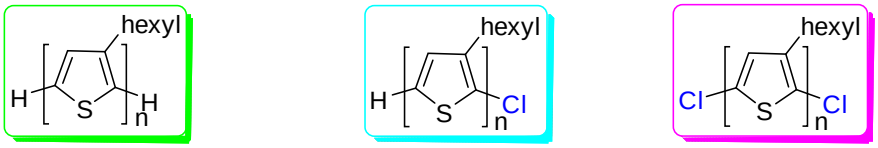

Scheme 6.3.1.10. Typical three types of oligomers possibly otained in the polymerization of 3-hexylthiophene

As shown in Figure 6.3.1.7, three types of oligomers with different end-groups could be identified in the progress of the polymerization (Scheme 6.3.1.10). On the basis of the results on the identification of the end groups, the author speculated that in the early polymerization stage, the propagation reaction exclusively yields the oligomer with hydrogen end groups. With the reaction progresses, the content of the oligomer with chlorine end group(s) increases, and the polymerization rate drastically lowers and becomes extremely low. These phenomena would arise from the substitution of hydrogen(s) with chlorine(s) at the terminus of the oligothiophenes. Thus, oligo(3-hexylthiophene)s with hydrogen atom(s) at the terminus (Scheme 6.3.1.10: A-type and B-type oligomer) can continue the polymerization by the reaction between the oligomers and between the oligomer and the monomer. In contrast, in the case of the oligomer with chlorine atoms at the termini (Scheme 6.3.1.10: C-type) the further propagation of the oligomer would be prevented.

6.3.2 Polymerization of bromo-substituted 3-hexylthiophene with anhydrous ferric halide ($FeCl_3$ and $FeBr_3$)

To confirm this hypothesis, bromo-substituted 3-hexylthiophene, which has bromine atom(s) at one terminus or both termini, was polymerized by using $FeCl_3$ or $FeBr_3$ in $CHCl_3$, and the structure of the corresponding products were determined by MALDI-TOF MS, ^1H NMR, ^{13}C NMR, and gel permeation chromatography (GPC).

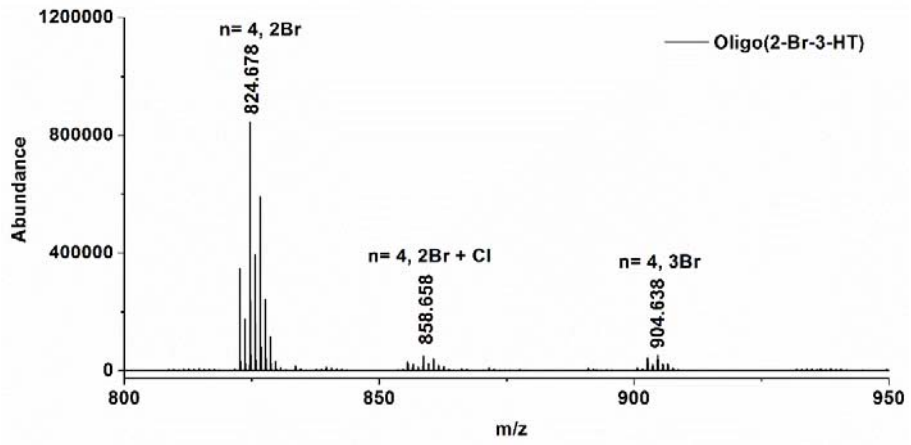

Scheme 6.3.2.1. MALDI-TOF MS spectrum of oligo(2-bromo-3-hextlthiophene) prepared with $FeCl_3$ in $CHCl_3$ at 0 °C for 2 h

As evidenced by the GPC analysis of the corresponding product (Mn=1100; Mw=1300; PDI=1.1), 2-bromo-3-hexylthiophene was polymerized by the $FeCl_3$ oxidative method to just afford oily oligomer, implying its poor polymerization activity. From Scheme 6.3.2.1, other than a Cl atom, oligomers were found to have more than two bromine atoms. Taking the origin of bromine atoms into consideration, the author confirmed that the bromine atom was released by the cleavage of the C-Br bond in the monomer and could be reincorporated into the oligomer by a covalent band.

In the MALDI-TOF MS spectrum of oligo(2,5-dibromo-3-hexylthiophene), only tetramer and pentamer, which contain two or more bromines, were observed (Figure 6.3.2.2). The

existence of various ion series ($[M+2Br]^+$, $[M+3Br]^+$, and $[M+4Br+H]^+$ for the tetramer, $[M+4Br]^+$, and $[M+5Br]^+$ for the pentamer) clearly indicates that some protons at the 4-position of the thiophene ring in the tetramer and pentamer were substituted with bromine(s), similar to the case of the 3-hexylthiophene oligomer obtained during the polymerization of 3-hexylthiopnene by $FeCl_3$.

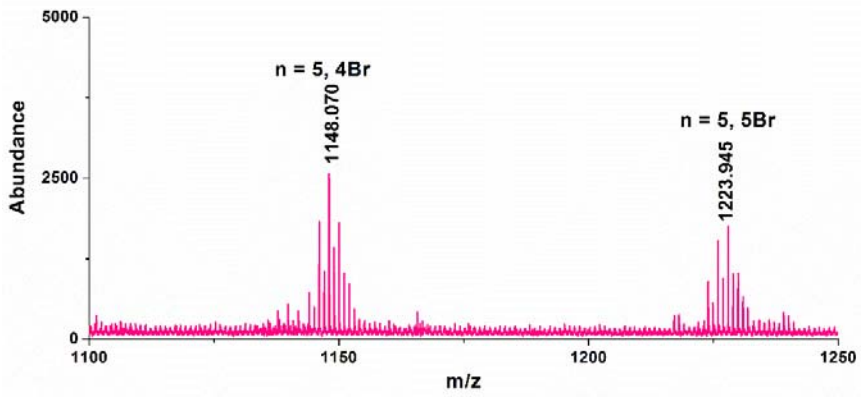

Figure 6.3.2.2. MALDI-TOF MS spectrum of 2,5-dibromo-3-hexylthiophene oligomer synthesized by employing $FeBr_3$ (CCA as the matrix)

In the ^1H NMR spectrum of the oligomer thus obtained (Figure 6.3.2.2), there were many signals between 6.5 and 7.2 ppm, indicative of a mixture of isomers with various possible bromine-substituted end groups (Scheme 6.3.2.3). The generation of the tetramer and pentamer can be ascribed to the homo-coupling reaction of 2,5-dibromo-3-hexylthiophene in the presence of $FeBr_3$. On the other hand, the formation of the 2,5-dibromo-3-hexylthiophene oligomers shows that the C-Br bond of 2,5-dibromo-3-hexylthiophene monomer can be cleavage by $FeBr_3$ and that the 3-hexylthiophene oligomers with two bromines as terminal groups still can polymerize. The result of the oligomerization of 2,5-dibromo-3-hexylthiophene strongly indicates that in contrary to our hypothesis, the oligomer with chlorine atoms at the termini (C-type) is still reactive,

although the polymerization activity is rather low. To date, the mechanism of the chlorination of the terminal and 4-positioned protons in the chain of poly(3-hexylthiophene) is still less understood. However, the author would like to propose one possibility that the introduction of a chlorine atom to a polymer chain takes place by the reaction of 3-hexylthiophene radical, produced by the action of $FeCl_3$, with Cl radical from $FeCl_3$ dissolved in chloroform.

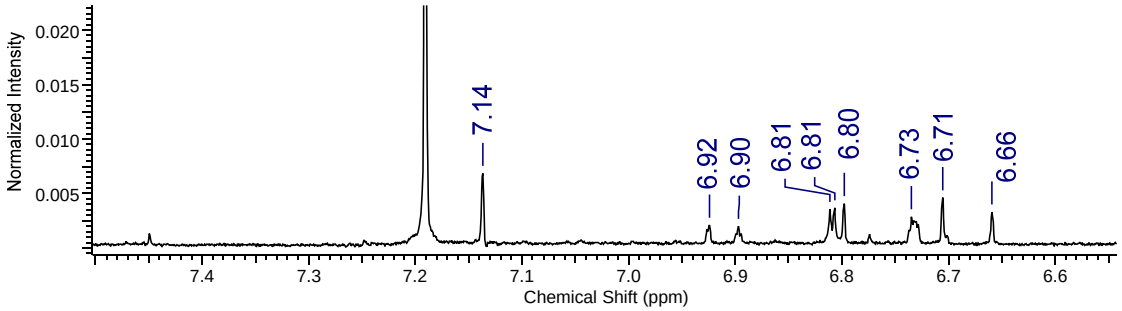

Scheme 6.3.2.3. ^{1}H NMR of oligo(2,5-dibromo-3-hexylthiophene)

In conclusion, the reaction profile for 3-hexylthiophene polymerization with $FeCl_3$ in chloroform has been established. The highest rate of polymerization is obtained in the initial reaction stage, and followed by a moderate decay to a stationary stage of polymerization. The polymerization activity of 3-hexylthiophene remarkably increased with elevating the reaction temperature. The overall activation energy for the polymerization of 3-hexylthiophene with $FeCl_3$ was calculated to be 15.4 kJ mol^{-1}, which was determined from the slope of the Arrhenius plot. 2,5-Dibromo-3-hexylthiophene was oligomerized by $FeBr_3$ in chloroform. This result implied that oligomers with two chlorine atoms as terminal groups still can propagate, even though the activity is extremely low. The results will provide a fundamental insight for further study on the syntheses of poly(alkylthiophene)s by using transition metal halides.

6.4 References to Chapter 6

1. R. Sugimoto, S. Takeda, H. B. Gu, and K. Yoshino, *Chem. Express*. **1986**, 1, 635- 638.
2. J. Janata and M. Josowicz, *Nat. Mater*. **2003**, *2*, 19-24.

   R. Taylor, The Chemistry of Heterocyclic Compounds, John Wiley and Sons, **1986,** 159-522.
3. J. Liu, N. R. Davis, D. S. Liu, and P. T. Hammond, *J. Mater. Chem*. **2012,** *22*, 15534.
4. R. M. Kellogg, Comprehensive Heterocyclic Chemistry, Pergamon Press, **1984**, 741-861.
5. H. Ritter, Desk Reference of Functional Polymers, Syntheses and Applications, American Chemical Society, 1997, 103-113.
6. F. Jonas, G. Heywang, W. Schmidtberg, J. Heinze, M. Dietrich, U.S. Patent 5035926 (1991).

   L. A. P. Kane-Maguire and G. G. Wallace, *Chem. Soc. Rev*. **2010**, 39, 2545-2576.

   J. Roncali, *Chem. Rev*. **1992**, *92*, 711-738.

   A. Marrocchi, D. Lanari, A. Facchetti, and L. Vaccaro, *Energy Environ. Sci*. **2012**, *5*, 8457-8474.

   A. Gumus, J. P. Califano, A. M. D. Wan, J. Huynh, C. A. Reinhart-King, and G. G. Malliaras, *Soft Matter*. 2010, 6, 5138-5142.

   K. Yoshino, S. Morita, and R. Sugimoto, *Synthetic Met*. **1992**. 50, 491-497.
7. T. Olinga.; B. François, *Synthetic Met*. **1995**, *69*, 297-298.
8. Amou, S.; Haba, O.; Shirato, K.; Hayakawa, T.; Ueda, M.; Takeuchi, K.; Asai,

M., J. Polym. Sci. A Polym. Chem. **1999**, *37*, 1943-1948.

9. R. S. Loewe, P. C. Ewbankl, J. Liu, L. Zhai, and R. D. McCullough, *Macromolecules*. **2001**, *34*, 4324-4333.

   Marie, A.; Fournier, F.; Tabet, J. C., *Anal. Chem*. **2000**, *72*, 5106-5114.

10. T. D. McCarley, C. O. Noble, C. J. DuBois, and R. L. McCarley, *Macromolecules*. **2001**, *34*, 7999-8004.

11. P. Kovacic and N. O. Brace, *J. Am. Chem. Soc*. **1954**, *76*, 5491-5494.

    T. Fujimori, M. Takaoka, S. Morisawa, *Environ. Sci. Technol*. **2010**, *44*, 1974-1979.

12. Laskin, A.; Cowin, J. P., *Anal. Chem*. **2001**, *73*, 1023-1029.

13. Bradley, M.; Rowe, J., *Soft Matter*. **2009**, *5*, 3114-3119.

Conclusion and Perspectives

Through the studies explained above, the follows are concluded.

1. A novel ruthenium complex, di(isothiocyanato)bis(4-methyl-4'-vinyl-2,2'-bipyridine)ruthenium(II) [$(NCS)_2(mvbpy)_2Ru(II)$], was synthesized and immobilized onto a TiO_2 electrode surface by a newly developed method.

2. The Ru(II) complex film on TiO_2/FTO thus obtained showed maximum incident photon-to-current efficiency (IPCE) of 1.2%. In contrast, the composite film consisting of the Ru(II) complex and sodium 4-vinylbenzenesulfonate showed much higher maximum IPCE of 31.7% at 438 nm.

3. In the studies on the kinetics of 3-hexylthiophene polymerization by $FeCl_3$, the reaction profile and activation energy have been determined.

4. The effect of reaction time, temperature and solvent on the chemical polymerization of 3-hexylthiophene was investigated. When the polymerization reaction was conducted in an aromatic solvent, the solvent molecule(s) was incorporated into the polymer main chain.

5. TEMPO increased the molecular weight of P3HTs sharply. TEMPO-mediated oxidation may produce halogen-free P3HTs.

6. Bromo-substituted 3-hexylthiophene was found to undergo chemical polymerization with a very low activity. Based on this result, new polymerization methods may be developed.

ACKNOWLEDGEMENTS

At the end of my journey towards Ph.D. degree, I would like to express my heartfelt gratitude to my supervisor: Prof. Ryuichi Sugimoto at Kochi University of Technology for giving me one opportunity to work in his research group, for affording unreserved guidance, suggestions, and consistent encouragements. Without the supports from him, this thesis will not see the light.

I am also extremely grateful to Prof. Kazuhiko Saigo (one of my dissertation committee) for his constructive input, insightful discussions, motivation, inspiration, and true desire to keep me on track. What I learned from him is not only how to conduct research, but also how to push myself ahead. Working with him is a really memorable and valuable experience for me.

I also would like to offer my sincerest appreciations to Prof. Katsuhiro Sumi (former supervisor), and Prof. Masaoki Furue for helpful guidance and suggestions regarding various aspects of research, and their unconditioned support during the rough time of Ph.D. pursuit.

I want to take this opportunity to thank the remaining members of my dissertation committee: Prof. Nagatoshi Nishiwaki, Prof. Kazuya Kobiro, for severing in my defense committee and reviewing my thesis despite their overwhelmingly schedule.

Special thanks was given to Prof. Zhao-yong Bian at Beijing Normal University, China, for introducing me to Kochi University of Technology. Prof. Bian is a respectable mentor and dear friend for me. When I am depressed about research and private life, he gave me hearty and timely supports.

Special thanks was extended to my dearest friends：Dr. Khanit Matra, Dr. Xin Chen, Dr. Shi-xun Zhang, and Mr. Kotaro Nabeshima for sharing with me achievements, fears, pains and joys of last three years.

Special acknowledgement was made to Dr. Peng-yu Wang for the EDX measurements, Mrs. Maki Inoue, Mr. Kazushige Matsumoto, and Takuya, Nakashita, Kanami Inoue for their friendship and assistance in this thesis.

Finally, I am indeed indebted to my girlfriend Ling-lin Yang, my brother Hou-yun LIU, and my parents Zhong-kun LIU (dad), Zheng-yin Rao (mom) for their love, patient understanding, unfailing belief in me, and undiminished support.

Publication and presentation lists

Paper

1. Liu, Y.; Nishiwaki, N.; Saigo, K.; Sugimoto, R., *Bull. Chem. Soc. Jpn.* **2013**, in press.

2. Liu, Y.; Sugimoto, R.; Sumi, K., *Green and Sustainable Chem.* **2013**, 3, 61-67.

Presentation

1. Liu, Y.; Sugimoto, R.; Nishiwaki, N.; Saigo, K.

"Kinetics studies of 3-hexylthiophene with Iron(III) Chloride"

93rd Spring Meeting of Japan Chemical Society; Shiga, March 22-25, 2013.

2. Liu Y.; Shinohara T.; Sumi K.

"Immobilization of Novel Ruthenium(II) Complex with Viny Group by Electrochemically Initiated Polymerization on Titanium Oxide in Dye sensitized Solar Cell"

Annual Meeting of the Society of Polymer Science, Yokohama, May 29-31, 2012.

3. Liu Y.; Tamura M.; Shinohara T.; Yamasaki Y.; Sumi K.

"Dye-sensitized solar cell with vinyl monomers immobilized on TiO_2 by electrolytic initiated polymerization"

61th Symposium on Mmacromolecules, Nagoya, Sep 19-21, 2012.

4. Liu Y.; Yamasaki Y.; Shinohara T.; Sumi K.

“Polymeric films of vinyl metal complex on titanium oxide immobilized by a new electrochemically-initiated polymerization in dye-sensitized solar cell”

9th International Polymer Conference, Kobe, Dec 11-14, 2012.